Order Number 9304686

Synthetic analogs of retinal with spacer arms attached to the seco-ring for the structural probes of retinal proteins: Rhodopsin and bacteriorhodopsin

Kozak, Wei Xing, Ph.D.

City University of New York, 1992

U·M·I

300 N. Zeeb Rd.
Ann Arbor, MI 48106

SYNTHETIC ANALOGS OF RETINAL WITH SPACER ARMS ATTACHED TO THE SECO-RING FOR THE STRUCTURAL PROBES OF RETINAL PROTEINS: RHODOPSIN AND BACTERIORHODOPSIN

by

WEI XING KOZAK

A dissertation submitted to the Graduate Faculty in Chemistry in partial fulfillment of the requirements for the degree of Doctor of Philosophy, The City University of New York.

1992

This manuscript has been read and accepted for the Graduate Faculty in Chemistry in satisfaction of the dissertation requirement for the degree of Doctor of Philosophy.

Date	Chair of Examining Committee
9/3/92	Executive Officer
	Neil McKelvie
	John Lomabardi
	Supervisory Committee

THE CITY UNIVERSITY OF NEW YORK

ABSTRACT

SYNTHETIC ANALOGS OF RETINAL WITH SPACER ARMS ATTACHED TO THE SECO-RING FOR THE STRUCTURAL PROBES OF RETINAL PROTEINS: RHODOPSIN AND BACTERIORHODOPSIN

by

WEI XING KOZAK

Advisors: Professor William F. Berkowitz, Neil McKelvie and John Lomabardi

Retinal proteins in vertebrates and invertebrates comprise rhodopsin: visual pigments which serve as light detectors for the sensory system; whereas the pigment present in *Halobacterium halobium*, called bacteriorhodopsin (bR) functions as a photosynthetic energy source. The retinal chromophores in both proteins are the 11-cis isomer with a linkage to Lys-296, and the all-trans isomer with a linkage to Lys-216 of their respective apoproteins via a protonated Schiff base. Incident light causes both to undergo a series of conformational changes of retinal moiety, related to formation of photointermediates. They are responsible for visual transduction coupled with the permeability of the cytoplasmic membrane to sodium ions, and the proton translocation coupled with the synthesis of ATP in the bR photocycle.

In order to understand both processes in molecular detail, the tertiary structures of these photointermediates and the proteins must be precisely

established. Synthetic retinal analogs confer great advantages for this purpose. A series of seco-ring spacer armed retinal analogs connected to an ester linkage were synthesized. Up to ten carbons in length, all of these analogs efficiently reacted with bacterioopsin to form bacteriorhodopsin analogs with absorption maxima ranging from 530 nm to 536 nm, indicative that the distance between the ring-binding site and the exterior surface of the membrane is about 11-12 Å. Moreover, that these synthetic retinals fully occupy the native binding site is shown by the result of inhibition due to the native chromorphore displacement. These bR analogs function similar to native pigment as shown by the CD spectrum and light-dark adaptation experiments. The all-trans seven-carbon spacer armed retinal was photoisomerized to its cis isomers which were also bound to bovine opsin at maximum absorption of 450 nm. The synthesis of seco-ring retinal analogs with an attached terminal photoactive group has been attempted with great effort using several different methods.

Acknowledgments

I am greatly indebted to my Thesis Committee members for their reviews, editions and supports. They are Professor William F. Berkowitz, Neil McKelvie and John Lomabardi.

I thank Dr. V. Balogh-Nair for giving me the chance to perform all the work and to gain much knowledge about the subject in her lab for these five years.

I thank my colleagues and my friends at the City College of New York for their many helpful suggestions and contributions to this work.

I am grateful to many people at the Graduate School of the City University of New York, especially Professor Pizer, the Executive Officer in the Chemistry Department.

I thank my parents and brothers for their special contributions and concerns; and I thank my husband Ron for his special and long-term support. This work is affectionately dedicated to them.

TABLE OF CONTENTS

SECTION I.

SECTION II.

I. General Introduction

Life on earth obviously could not continue indefinitely without sunlight. The necessity of input of energy is provided by the sunlight. Photosynthetic organisms and plants use electromagnetic energy of sunlight to convert into chemical energy through the process of photosynthesis. They use light as a source of energy whereas animals that can see use light to obtain very detailed information about their surrounding through the visual sense. Humans are especially visually oriented. However, vision and photosynthesis both are initiated from the incidence of light to cause the excitation of an electron.

In the case of vision, after absorption of light, the visual pigments transmit signals across synapses to nerve cells and then the signals travel along the optical nerve cells until they finally reach the brain. The visual pigments are located in light sensitive cells, termed photoreceptors. Vertebrates and invertebrates have different types of cells, ciliary cells and rhabodomeric cells respectively, both possessing an inner and out segment.

Invertebrates have evolved a variety of morphologically distinct visual systems that are very different from those of vertebrates. On the other hand, all vertebrates have similar visual systems with an extremely complex eye which contains many different types of specialized cells (see Figure 1.). Upon entering the eye, the light is refracted by the cornea, the transparent tissue at the front of the eye, and then traverses an aqueous chamber and reaches

the lens, a thin layer tissue of variable thickness regulated by the ciliary muscle, which focuses an optical image on the retina. Finally the light hits neural photoreceptor rod cells and cone cells present in several different layers of the retina (see Figure 2a.). These photoreceptors contain visual pigments. The rod visual cells are specially responsible for vision in dim light and transmit signals to the brain so that we perceive colorless objects in shades of gray. The cone visual cells are concentrated in the central fovea region of the retina and serve for visual acuity, as well as for perception of color distinguished by three different types of cone cells which absorb at 450 nm (blue), 535 nm (green) and 560 nm (yellow).[1] Rods and cones convert the light to a neural signal and the signal is transmitted to the brain via the optical nerve, causing visual perception. In addition, the electrophysiological response of the rods and cones to light involves a change in the permeability of the cytoplasmic membrane to sodium ions. In the dark, sodium ion conductance of the vertebrate rod outer segment (ROS) plasma membrane is high. Flowing into the outer segment from the inner segment, the sodium ions diffuse back to the inside to be pumped out again by a Na^+/K^+-ATPase located in the plasma membrane in the dark (see Figure 2b.). Blocking the sodium ion channels in the plasma membrane and reducing the sodium ion current is one of the major features of the visual transduction process.[2] This event causes a transient hyperpolarization of the membrane,[3] and as visual agents calcium ions and 3',5'-cyclic-GMP (cGMP) might be the major

a)

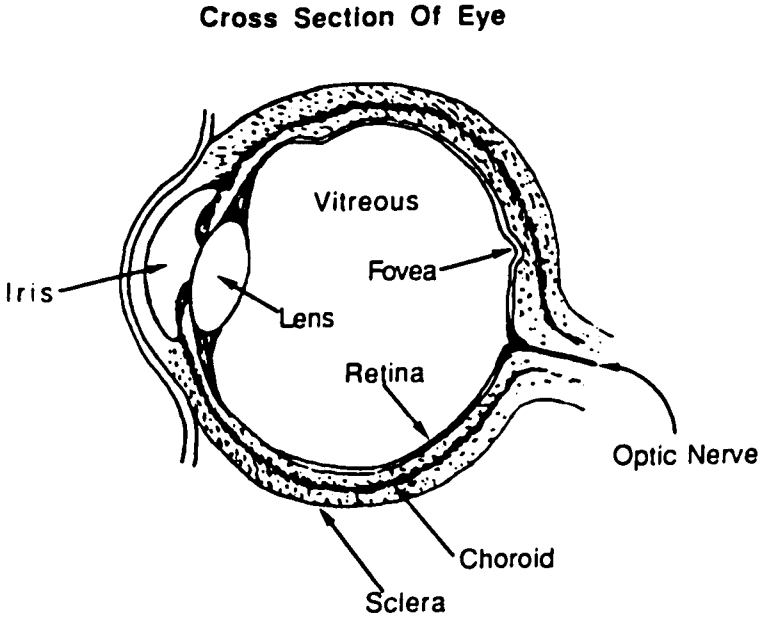

b)

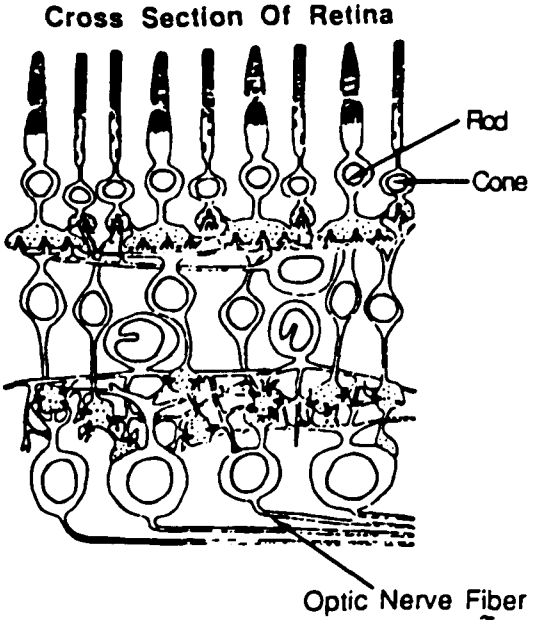

Figure 1. a) A horizontal cross-section diagram of the human eye, from W. K. Noell et al; *Invest. Ophthalmol.* **1966**, *5*, 450-472. b) A horizontal cross-section diagram of the vertebrate retina, from J. E. Doeling & B. B. Boycott; *Pro R. Soc. London, Ser. B* **1966**, *166*, 80-111.

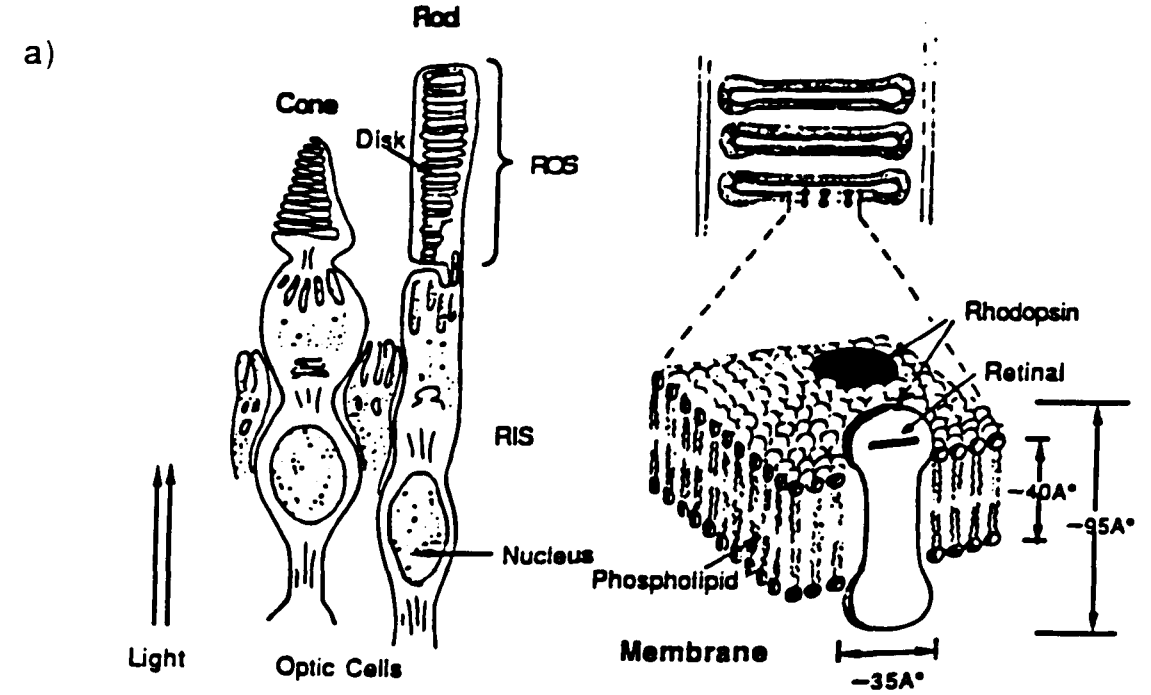

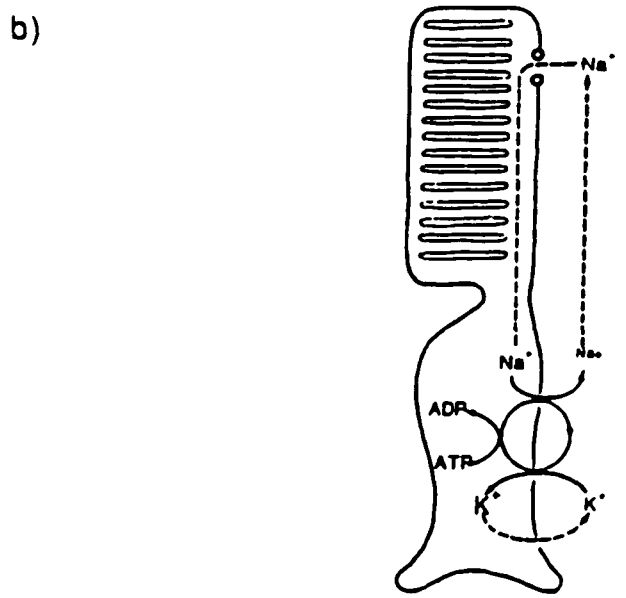

Figure 2. a) Schematic diagram of photoreceptor cells. In the retina, rod cells are stacked side-by-side and light enters the cells end on through the inner segment after passing through several layers of other neural cells. In cone cells the outer segments are shorter and are conical instead of cylindrical. From V. Balogh-Nair & K. Nakanishi; *New compr. Biochem.* **1982**, *3*, 283-334. b) The sodium ion channel in rod cells. Na^+ is pumped out of the inner segment (solid arrow) and diffused back in through channels in the outer segment (dashed arrow).

candidates.

In the rod outer segments, a few thousand stacked disks are incased in a sack of plasma membrane. The protein rhodopsin floats in the phospholipid bilayer of the disks (Figure 2a.).[4] The disk membranes of the vertebrate photoreceptor rod outer segments have a particularly simple composition, as about 95% of the total membrane protein is the visual pigment rhodopsin. The center-to-center repeat spacing of the disks is approximately 300 Å and the cytoplasmic layer between disk membrane less than 150 Å thick and the space inside the disk is about 25 Å.[5] The protein

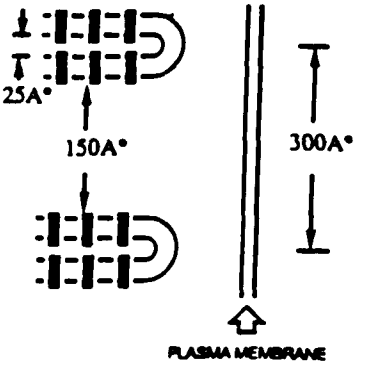

rhodopsin contains 11-cis retinal as a chromophore which undergoes a series of conformational changes during the process of vision. Light-excited rhodopsin stimulates a large number of guanosine triphosphate (GTP)-binding proteins on the membrane surface to bind GTP which then trigger enzymes to degrade cyclic guanosine monophosphate.[6]

II. The Characteristics of Rhodopsin

Rhodopsin is composed of a light-insensitive protein moiety and a light-sensitive chromophore, 11-cis retinal linked to it by a protonated Schiff base. The use of retinal as the chromophore by rhodopsin is almost universal and even the light-sensitive proteins of some unicellular organism, like Halobacteria[7] and Chlamydomonas,[8,9] use retinal.

Rhodopsin, the visual pigment of the rod cell in the disk membrane is a hydrophobic intrinsic membrane protein and contains several carbohydrate groups bound near the amino terminal end of the protein. It is, like the other pigments, a transmembrane protein that is located in the plasma and disk membranes of the receptor outer segment, and has a molecular weight of 39 kDa (including two oligosaccharides) based on sodium dodecyl sulfate (SDS)-gel electrophoresis analysis.[10-13] The carboxyl-terminal end of the protein is exposed to the cytoplasmic space outside the disk and the amino end is exposed to the space inside the disk with hydrophobic stretches of the protein making several excursions back and forth across the lipid bilayer.[14-23] From X-ray diffraction studies of retinal rod cells by Chabre,[20] the most probable distance between rhodopsin molecules aligned on the long axis perpendicular to the disks is 55 Å in oriented ROS indicating the nature of rhodopsin in situ. The complete primary structure of bovine and ovine rhodopsin have been determined,[24-28] and there are 348 amino acid residues, with 23 amino acid

differences between these two rhodopsins,[29] and they are thought to be folded into seven transmembrane helices.

The Properties of Visual Pigment Chromophore

Rhodopsin contains an 11-cis retinal chromophore covalently attached to the apoprotein opsin through a protonated Schiff base linkage to the amino group of Lys-296.[30,31] Retinal has four double bounds in an isoprenoid chain. In 11-cis retinal, steric strain is relieved by twisting about the C_{12}-C_{13} single bond. A twisted nonplanar conformation close to the 12-s-cis conformation is predicted to be the lowest in energy. A nonplanar conformation close to 12-s-trans has a slightly higher energy because of steric hindrance between the 13-methyl group and the 10-hydrogen atom. Earlier Raman spectroscopy studies by Callender et al,[32] showed the chromophore of rhodopsin to be in a 11-cis, 12-s-trans configuration. X-ray analysis of the crystals,[33-35] showed crystalline 11-cis retinal to have three cis bonds: 6-s-cis, 11-cis and 12-s-cis (see Figure 3.). NMR studies of 11-cis retinal indicate that both 12-s-cis and 12-s-trans configurations are present in solution as an equilibrium mixture at room temperature.[36] Moreover, the C_6-C_7 bond is twisted about 40° from the s-cis orientation, close to a 6-s-cis conformation.[34] Compared to absorption spectra of other cis isomers (see Figure 4.), the ratio of the "cis" band at 250 nm to "trans" band at 370 nm is the highest in the 11-cis retinal. The absorption maxima of the 11-cis retinal and the all-

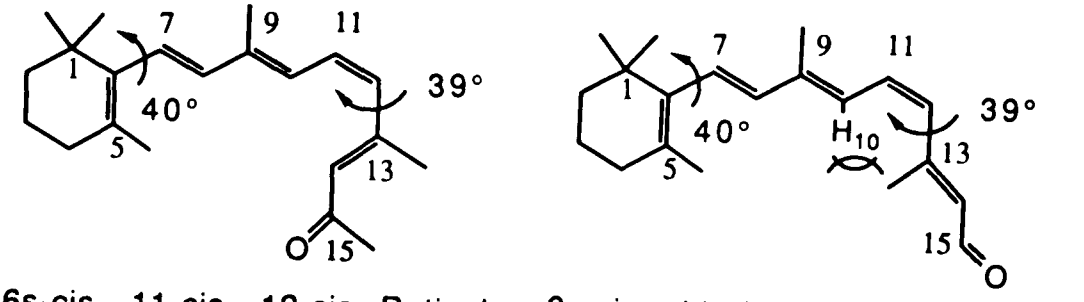

6s-cis, 11-cis, 12-cis Retinal 6s-cis, 11-cis, 12-trans Retinal

Figure 3. Chemical Structure of 11-cis retinal. The C_6-C_7 bond is twisted about 40 °, and C_{12}-C_{13} is about 39 ° from the planar s-cis or 141 ° from the planar s-trans.

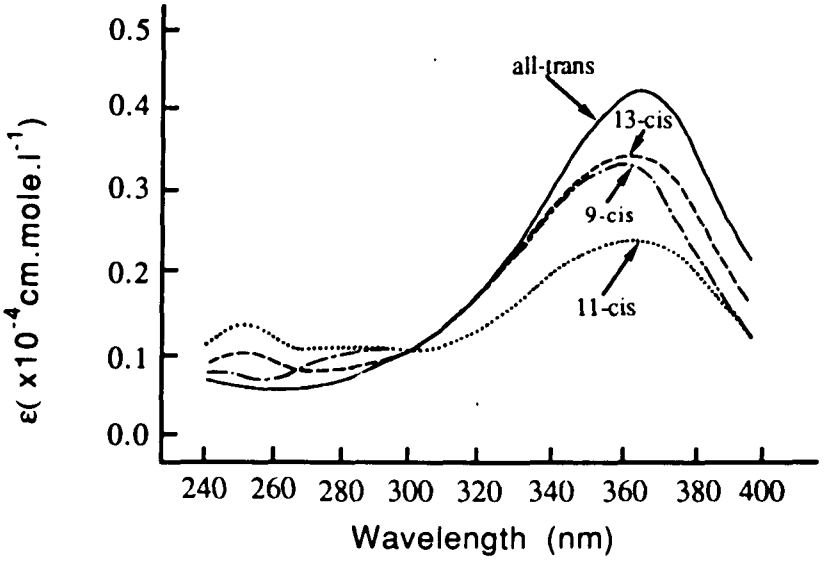

Figure 4. Absorption spectra of retinal isomers. The soectrum of 11-cis retinal represents an equilibrium mixture of 12-s-cis and 12-s-trans isomer.

trans retinal are about 5 nm apart in MeOH. The 11-cis retinal as a chromophore in rhodopsin can be found in terrestrial vertebrates (such as cow, pig, sheep, frog and etc.) and some marine fish. The absorption maxima visual pigments range from 350 nm to 600 nm, attributed to variations in the opsin protein.[37-42] In the case of bovine rhodopsin, the absorption maximum of the pigment is shifted to about 120 nm longer than the free chromophore: 11-cis retinal which absorbs at maximum 380 nm in MeOH. The explanation for this depends partly on the fact that the N of the Schiff base linkage in rhodopsin is protonated and is therefore positively charge, as proved by Raman resonance spectroscopy[43-46] and Fourier-Transform Infrared (FTIR) difference spectroscopy.[47] In addition, low temperature solid-state ^{13}C NMR studies indicate that the Schiff base, a C=N linkage, is protonated in an anti configuration.[48]

The Point Charge Model of Rhodopsin

The 11-cis retinal which functions as a chromophore in rhodopsin is covalently bound to the protein via a protonated Schiff base, leading to an absorption maximum of 500 nm with an extinction coefficient of 40,500.[49] The absorption maximum of retinal itself is at ca. 380 nm in MeOH, and that of the protonated Schiff base with n-Butylamine in MeOH solution is at 440 nm.[50,51] This red shift, termed the Opsin Shift[52,53] which is defined as the difference between the absorption maxima of the protonated Schiff base with

n-butylamine and with opsin, in cm^{-1} unit, is 60 nm (2700 cm^{-1}) and is attributed to the interaction between the protein and the chromophore. The external point charge model of the visual pigment (see Figure 5.), proposed by the Nakanishi group, explains this drastic red shift. Theoretical calculation and experimental data from a series of synthetic dihydro retinal bound to bovine opsin to form rhodopsin analogs indicate that the shortest chromophore, the 11,12-dihydro retinal, has the largest opsin shift, 3000 cm^{-1}, even larger than that of 11-cis retinal itself (2700 cm^{-1}). From theoretical electron calculations, the double point-charge model shown in the Figure 5 shows two negative point charges, one counterion for the protonated Schiff base nitrogen at a distance of about 3 Å and another negative charge in 3 Å away from C-12 and C-14. It is generally believed that the first negative charge, which is a counterion for stabilizing the positive charge on the Schiff base, corresponds to a nearby carboxylate group which hydrogen bond to the Schiff base and is the source of a negative electrostatic potential, or to a cluster of water molecules which hydrogen bonds to neutralize the positive charge.[54,55] However, the Schiff base may interact with the protein environment in a more complex way than with a single nearby carboxylate group, or water molecules.[56-62] Recent evidence from mutagenesis studies of visual pigments[63-65] indicates that glutamate-113, located outside of the membrane-embedded region, seems to be the counterion to the protonated Schiff base and apparently effects the wavelength modulation in visual pigments.

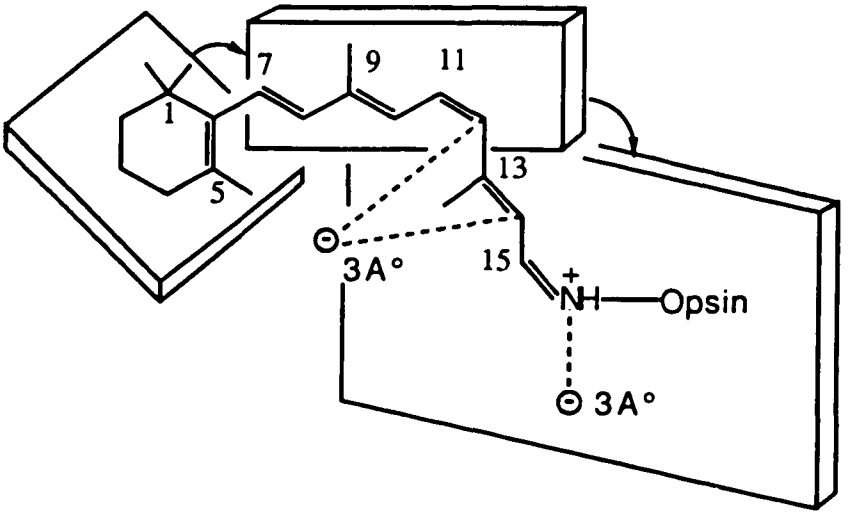

Figure 5. External point charge model of visual pigmentchromophore. The β-ionone ring, C_7-C_{12} conjugated system and C_{12}-C_{15} conjugated system are not in the same plane. One negative charge is located 3A° away from the Schiff base and another negative charge 3A° away from C_{12} and C_{14}.

Nevertheless, to this weakened interaction of the Schiff base with a negative electrostatic potential (weakened with respect to the Schiff base in methanol) is attributed to one of explanations for the opsin shift in rhodopsin, because decreasing this potential causes a red shift of the spectrum and a decrease in affinity for the site of protonation. On the other hand, the second negatively charged group near the middle of the polyene chain is the cause of the bulk of the opsin shift, and it suggests the presence of an interaction close to carbon-13.[66-68] From the studies of opsin shift values of octopus pigments and chicken iodopsin,[66,69] it is found that octopus rhodopsin has the same charge distribution as rhodopsin but chicken iodopsin does not. Since the amount of the shift induced from external charges depends on the conjugated π system, the fact that the introduction of a conjugated double bond at C_3-C_4 monotomically increased the opsin shift in the case of chicken iodopsin strongly suggests the existence of the negative charge at the ring site.

The Circular Dichroism Phenomenon of the Visual Pigments

Rhodopsin shows three distinct absorption maxima at 500 nm, 340 nm and 278 nm corresponding to the α, ß and ν bands respectively (see Figure 6.). The α band (500 nm) and ß band (340 nm) are attributed to the bound chromophore, and ν band (278 nm) in the UV region is from the absorption of the π - π^* and n-π^* transition of aromatic amino acid residues of opsin.[70]

Another spectral property of the visual pigment chromophore is optical activity, which is studied by Circular Dichroism (CD) measurements. Visual pigments significantly show optical activity in solution, whereas the chromophore itself does not. The retinal chromophore of rhodopsin has two distinct circular dichroism bands at ca. 490 nm and ca. 340 nm corresponding to the α and ß absorption bands with a strong Cotton effect (see Figure 7.).[71,72] Bovine rhodopsin also shows a CD band at ca. 280 nm due to the π - π^* transition of aromatic residues and the $n-\pi^*$ transition of cysteine. Induced optical asymmetry on the part of retinal from an asymmetric protein environment would be one of the reasons for the optical activity of the visual pigment. Alternatively, the protein may adopt the distorted conformation of the 11-cis retinal.[73] It is also noteworthy from CD spectra in the far ultraviolet region that rhodopsin contains about 50% α-helix structure.[74]

Spectra & Properties of Photolysis Intermediates in Visual Pigments

When rhodopsin is exposed to the light, it undergoes a series of color changes from its original reddish-pink to yellow in a series of steps. The entire process is named "Bleaching". In the process, the photolysis of visual pigments results in the formation of an initial photoproduct which then decays thermally in the dark through several spectrally distinct intermediates, accompanied by conformational changes of the retinal moiety from the 11-

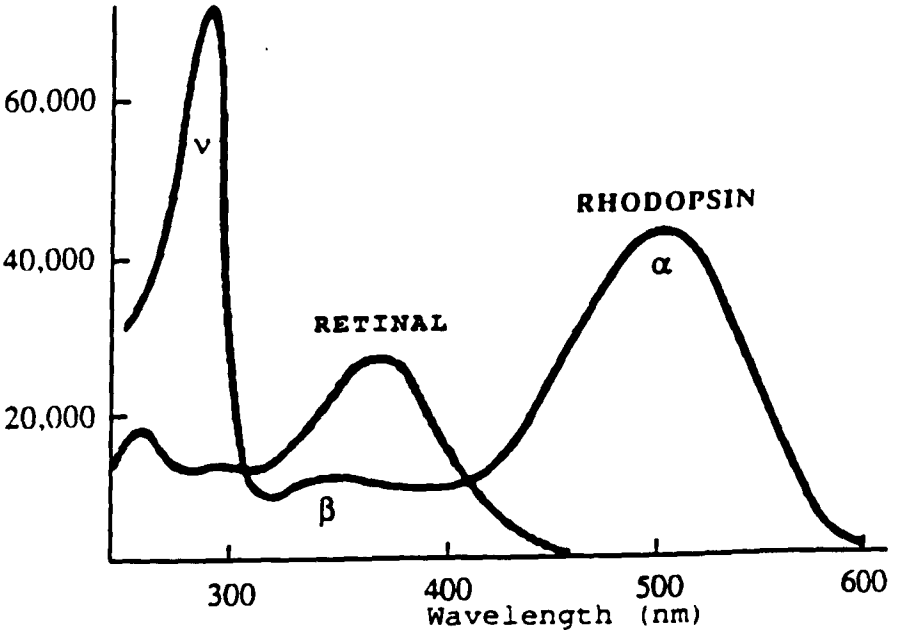

Figure 6. The absorption spectra of purified rhodopsin in the detergent and 11-*cis*-retinal in hexane solustion, from M.Ottolenghi, *Ave. Photochem.*, **1980**, *12*, 97.

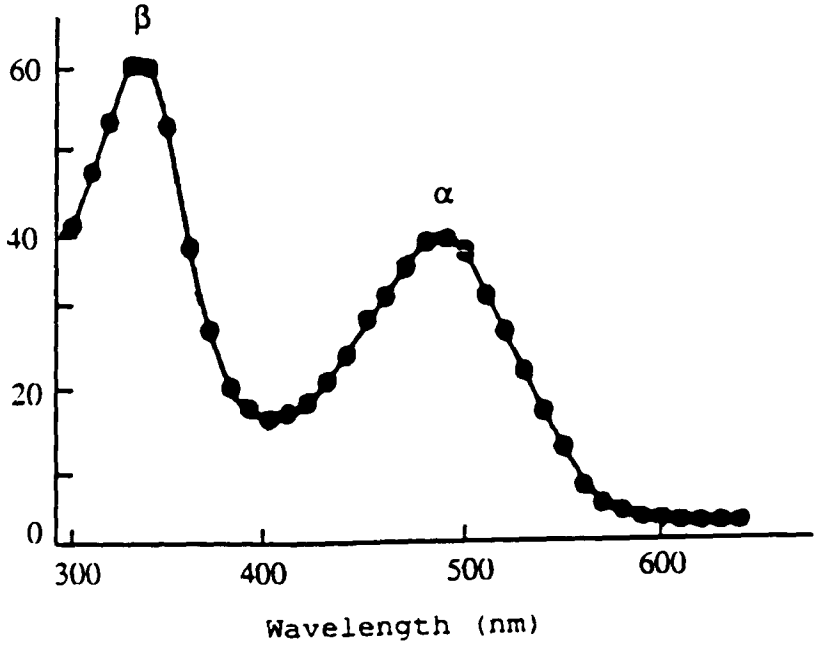

Figure 7. Circular dichroism spectrum of bovine rhodopsin.

cis to the all-trans form, until the isomerized retinal (all-trans retinal) is liberated from the apoprotein. The quantum efficiency of stimulation of rhodopsin is very high, nearly 0.67.[75] In the eye, bleached rhodopsin is regenerated by the enzymatic conversion of all-trans retinal into 11-cis retinal. The 11-cis retinal spontaneously combines with bleached rhodopsin (opsin) to regenerate rhodopsin. The entire process from the bleaching of rhodopsin to its regeneration is called the visual cycle. Figure 8 shows the series of intermediate steps in the bleaching process that have been identified, their absorption maxima, and approximate half-times of interconversion in bovine rhodopsin.

The first change from rhodopsin to bathorhodopsin (batho) is the only light-induced step, called the primary event (or step). All other subsequent changes from it are thermal. The light energy absorbed in this process is channeled into the protein where it initiates a biochemical chain of events leading to the closure of sodium channels in the plasma membrane.[76,77] For many years, it was believed that bathorhodopsin was the first product (formed in a low picosecond time region) and that this was basically generated by an isomerization of 11-cis to all-trans with a twisted angle to some extent.[78-81] Later efforts[82] indicated another intermediate called hypsorhodopsin, between bathorhodopsin and rhodopsin, which has a blue shift of its absorption maximum compared to rhodopsin due to deprotonation. More recent results[83,84] strongly indicate that hypsorhodopsin is formed by multiphoto absorption and

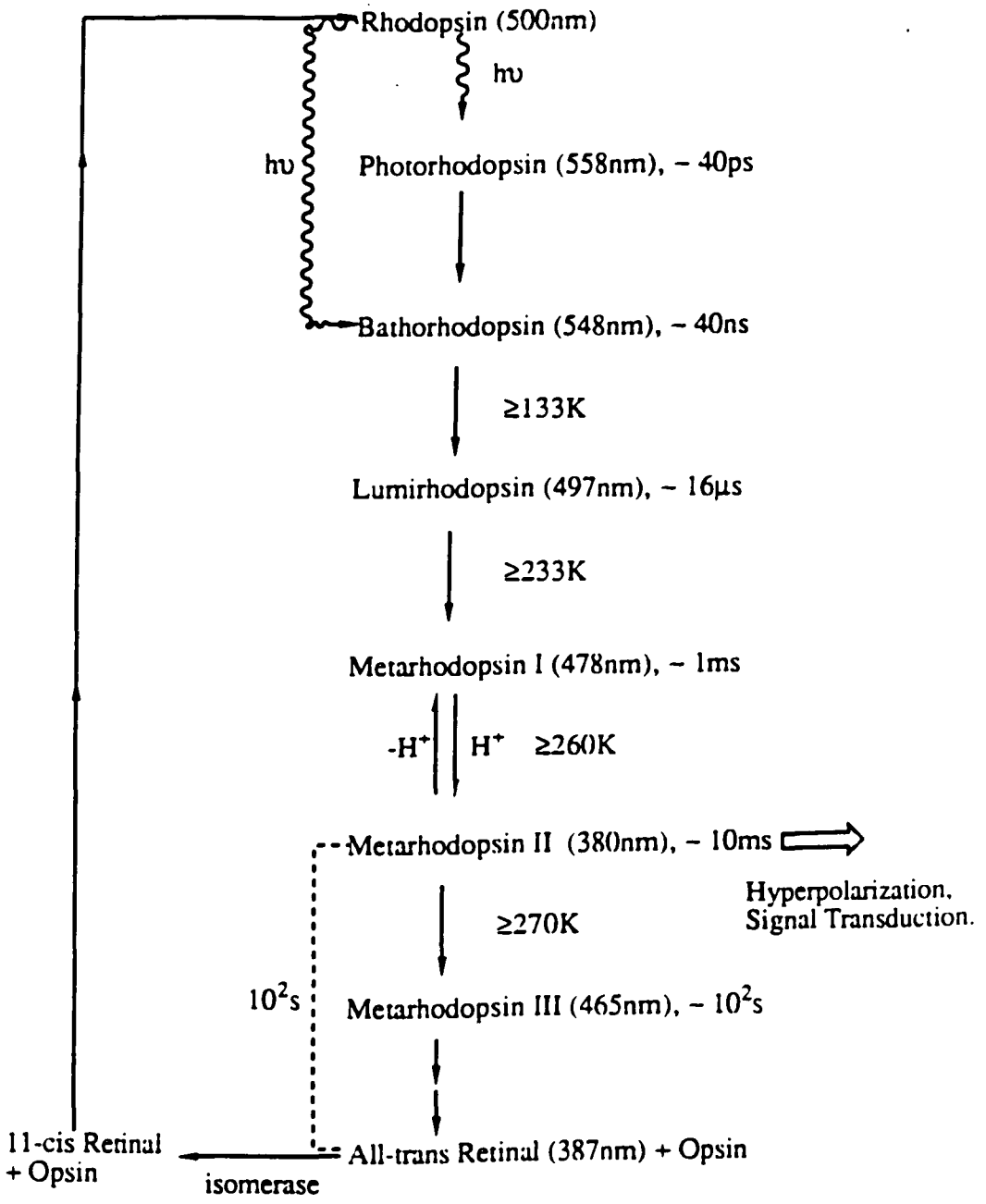

Figure 8. Intermediates in the bleaching process of bovine rhodopsin. Approximate maxima of absorption are given in parenthesis and the temperature shows the interconversion between intermediates occurring in the sequence. Approximate decay constants near room temperature are shown beside the wavelength. From R. S. Becker; *Photochem. Photobiol.* **1988**, *48*, 369-399.

should not be considered as a precursor to bathorhodopsin. Moreover, a new "first" intermediate, termed prebathorhodopsin[85,86] or photorhodopsin[83,84,87] preceding bathorhodopsin has been observed at very low excitation energies (20 uJ). It absorbs at about 10 nm longer wavelength than bathorhodopsin and decays on a time scale of 10^{-11} s to bathorhodopsin.[88] Nevertheless, bathorhodopsin has a 6-s-cis, 11-cis chromophore whose ground state energy is nearly 33 Kcal/mole above that of rhodopsin and whose absorption maximum at 548 nm is shifted to a longer wavelength relative to rhodopsin (500 nm).[89-91] This energy is used in subsequent thermal transitions through lumirhodopsin and metarhodopsin, and ultimately leads to an activated form of the protein which catalyzes the visual transduction process. Moreover, from a study of bathorhodopsin, Smith et al[92] very recently provided results contrary to another mechanism for energy storage;[56] that is, charge separation upon isomerization during the Batho transition, due to the interaction between the protonated Schiff base and charged protein residues in the retinal binding pocket, as the main mechanism for energy storage in the Batho photoproduct. Also, they suggested that energy storage occurs in the form of the distortions of the bathorhodopsin chromophore.

The next well-characterized intermediate, lumirhodopsin, has a room temperature lifetime on the order of 10^{-5} s and is stable up to 200 K. FTIR date[93] indicates that the chromophore strain in lumirhodopsin has relaxed and that protein changes, which are already present at the bathorhodopsin

stage, have significantly increased. Recently, a new intermediate blue-shifted (λ max = 430 nm) relative to the lumirhodopsin intermediate has been first observed with use of nanosecond photolysis experiments and low-temperature studies [94] in the study of the artificial pigment cis-5,6-dihydroisorhodopsin. It was suggested that this blue-shifted intermediate was a decay product of bathorhodopsin. Similar observations [95-97] were made with other artificial pigments, such as 4,5-dehydro-5,6-dihydro-isorhodospin, 11-cis-13-demethyl retinal and ring-modified analogs. In addition, current time-resolved spectral studies [98] have confirmed the existence of this photolysis intermediate in native rhodopsin as well and indicate that bathorhodopsin produced by photolysis of rhodopsin does not decay directly to lumirhodopsin (Lumi), but rather forms this blue-shifted intermediate with higher enthalpy than that of bathorhodopsin,[99] which then decays to lumirhodopsin. In the light of consideration, a mechanism involving an equilibrium between bathorhodopsin (Batho) and the blue-shifted (BSI) intermediate is suggested:[99,100]

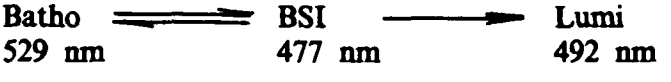

On the other hand, because of the short period of time elapsed (45 ps) between light absorption and formation of bathorhodopsin, it is generally believed that a relatively larger change in chromophore-opsin interactions could take place during the Batho-to-Lumi transition. From earlier low-temperature CD data,[101-103] recent FTIR measurements,[104,105] and studies of

synthetic retinal analogs,[106,107] it is suggested that the Batho-Lumi transition is due to a change in the interaction between the chromophore and opsin is likely to involve the region adjacent to the cyclohexenyl ring of the chromophore.

The next intermediate, metarhodopsin I (Meta I, λmax = 478 nm), is formed from lumirhodopsin within a few microseconds at physiological temperature. Meta I decays to metarhodopsin II (Meta II) with a lifetime of a few milliseconds. There is a tautomeric equilibrium, pH and temperature sensitive, between Meta I and Meta II, accompanied by considerable protein conformational change that is markedly influenced by the environment. A proton is taken up by rhodopsin during this transition.[108,109] Therefore, Meta I is linked to the protein via a protonated Schiff base, whereas Meta II is linked an unprotonated Schiff base.[110] Meta II (λmax = 380 nm) which is formed milliseconds after bleaching, is the last photointermediate formed on a time scale fast enough to be implicated in visual signal transduction. Previous studies [111-114] indicated that Meta II is generally spectrally identified with the photolyzed conformation of rhodopsin (Rho*) which binds and activates the visual G-protein (Gt) resulting in the exchange of GTP for bound GDP on Gt. This is based on the enhancement of the concentration of Meta II in the Meta I - Meta II equilibrium upon reduction of the concentration of Meta I and an increase in the level of Gt activation, using the criteria of Gt binding.[115] Relatively recent study [116] provides evidence of

the similarity of decay times of Meta II and Rh* in parallel experiments, and further supports the functional equivalence of photointermediate Meta II and the visual G-protein activating form of photolyses rhodopsin. Therefore, the presence of Meta II serves as an indicator of the Gt-activating conformation of photoactivated rhodopsin. In the subsequent step, Metarhodopsin II decays either to Metarhodopsin III (Meta III, λmax = 465 nm) or directly to all-trans retinal and the opsin depending on the pH of the medium.[117] Metarhodopsin III is then slowly hydrolyzed and releases all-trans retinal.

Visual Transduction of Rhodopsin

Two major phenomena in the visual transduction mechanism were found in the late 1960's. First, the electrophysiological response results from the reduction of the Na^+ inward current that flows in the dark through the ROS external membrane. The important agent which controls this event, either calcium ion or cyclic GMP, was considered. Based on the interpretation of extracellular effects of calcium ions, a potent effector of the light-sensitive sodium current was thought to be calcium. A classical calcium hypothesis was postulated by Hagins:[118] photoexcitation of rhodopsin leads to the release of calcium ions from the inside of the disks into the cytoplasm, followed by diffusion toward the external membrane where it interacts with the sodium ions. However, the observation of a modulation of cyclic nucleotide

concentration in the rod on illumination indicated cGMP might be involved in visual transduction.[119-121] Recently, it has been found that the addition of cyclic GMP to the cytosolic side of the excited patch of plasma membrane opens the sodium channels, whereas calcium ion are totally ineffective. Moreover, the calcium ions close the sodium channels more slowly than light does.[122,123] This solid evidence strongly supports the idea that cyclic GMP controls the sodium channels in the plasma membrane during visual transduction.

Second, light absorption of visual pigments initiates the photoisomerization of the retinal chromophore tightly bound to rhodopsin, accompanied by a series of conformational changes in the protein and eventually generating all-trans retinal and protein. As mentioned above, the photointermediates metarhodopsin II physiologically identified with photolyzed rhodopsin Rh* is able to activate the visual G-protein, or transducin peripherally bound to the protein membrane, via a catalyzed exchange of Gt-bound GDP for GTP on the Gα subunit, and dissociation of Gα from Gαβν (a complex of three subunits, α, ß and ν of Gt).[124,125] The active form of Gt effects the removal the inhibitory ν subunits from the inactive PDEαβν (a complex form of phosphodiesterase of the rod outer segment) activating the enzyme. This results in hyperpolarization of the rod cell, [126,127] and the visual stimulus is transferred from rhodopsin to the rod cell plasma membrane sodium channels, c-GMP is rapidly hydrolyzed to GMP causing closure of the

sodium channels (see Figure 9.), resulting in a nerve impulse and visual transduction. The activated Metarhodopsin II is eventually deactivated by serine and threonine residue phosphorylation by ATP and rhodopsin kinase at the carboxyl terminal. The inactive form of rhodopsin is then dephosphorylated by phosphatase and all-trans retinal is finally released from the protein.[77]

The Structure of Rhodopsin

Rhodopsin is the photoreceptor protein of the rod cells in the vertebrate retina. It is located on a regularly stacked array of disk membranes in the rod outer segment. It is an integral membrane protein consisting of hydrophilic domains linked by seven helices which span the disk membrane, and is converted to a physiologically active species by photo absorption. Its photolyzed form accomplishes its signal transduction function by binding and activating a peripheral guanine nucleotide binding regulatory protein Gt: visual G-protein in vertebrate retinal rod outer segments. The primary structure of rhodopsin has been determined, and confirmed by sequencing both the DNA and the gene.[128] Although the primary structure of the protein is vital as a construction template, the secondary structure and its three dimensional organization may have important effects on the visual pigment function and spectra. Figure 10 shows a schematic structure of vertebrate rhodopsin and Figure 11 shows more detail regarding amino acid arrangement, location of

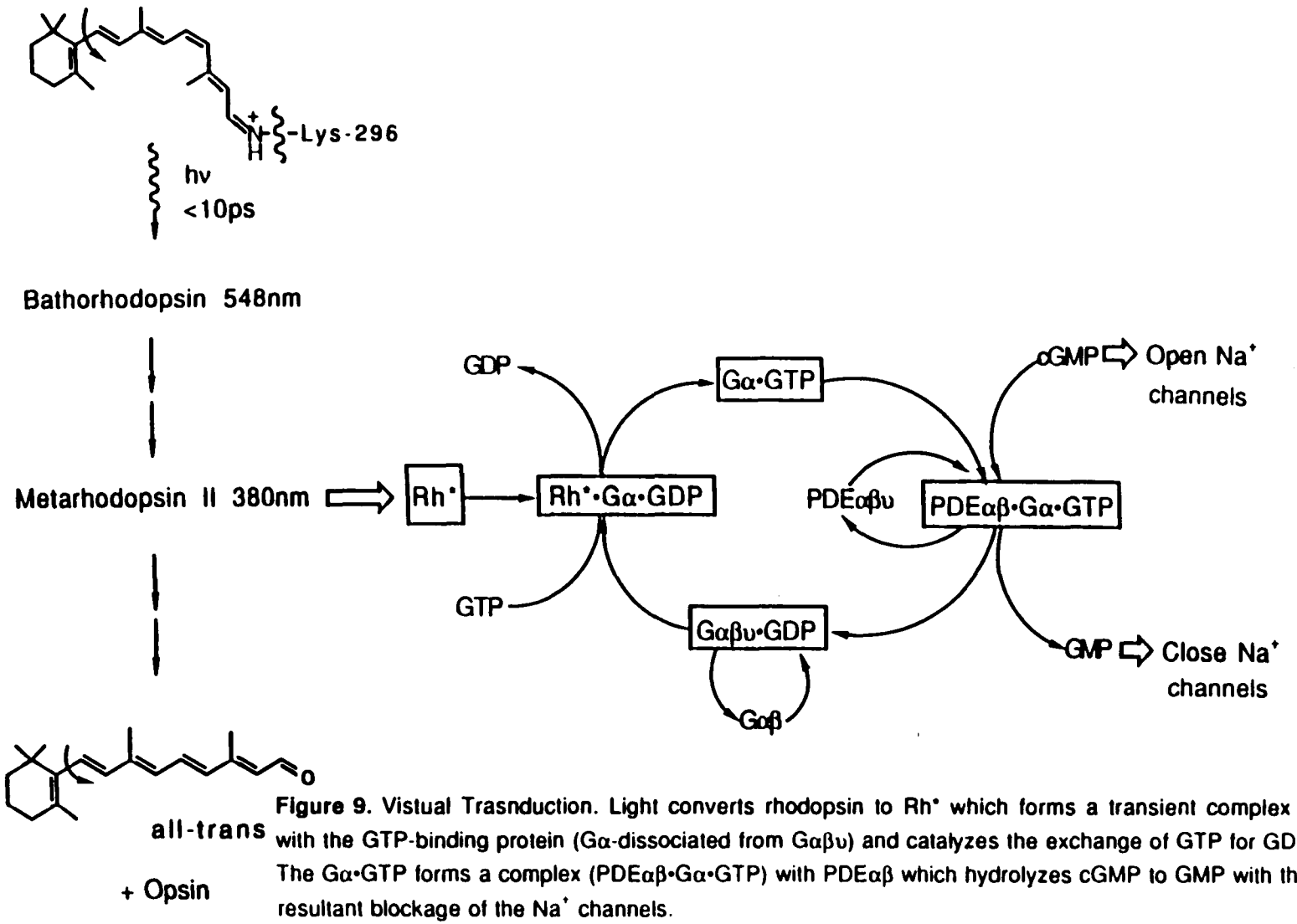

Figure 9. Vistual Trasnduction. Light converts rhodopsin to Rh* which forms a transient complex with the GTP-binding protein (Gα-dissociated from Gαβυ) and catalyzes the exchange of GTP for GDP. The Gα·GTP forms a complex (PDEαβ·Gα·GTP) with PDEαβ which hydrolyzes cGMP to GMP with the resultant blockage of the Na^+ channels.

charged amino acids and their charges. It exhibits even slightly bent transmembrane helices with a retinal moiety oriented perpendicular to the helix axis in a "basket" of bent helices. The bovine sequence suggests a strongly asymmetric charge distribution across the membrane with a positive charge on the cytoplasmic surface due to the protein and a negative charge on the lipid.[129-131] Rhodopsin has two short oligosaccharide chains, consisting of mannose and N-acetylglucosamine, which protrude into the aqueous region.[132] The carbohydrates are located at two sites, Asn-2 and Asn-15, in the amino-terminal region of the protein facing the intradiskal surface.[133] Recent data indicates that hclix 7, which contains the 11-cis retinal linkage, helix 1 and helix 4 contain significant distortions from the normal α-helical backbone.[134] Enzymatic proteolysis of rhodopsin shows that its carboxyl terminus is in contact with the cytoplasm and is rich in hydrophilic amino acids: it contains seven serine and threonine residues.[135,136] The seven hydrophobic membrane segments of rhodopsin span the lipid core of the lipid bilayer membrane, and are interconnected by three hydrophilic loops on both sides of the membrane boundaries. The retinal chromophore is bound to lysine-296 in the seventh helix via a protonated Schiff base and is at an angle of approximately 16 ° with the plane of the membrane, based on CD measurements.[137] The resultant bathochromic shift of rhodopsin from its isolated chromophore can be explained by the external point charge model proposed by the Nakanishi group. A three-dimensional structural

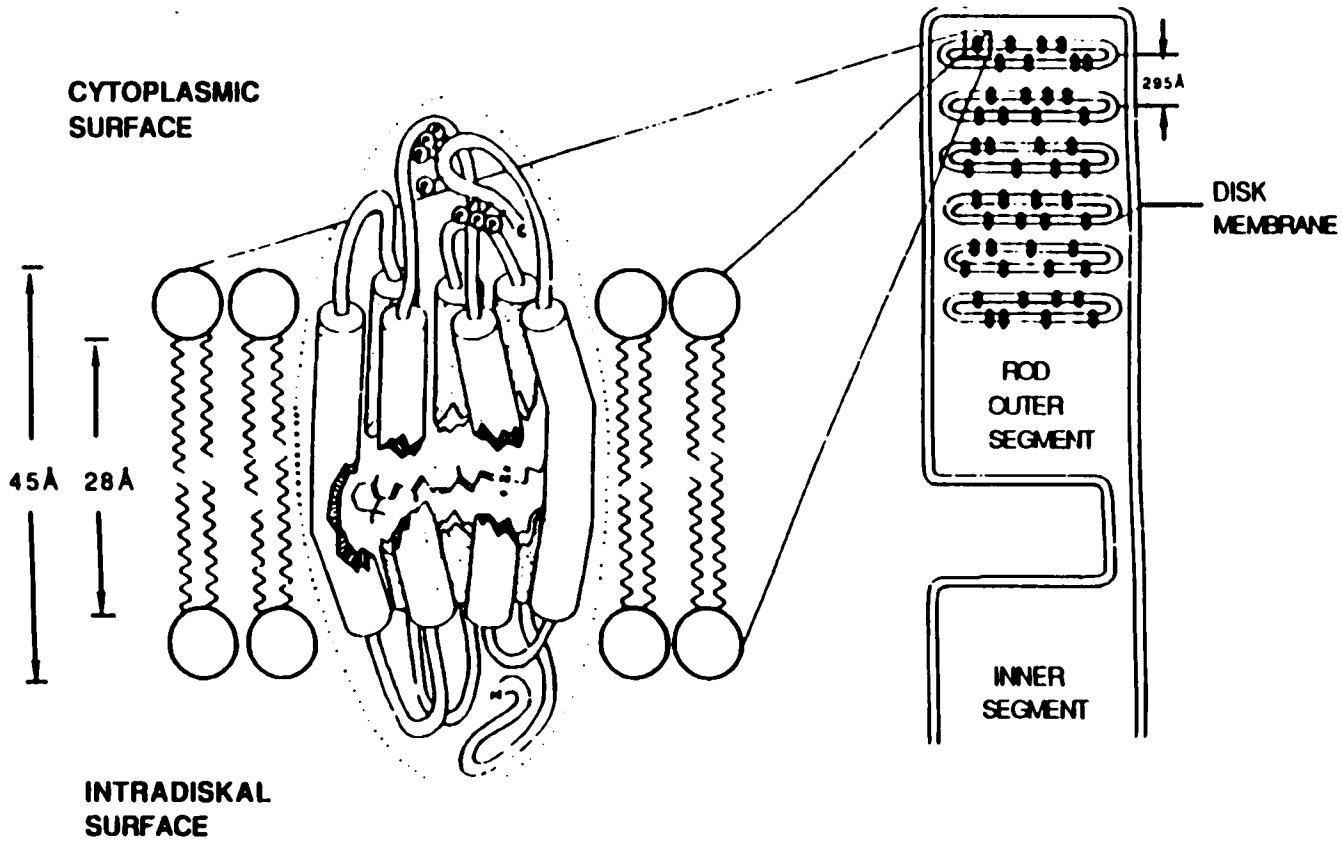

Figure 10. Diagram of a cross-section of the rod outer segment. On the left, a schematic model of the structure of rhodopsin is shown. Rhodopsin is represented as an elongated bundle of seven irregular helices embedded in the lipid bilayer, and the 11-cis-retinal binding site is oriented nearly parallel to the membrane plane. From E. A. Dratz & P. A. Hargave; Trends Biochem. Sci. **1983**, 8, 128-131.

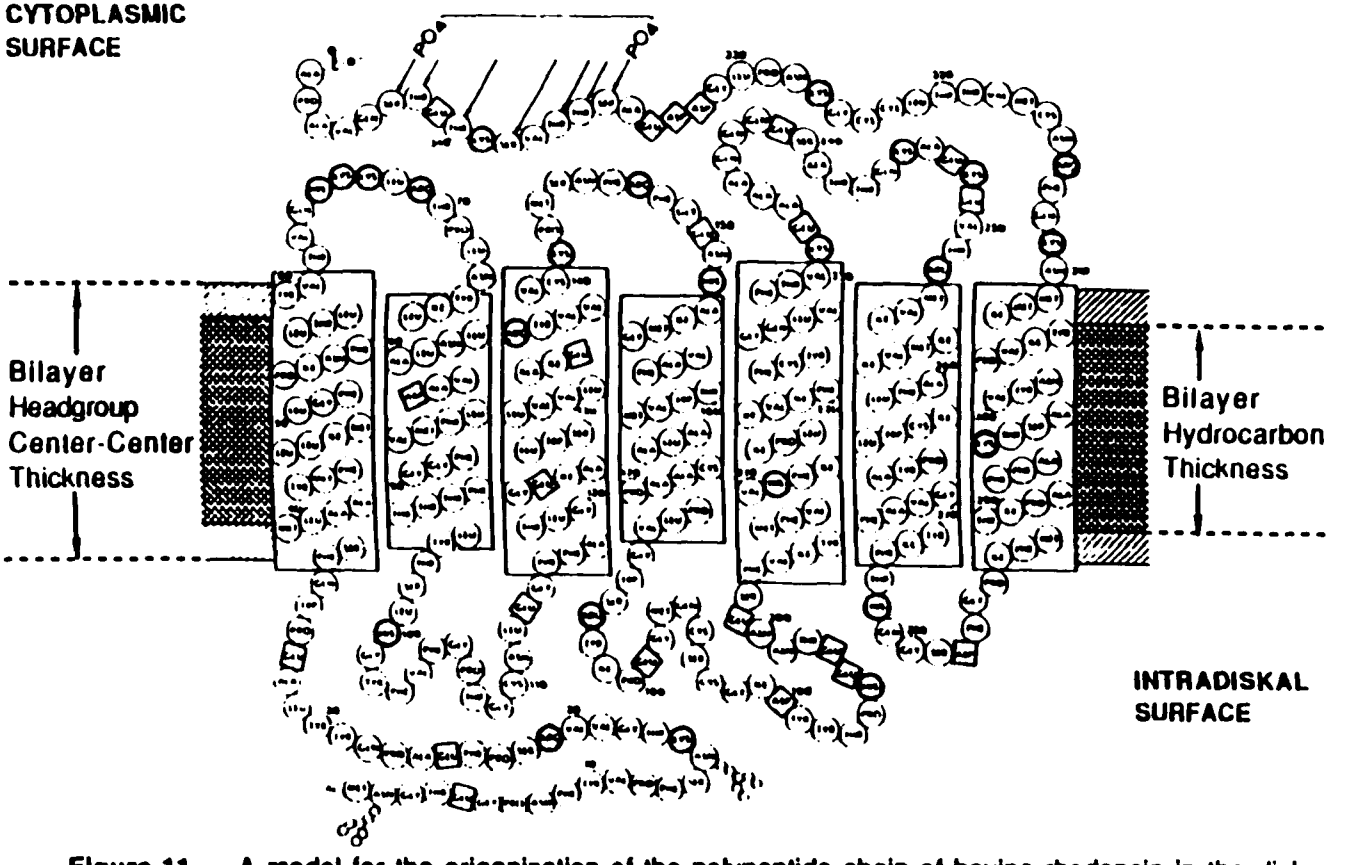

Figure 11. A model for the organization of the polypeptide chain of bovine rhodopsin in the disk membrane. The carboxyl terminus is exposed to the rod cell cytoplasm. Amino acids with potentially positively charged side are shown as outlined shaded circles, and amino acids with potentially negatively charged side chains are shown as shaded squares. Carbohydrates are indicated by the strings of smaller circles near the amino terminal end. From E. A. Dratz & P. A. Hargrave; *Trends Biochem. Sci.* **1983**, *8*, 128-131.

representation of the protein has to be generally based on the known low-resolution electron density map of bacteriorhodopsin, since neutron diffraction or electron microscopy data for the tertiary structure of rhodopsin has not been available. A three-dimensional model for ovine rhodopsin has been established by Findlay et al,[138,139] in which the region of the cytoplasmic loops 3-4 and 5-6 may be involved in binding and activating the G-protein in the cytoplasmic domain of the disk.

III. The Characteristics of Bacteriorhodospin

Halobacterium halolium, a bacterium, lives in salty, sunny areas and sometimes can survive even in hot places such as saturated salt solutions having maximal 20% of the oxygen content of normal seawater. When oxygen is lacking in such brine, respiration (the normal metabolic pathways) can stop and the bacterium produces patches of light sensitive membrane, purple in color,[140] found by G. Wald in 1968. Analysis showed that the purple membrane can occupy more than 50% of the total surface area of the cell and can be isolated after hydroponic lysis of the cell.[141,142] This purple membrane contains a retinal-based integral membrane protein, termed bacteriorhodopsin (bR) due to its similarity with rhodopsin in visual pigments, Mr. 27,000. It functions as a light-driven proton pump, pumping protons from the inside to the outside of the cell, creating an electrochemical gradient. A proton translocating ATPase uses this thermodynamic potential to synthesize ATP.[143]

The Properties of Bacteriorhodopsin

Bacteriorhodopsin constitutes 75% of the total weight of the purple membrane, the remainder are phospholipids.[144] Like the visual pigments, at the molecular level bacteriorhodopsin contains one retinal molecule per protein molecule (apoprotein opsin) and this is linked as a protonated Schiff base to

the e-amino group of lysine residue, Lys-216.[145] The opsin consists of a single polypeptide chain [146] containing a continuum of seven trans membrane α-helices (see Figure 1.) each of which spans the membrane and is largely embedded in it, showed by an 7 Å-resolution electron density map of bacteriorhodopsin using an electron diffraction technique.[147] The retinal bound in the bacteriorhodopsin is present only in either the all-trans or 13-cis isomer configuration.[148,149] Two types of bacteriorhodopsin, dark adapted (bR^{DA}) and light adapted (bR^{LA}), absorb at maxima 560 nm and 570 nm respectively (see Figure 2.). The chromophore of bR^{LA} is the all-trans isomer, while that of bR^{DA} is a mixture of 13-cis and all-trans isomer with a ratio of one-to-one.

Bacteriorhodopsin from the light adapted form shows maximum absorption bands at 400 nm (minor) and 570 nm (major). The chromophore of the adjacent molecules interact asymmetrically and demonstrate circular dichroism bands (see Figure 3.) due to exciton splitting. The ultraviolet circular dichroism of membrane suspensions indicates that 70-80% of the conformation of bacteriorhodopsin is α-helical.

The Photocycle of Bacteriorhodopsin

Light absorption by the retinal moiety (bR^{LA}) in the pigment initiates isomerization about the C_{13}-C_{14} double bond of the retinal chromophore to the 13-cis isomer and produces a primary photoproduct. This event is called the primary event [150] and unlike that of the visual pigment, starts the

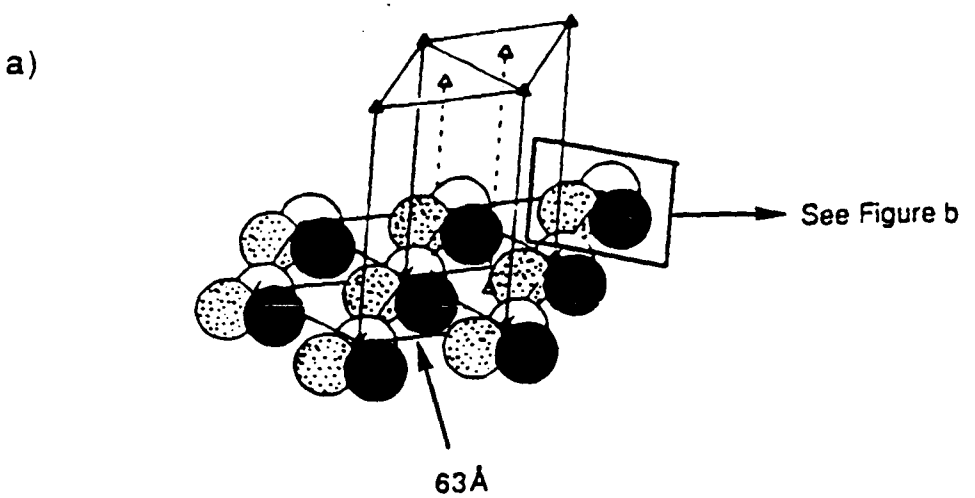

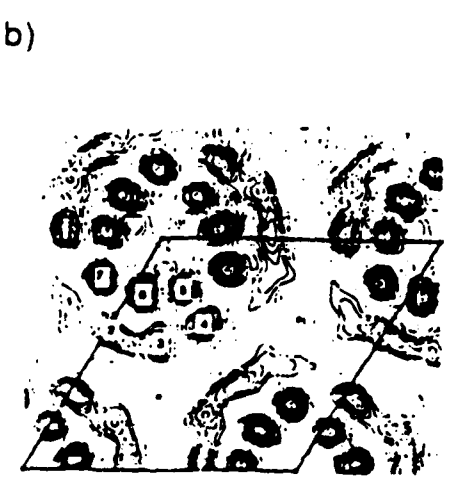

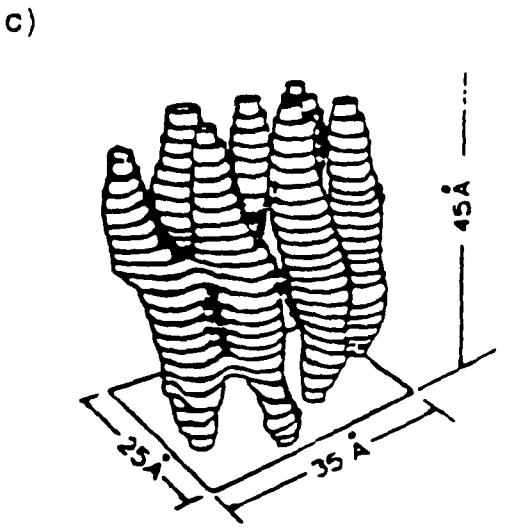

Figure 1. a) Hexagonal arrangement of bacteiorhodopsin trimer;
b) Electron-density contour map of a trimolecular bR unite;
c) Arrangement of α-helical columns in bR.
From H. Shichi; In "*Biochemistry of Vision.*" 1983. Academic Press.

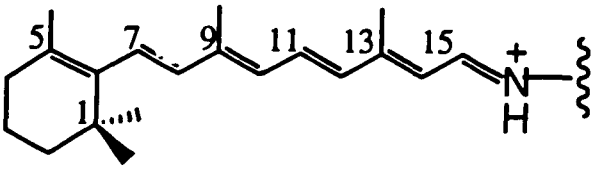

bR^{LA} : λmax=570nm all-trans

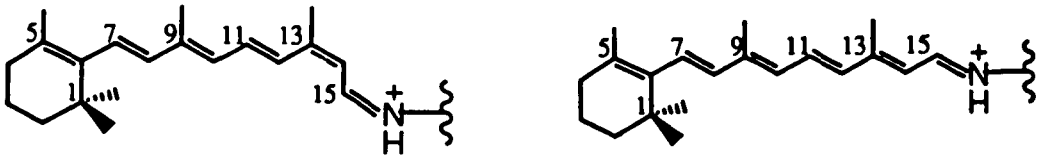

bR^{DA} : λmax=560nm all-trans : 13-cis = 1:1

Figure 2. The chemical structures of retinal moieties of light-adapted (LA) and dark-adapted (DA) bacteriorhodopsin.

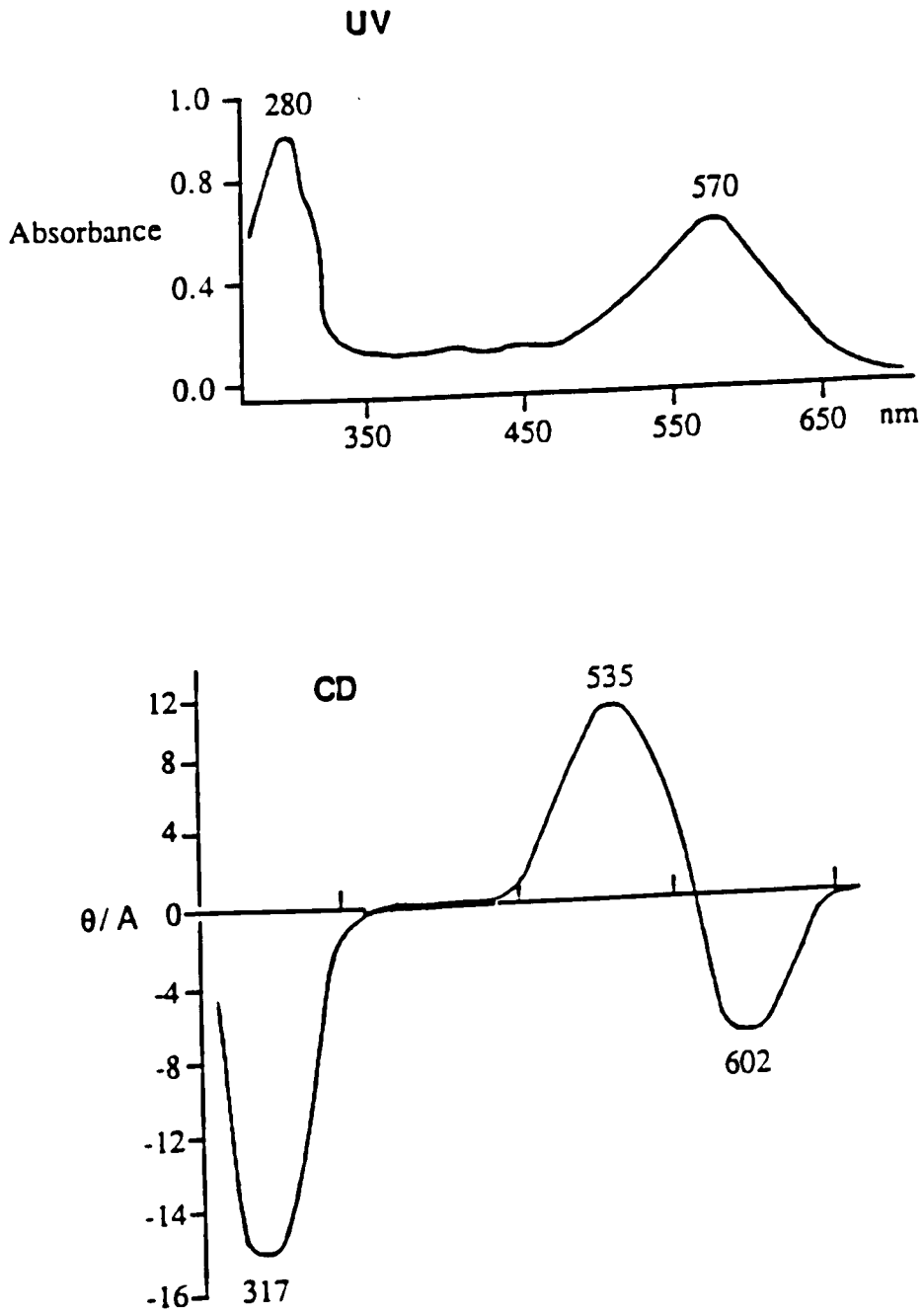

Figure 3. The UV and CD spectra of bacteriorhodopsin. From T. G. Ebery, B. Becher, B. Mao & P. Kilbride; *J. Mol. Biol.* **1977**, *112*, 377.

photocyclic process (not bleaching), following formation of several spectroscopically different intermediates then returns to the ground state in about 10 ms (see Figure 4.). This is associated with proton translocation from the inside to the outside of the cell, termed proton pumping.[151-153] These photointermediates formed from the photoreaction of bacteriorhodopsin have been intensively studied since the 1970's.[152,154] Since then a large number of different schemes have been proposed.[155-160] The photochemical reaction thermal decay scheme is approximately presented for this photocycle: bR → K_{625} → L_{550} → M_{412} → N_{520} → O_{640} → bR. The letters denote the successive intermediate states and the numbers indicate the estimated absorption maxima. In the pioneering work of Stoeckenius et al,[161] the main set of intermediates which were trapped at low temperature or observed kinetically at room temperature have been identified. They also indicated, further proven by Konyama et al,[162] that in the light, bR translocates protons across the cell membrane and generates an electric potential and a pH gradient which can be as large as 4 pH units. Preilluminated bR (bR^{LA}) contains only all-trans retinal; but in the dark, an equilibrium between the 13-cis and all trans isomers is slowly established in a one to one ratio. It is generally believed that in the first part of the photocycle, the all-trans-retinal chromophore is isomerized to a distorted 13-cis form and Schiff base is deprotonated and a proton is released to the extracellular medium. In the second part, a proton is taken up from the cytoplasm and the Schiff base is reprotonated and the retinal returns to

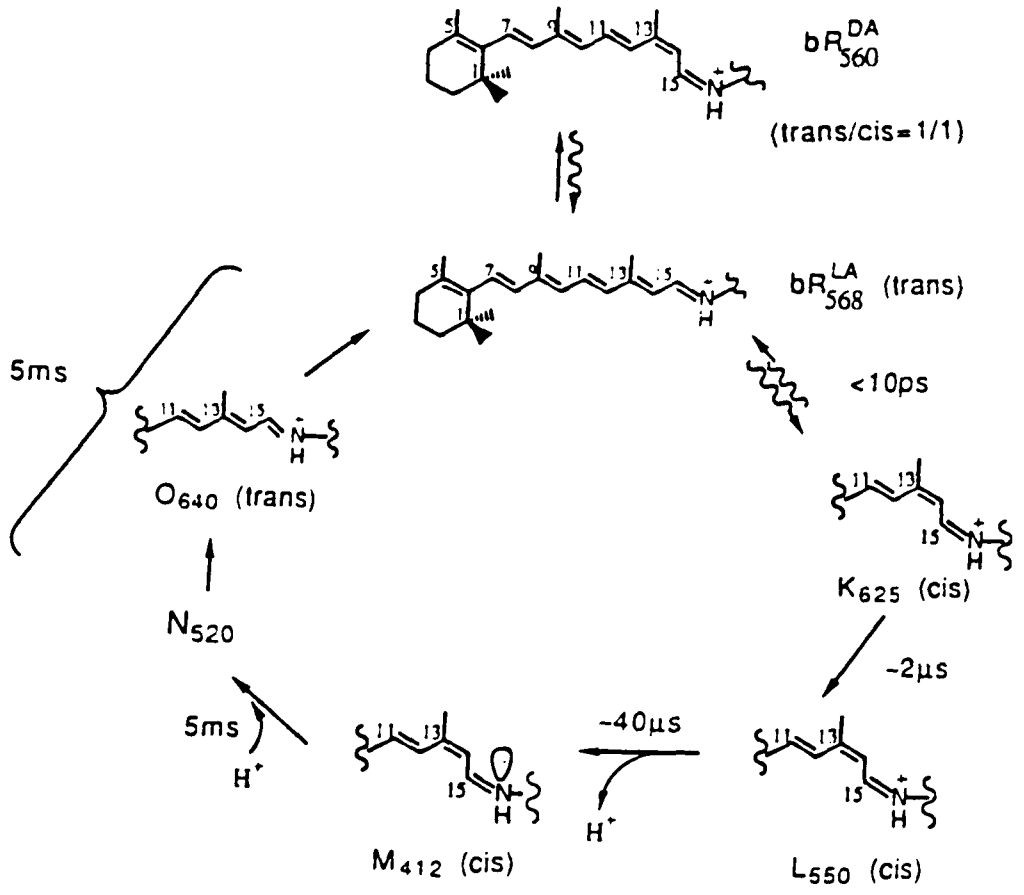

Figure 4. The photocycle of bacteriorhodopsin. LA and DA denote light-adapted and dark-adapted, trans and cis in parentheses refer to the C-13 configuration, and wavy and straight arrow indicate photochemical and thermal transformation. From S. O. Smith, A. B. Myers, J. A. Pardoen, C. Winkel, P. P. J. Mulder, J. Lugtenburger & R. A. Mathies; *Proc. Natl. Acad. Sci.; USA* **1984**, *81*, 0255-2059.

the all-trans configuration. From optical and electric measurements, it has been shown that one proton is translocated per cycle, making it very likely that the Schiff base proton is directly involved in the proton transport.[163-166] R. R. Birge et al [167,168] showed that nearly 16 Kcal/mole enthalpy energy is stored in the primary photointermediate, sufficient to pump two protons per photocycle. Recently, however, they [169] recalculated the energy based on the forward (Φ_1) and reverse (Φ_2) quantum yields associated with the bR = K photoreaction: $\Phi_1 = 0.65 \pm 0.05$ and $\Phi_2 = 0.95 \pm 0.05$,[170] giving 11.6 ± 3.4 Kcal/mole of energy storage in the primary photochemical event, not sufficient to pump two protons.

Vibrational spectroscopy studies [171-174] have shown that after light absorption, the retinylidene chromophore undergoes an isomerization from all-trans to a distorted 13-cis configuration during the $bR_{568} \rightarrow K_{625}$ transition, the only light-driven transition, comparable to the bathorhodopsin transition in the rhodopsin bleaching process. It is generally believed that in the K_{625} transition, the Schiff base proton is translated across the retinal binding site to a new protein environment and some enthalpy is stored. The following thermal steps use this energy for the proton transport. In the subsequent $K_{625} \rightarrow L_{550}$ step, the retinal relaxes to the planar cis structure. In the $L_{550} \rightarrow M_{412}$ transition, the Schiff base proton is released. The M_{412} photointermediate is the only one which is not protonated in the photocycle. The crucial proton transport step is believed to occur at the transiently deprotonated Schiff

base,[175,176] termed a crucial conformational switch, at or after the formation of M_{412} and the proton is first released towards the outside of the cell into a proton pathway in which the carboxylic group of the residue in the bacteriorhodopsin serves as a proton acceptor. Therefore, M_{412} , the most blue-shifted and solely deprotonated species in the bR photocycle, is generally believed to be the photoactivated form of the protein, which directly triggers proton translocation from the cytoplasm to the external medium in the purple membrane, comparable to Meta II, the photoactivated form of rhodopsin in visual bleaching process. In kinetic resonance Raman studies of bacteriorhodopsin, Diller and Stockburger found that L_{550} decays with two different time constants at 23 °C,[177] one is 60 μs, in which a proton is released from the chromophore; the other is 220 μs, in which the chemical structure of this new intermediate is only slightly different from that of L_{550}. This observation led to a two-cycle mechanism starting from two different states of bacteriorhodopsin. The Schiff base is reprotonated in the $M_{412} \rightarrow N_{520}$ step from the opposite side through a proton pathway. Two M states (same absorption) and an irreversible reaction between them were found in a pH 7 phosphate buffer solution in the presence of 100 mM NaCl, by Varo and Lanyi,[178] and recently the M intermediate was kinetically and spectroscopically resolved into two sequential substrates: M_1 and M_2.[179] Moreover, upon thermodynamic analysis they found [180,181] a large entropy decrease resulting from the irreversible reaction of M_1 to M_2, which suggested

that a protein conformational change occurs in this step. They believe that the $M_1 \rightarrow M_2$ transition is the switch step in the photocycle and the irreversibility of the reaction provides a large free energy barrier to ensure the proton transfer. In the $N_{520} \rightarrow O_{640}$ step, cis-trans isomerization of the retinal occurs and finally the protein relaxes to its initial state. According to these results, proton release and uptake by the Schiff base occur on different sides, and protein conformational changes during the photocycle are very important for proton pumping: M formation leads to a rearrangement of the group near the Schiff base, providing a mechanism for deprotonation and reprotonation of the Schiff base from different sides. This was further proven very recently by FTIR difference spectroscopy studies of the bacteriorhodopsin photoreaction.[182]

Unraveling the bacteriorhodopsin mechanism not only requires elucidation of structural changes in the retinal moiety, but also in the protein moiety, and for this FTIR difference spectroscopy provides a powerful method.[183] Rothschild et al [184] inferred the first FTIR difference measurement on bacteriorhodopsin which implicated protonation changes in a carboxyl residue during the bR photocycle. Subsequent studies [185-187] indicated that more than one residue was involved in the photocycle. Eisenstein et al [188] demonstrated that all of the residues involved are Asp rather than Glu by using selective isotope labeling: [4-^{13}C]Asp and [5-^{13}C]Glu coupled with FTIR difference spectroscopy. Of the nine Asp residues in bacteriorhodopsin, only

four: Asp-85, 96, 115 and 212 are thought to be buried in the bilayer.[189,190] Evidence [191] from individual aspartic acid substitutions by Asn and /or Glu recently obtained showed for the first time that Asp-85, 96 and 212 are involved in a proton-conductance mechanism. Mutations at Asp-115 were also found to affect proton-pumping activity. The projection model of the protein given by these authors (see Figure 5.), which positions the helices in the contours of the electron diffraction map of bR based on diffraction, fluorescence energy transfer and mutagenesis,[192] attempts to show rough spatial interrelationships between the amino acids relevant to proton translocation. Several questions remain: where does proton translocation begin and where does it end, how does the proton arrive at this site and which aspartic acid residue is the first proton acceptor if the proton translocation begins at the Schiff base. Braiman et al [193] derived a model for the proton pumping mechanism from FTIR difference spectra of the bR → K, bR → L and bR → M (see Figure 6.) photoreactions using of bR mutants in which Asp-85, 96, 115 and 212 were replaced by Asn and Glu, as well as previous work.[194,195] The model can explain almost all of the carboxylic acid bands observed in the FTIR difference spectra of bR with its K, L and M photoproducts (see Table). In this model, the connectivity of the proton path is cytoplasm ⇒ Asp-96 ⇒ Asp-212 ⇒ retinal-lysine Schiff base ⇒ Asp-85 ⇒ external medium. However, the Asp-115 residue is believed not to change its protonation state during the photocycle but only to change an interaction

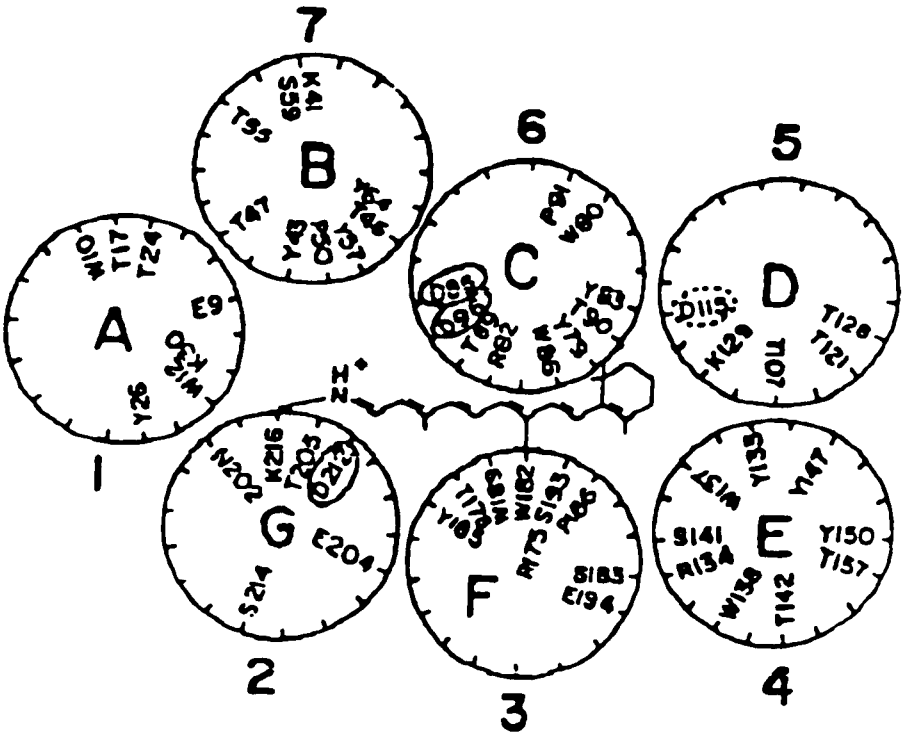

Figure 5. A helical wheel projection map for bacteriorhodopsin. Asp-85, Asp-96, and Asp-212 in solid ovals denote strong effect in proton pumping. From T. Mogi, L. J. Stern, T. Marti, B. H. Chao & H. G. Khorana; *Proc. Natl. Acad Sci.; USA* **1988**, *85*, 4148-4152.

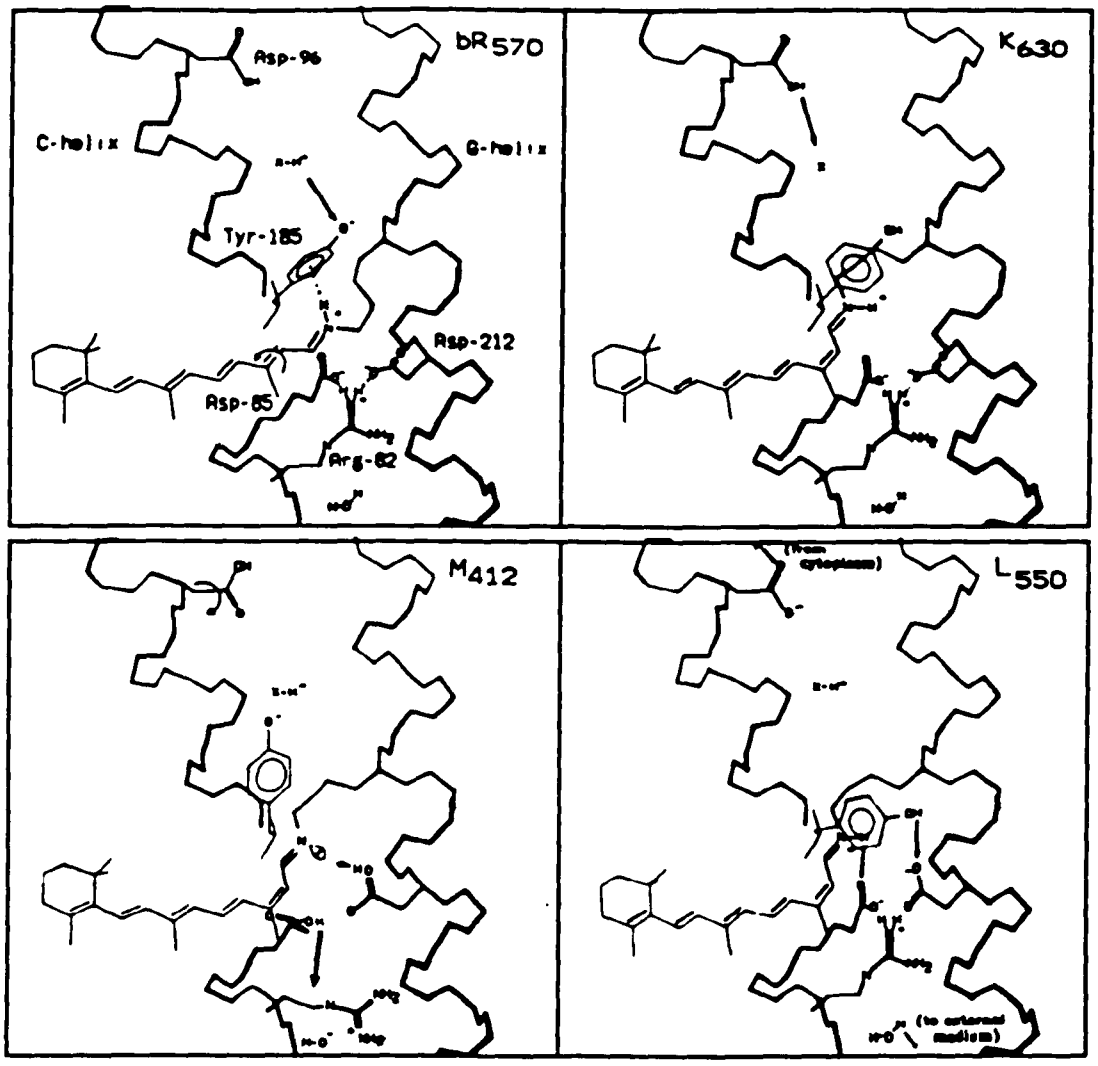

	bR	K	L	M
ASP-85	COO⁻	COO⁻	COO⁻	COOH(1761)
ASP-96	COOH (1742)	COOH	COO⁻⇔COOH(1748)	COO⁻⇔COOH(1748)
ASP-115	COOH	COOH	COOH(1729)	COOH(1729)
ASP-212	COO⁻	COO⁻	COO⁻	COOH(1738)

Figure 6. A hypothetical proton-pumping mechanism for bR. From M. S. Braiman, T. Mogi, T. Marti, L. T. Stern, H. G. Khorana & K. J. Rothschild; *Biochemistry* **1988**, *27*, 8516-8520.

with the chromophore during the photocycle. From the flash-photolysis measurement of the bR photocycle,[196] Otto et al indicated that Asp-96 serves as the internal proton donor to reprotonate the Schiff base of the retinal chromophore in the re-uptake pathway, because Asp-96 is protonated in bR and remains in the protonated form until the decay of the M transition.[197] Also, Asp-96 is positioned nearly 10-12 Å from the Schiff base in the cytoplasmic end of helix C.[198] Gerwert et al [197] further proved that the proton from the Schiff base can be transferred to Asp-85 in the L to M transition, but unlike Asp-85, Asp-96 is not a proton binding site in the proton uptake pathway but is a catalytic binding site in this pathway. They also found recently [199] that aspartic acid residues and the protonated Schiff base are not the only members of the proton translocation chain and two of eleven proline residues are involves in the structural changes during the proton pumping. Otto et al [200] have shown that Asp-85, Asp-212 and Arg-82 are involved in Schiff base deprotonation and Asp-85 functions as a proton acceptor from the protonated Schiff base. In addition, they have shown that proton release and uptake happen on the cytoplasmic side of the membrane. The role of tyrosine residues in the photocycle of bacteriorhodopsin can not be ruled out because the protonation and deprotonation of tyrosine residues were observed by FTIR difference spectroscopic measurements.[201-204] Nevertheless, it is generally now believed that the Asp-85 carboxylate accepts a proton from the retinal Schiff base in

the first part of the bR photocycle and Asp-96 as a proton donor reprotonate the Schiff base in the second part of the bR photocycle.[205-207]

The Structure of Bacteriorhodopsin

Obviously, the primary event in the function of the light-driven proton pump of bacteriorhodopsin is the absorption of light by the retinal chromophore and it is requisite to have a detailed three-dimensional structural model of bacteriorhodopsin with the exact location of the chromophore in the protein for the mechanistic studies of bacteriorhodopsin at a molecular level.

In 1971, Blaurock and Stoeckenius [208] found that the purple membrane consists of a regular arrangement of bacteriorhodopsin trimers which form a two dimensional hexagonal lattice (see Figure 1.), from X-ray diffraction studies. Subsequent electron diffraction and imaging experiments by Henderson and Unwin [209,210] indicated that bacteriorhodopsin has seven x-helical segments roughly perpendicular to the plane of the membrane. Bacteriorhodopsin contains a single polypeptide chain of 248 amino acids whose primary sequence has been determined by Ovchinnikov et al [211] and refined by Khornan et al,[212,213] and confirmed from the DNA sequence.[214] A secondary structure model of bacteriorhodopsin was proposed by Engelman et al,[215] generally consistent with recent data by Khorana. [216] In this model (see Figure 7.), the orientation of the protein in the membrane is such that the

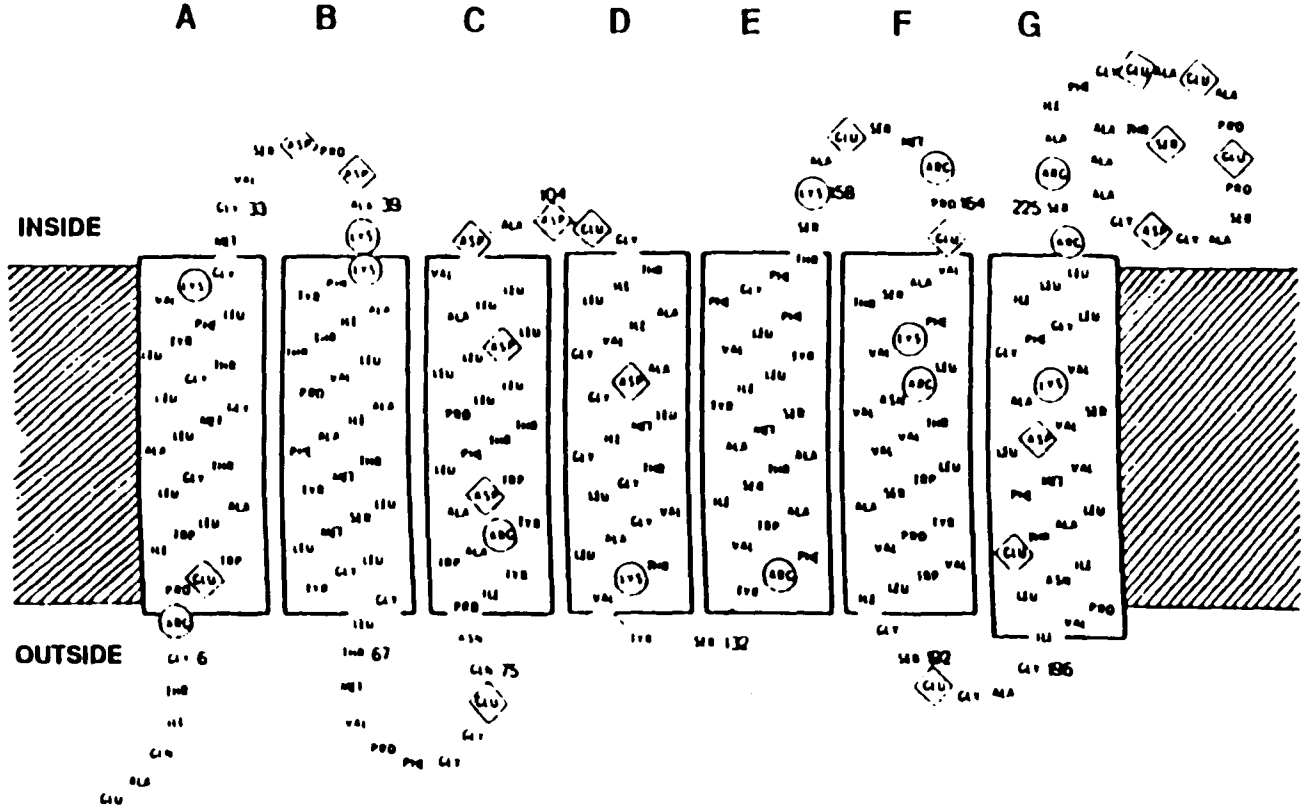

Figure 7. A secondary structure model for bacteriorhodopsin. Basic residues are indicated by circles and acidic residues by squares. The seven helices embedded in the membrane are designated by letters A-G. From D. M. Engelman, R. Henderson, A. D. McLachlan & B. A. Wallace; *Proc. Natl. Acad. Sci. USA* **1980**, *77*, 2023-2027.

carboxyl terminus is at the cytoplasmic side with about 20 amino acid residues protruding into the cytoplasm while the amino terminus is at the outside of the cell membrane with six residues exposed on the external surface of the membrane. However, on the basis of a high-resolution projection image of bR which exhibits a very narrow, high-density feature in the position of "rod one and two", Jap et al [217,218] proposed that "rod one and two" might be transmembrane ß-sheets rather than α-helices also consistent with CD and FTIR data. Since then, several other studies have supported the existence of a ß-structure, with disagreement about the amount.[219-225] More recently, Henderson et al [226] have shown a high-resolution three-dimensional density map of bacteriorhodopsin which rules out the hypothesis of a transmembrane ß-sheet. Earnest et al [227] also demonstrated that the membrane spanning regions of bacteriorhodopsin consist predominantly of α-helical structures, whereas most ß-sheet structures are located in the surface regions, directly accessible to water.

Like the 11-cis retinal in visual pigment, the chromophore in bacteriorhodopsin experiences a large bathochromic shift in binding to the opsin: bR^{DA} absorbs at maximum 560 nm (17857 cm^{-1}) and the maximum of the protonated Schiff base (SBH^+) formed from all-trans retinal and n-butylamine is at 440 nm (22727 cm^{-1}) in MeOH.[228] The termed Opsin Shift (cm^{-1}) has been defined as the difference between the wavelength of maximum absorption of the pigment (cm^{-1}) and that of SBH^+ (cm^{-1}), and is used to

exhibit the overall environmental effect of the protein binding site on the absorption maxima of the pigments. From the same studies on the artificial pigments with the 5,6-, 7,8-, 9,10- and 11,12- dihydro-all-trans retinals as that of 11-cis retinal,[229,230] it was found that the largest opsin shift is obtained from the longest chromophore, all-trans retinal, which is entirely contrary to the visual pigment case: the largest opsin shift from the shortest chromophore: 11,12-dihydro 11-cis retinal. These data led to the double point charge (or external charge) model (see Figure 8.) of bacteriorhodopsin, due to the large spectroscopic red shift resulting from a counterion for the Schiff base nitrogen at a distance of ca. 3 Å, and another negative charge positioned in the vicinity of the b-ionone ring. This model can explain different absorption maxima of the pigment due to through-space electrostatic interactions between charged or polar groups on opsin, or on retinal analogs, and the bound retinal chromophores or protein by changing the positions of the charges. According to calculations of stabilities of the ring-chain conformers,[231,232] most unbound retinal chromophores show a 6-s-cis configuration at ring sites with a C_5-C_6-C_7-C_8 torsional angle Φ^{5678} between -30° and -80° in solution and crystal. On the other hand, on the basis of the analyses of ^{13}C-NMR data in solid-state studies of bacteriorhodopsin,[233] Harbison et al indicates that protein-bound retinal chromophores can exist in the 6-s-trans configuration with Φ^{5678} = 180°: a planar s-trans configuration. Subsequent studies [234] of synthetic 6-s-trans and 6-s-cis locked retinal analogs:

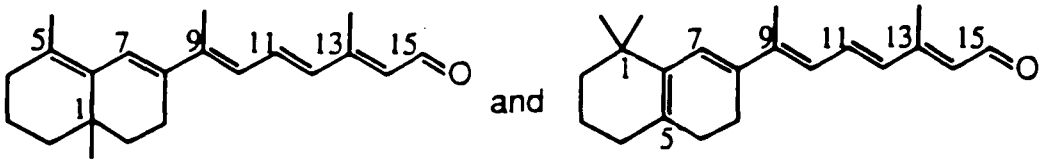

for bacteriorhodopsin, and opsin shift studies [235] of halorhodospin (hR, λ max = 578 nm) and sensoryrhodopsin (sR, λ max = 490 nm), which are family members of homologous membrane proteins, the light-driven chloride ion pump for hR and the phototactic pigment for sR, fully support the idea that bacteriorhodopsin requires the 6-s-trans chromophore configuration. Moreover, a newly revised bR external point charge model (see Figure 9.) has been suggested.[236,237] In this model, the negative charge is positioned adjacent to C_5 of the ß-ionone ring and a positive electrostatic interaction near C_7,[238] coupled with a 6-s-trans isomer of the chromophore. There are three factors which might cause this large opsin shift:[206] 1) the distance between the counter-anion and protonated Schiff base: the longer the distance is, the greater delocalization of the positive charge, resulting in a larger red shift; 2) the planarity of the conjugated system (6-s-trans): the 6-s-trans locked form of bR has 150 cm^{-1} greater opsin shift than the 6-s-cis locked form;[239] 3) the external point charge near the ß-ionone ring.

The retinal chromophore is approximately 15 Å length in the light-adapted state of bacteriorhodopsin (all-trans form including 6-s-trans configuration), and according to the linear dichroism absorption of bacteriorhodopsin: bR_{568}[240] the orientation of the retinal chromophore is an angle of about 20° between the polyene chain and the plane of the

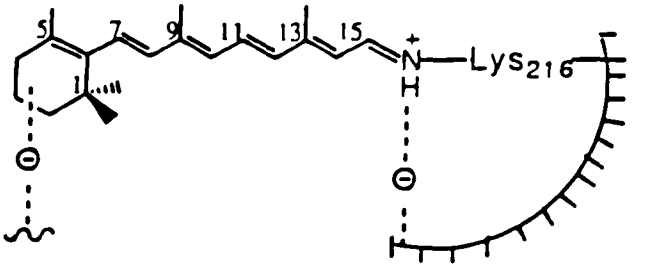

Figure 8. External point charge model for bacteriorhodopsi. From K. Nakanishi, V. Balogh-Nair, M. Arnaboldi, K. Tsujimoto & B. Honig; *J. Am. Chem. Soc.* **1980**, *102*, 7945-7947.

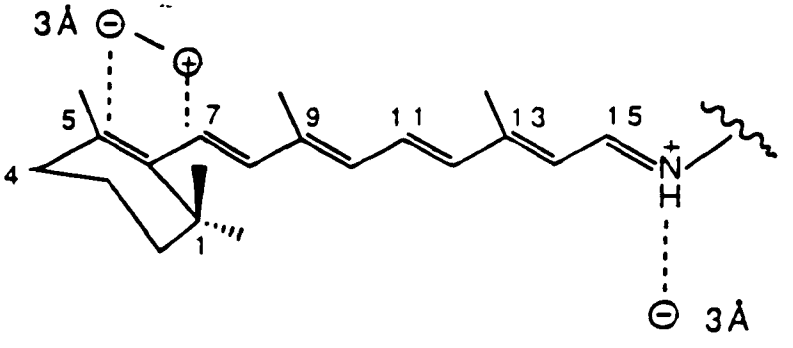

Figure 9. A newly revised external point charge model. From K. Nakanishi; *Pure & Appl. Chem.* **1991**, *63*, 161-170.

membrane. Moreover, the plane of the chromophore itself is almost perpendicular to the membrane, from polarized FTIR measurements.[241-243] However, the tilting direction of the chromophore, whether it is toward the cytoplasmic membrane surface or toward the extracellular membrane surface, has been interpreted differently from different experiments,[244,245] and contradictory results were obtained for the transmembrane depth of the chromophore as well. It is universally acknowledged that the Schiff base of the retinal in bacteriorhodopsin is formed at the amino acid Lys-216, which is roughly in the middle of the hydrophobic stretch of the carboxyl terminal helix G, and forms an electrostatic bond with the carboxyl group of aspartic acid at residue 212, and that it must be located approximately half way between the cytoplasmic and extracellular sides of the protein (see Figure 10.). Recently, by using high-resolution electron cryo-microscopy, Henderson et al[246] efficiently interpreted a bacteriorhodopsin structure map, 3.5 Å in diameter and 10 Å deep, and established the tertiary structure model of bacteriorhodopsin (see Figure 11.) which is currently applied in most other studies of bacteriorhodopsin. In this model, the ß-ionone ring of the retinal chromophore in bacteriorhodopsin is about 5 Å lower with respect to the vertical position of the Schiff base of retinal in the center of the protein and nearer the extracellular surface, leading to a tilting angle of roughly $20^{\circ}(\pm 10^{\circ})$ from the membrane plane.[247-250] In addition, the distance of the retinal ring site from the exterior membrane surface is about 10 Å, further supported by

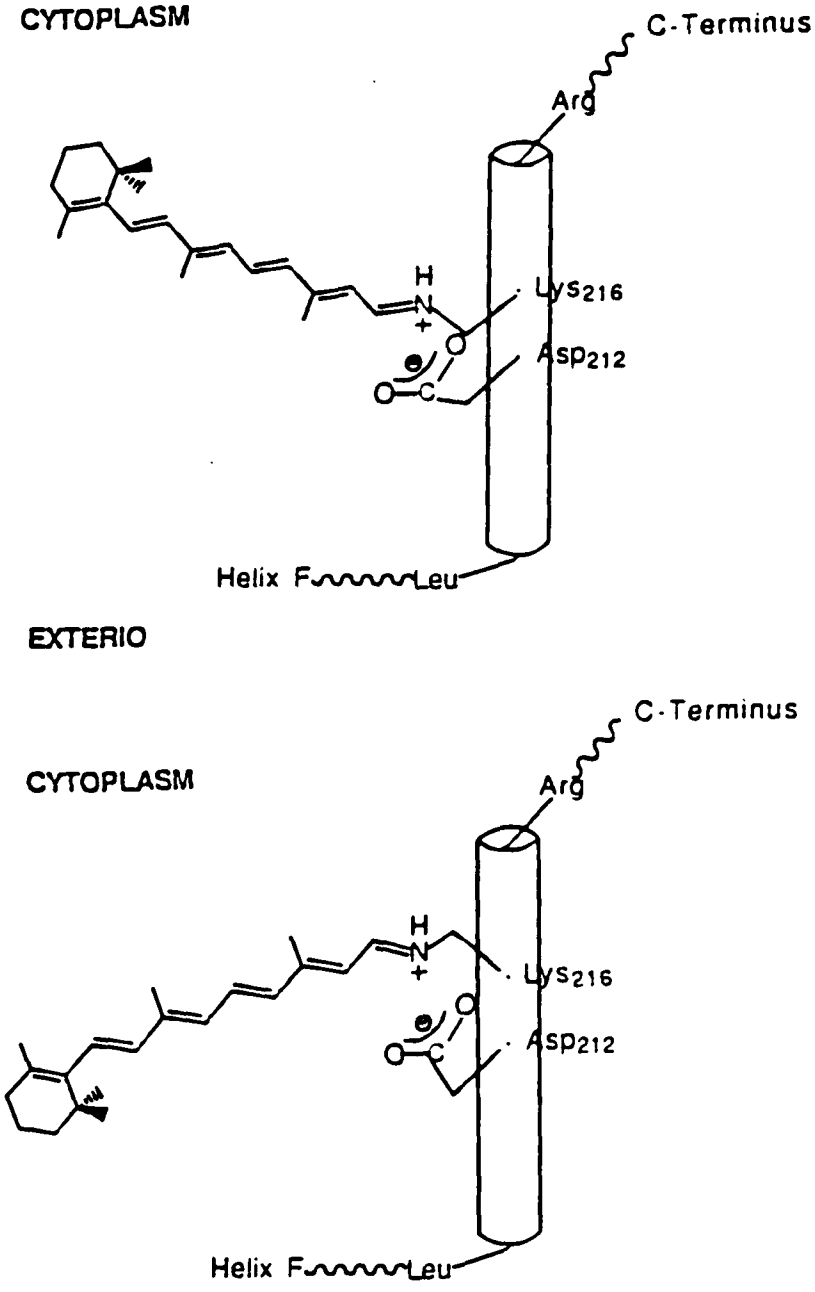

Figure 10. The two conceivable orientations of the Schiff base in bR.

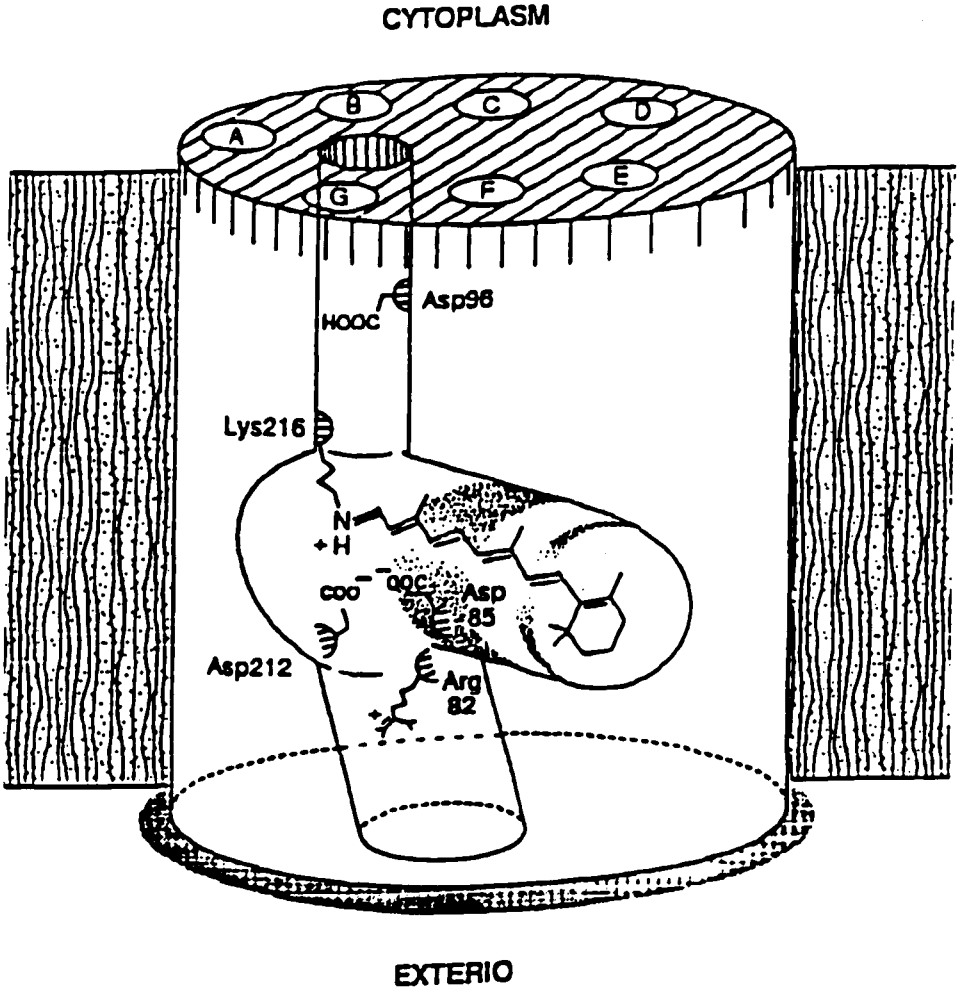

Figure 11. The three dimensional drawing of bR shows the relationship between Asp-85, Asp-96, Asp-212 and Asp-85, and the binding site and orientation of the retinal. From R. Henderson, J. M. Baldwin, T. A. Ceska, F. Zemlin, E. Beckmann & K. H. Downing; *J. Mol. Biol.* **1990**, *213*, 899-929.

Hauss et al [251] from elegant experiments using neutron diffraction measurements of bacteriorhodopsin with selectively deuterated synthetic retinals These studies provide clear indication of that the depth of C-2 of the b-ionone ring to the external surface of the membrane is nearly 10 Å and agree with the orientation of the polyene chain toward the extracellular surface. However, the methyl groups of the retinal moiety in Henderson's map cannot be clearly resolved. They agree with Lin and Mathies [252] that the densities of the methyl groups are upwards, facing the cytoplasmic surface of the membrane. From the linear dichroism data of Vitamin A2 whose chromophore has an extra double bond in the ß-ionone ring,

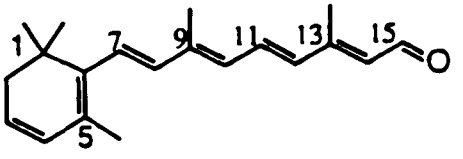

and by using Henderson's density map of bacteriorhodopsin, the methyl group direction is unambiguously indicated. This is in contrast to the results of Ding et al [253] from an entirely different experiment, chemical cross-linking measurement. In addition, from high-resolution ^{13}C-NMR data of biosynthetically labelled [methyl-^{13}C]-Methionine-bR, Seigneuret et al [254] indicated that seven of the nine Methionine residues of bR are located within the membrane-embedded segments. Met-23, Met-56 and Met-60 are found on the hydrophobic surface and Met-20, Met-118, Met-145 and Met-209 in the protein interior. These assignments further supported Henderson's results.[198]

III. Synthetic Analogs of Rhodopsin and Bacteriorhodopsin With Specific Purposes

In summary, retinal proteins in vertebrates and invertebrates comprise rhodopsins: visual pigments which serve as light detectors for the sensory systems, whereas the pigment present in *Halobacterium halobium*, bacteriorhodopsin, functions as a photosynthetic energy source. The retinal chromophores which are contained in both rhodopsin and bacteriorhodopsin are the 11-cis isomer with a linkage to Lys-296, and the all-trans isomer with a linkage to Lys-216 of their respective proteins via a protonated Schiff base. The maximum absorption of bovine rhodopsin is at 500 nm whereas that of light-adapted bacteriorhodopsin is at 568 nm. Upon illumination, they both undergo a series of conformational changes, through a bleaching process for bovine rhodopsin, and a photocycle for bacteriorhodopsin. These photointermediates formed from the bleaching process and the photocycle are responsible for the visual transduction coupled, respectively, with the permeability of the cytoplasmic membrane to sodium ions, and to proton translocation (the proton pumping) coupled with the synthesis of ATP. In order to understand both processes in molecular details, the structures of these photointermediates and the protein itself must be precisely established. However, there may be difficulties in meeting these requirements without knowing the tertiary structures of the proteins. Although extensive physical

measurements and biochemical and biological studies have been done with native pigments, there are still insufficient data to definitively establish the tertiary structures of rhodopsin and bacteriorhodopsin. Also, a great variety of synthetic retinals have been synthesized and bound to bleached proteins (opsins) to form artificial pigments. These include retinal analogs such as hydrogenated, substituted or desubstituted polyenes, more extensive structural modification substituting acyclic and aromatic rings in place of the ß-ionone ring, and isotopically labeled and photoactive (photoaffinity labeling) groups. The great advantage of synthetic analogs lies in the fact that retinal analogs can be designed so as to explain the absorption characteristics of proteins, assign the configurational and conformational characteristics of chromophores at the various intermediate stages of the bleaching process and the photocycle, and explore the proteins regarding structures and functions, which cannot be done with native pigments.[255-258]

Analogs For Bovine Rhodopsin

With additional substitution on the retinal chromophore, such as 11-cis-12-methyl-retinal,[259, 260]

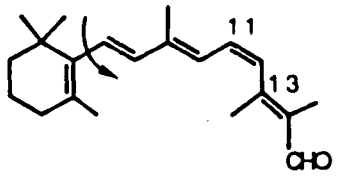

12-s-trans: λmax=338nm
pigment: λmax=502nm

and

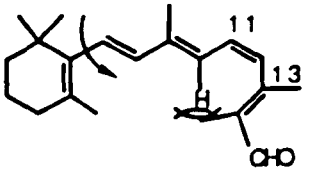

12-s-cis

the polyene can only exit in the 12-s-trans conformation due to hindrance between 10-H and 14-Me in the 12-s-cis form. It also binds to bovine rhodopsin giving a maximum absorption at 280 nm and 502 nm similar to the native chromophore. This suggests that the conformation of 11-cis retinal in rhodopsin must be 12-s-trans. Studies of retinal analogs with substitutions of methyl or ethyl on the polyene chain at the other positions [261-263] show that the chromophore binding site seems to be relatively flexible.

Bond locked retinal analogs such as analog A, B and C,[264-266]

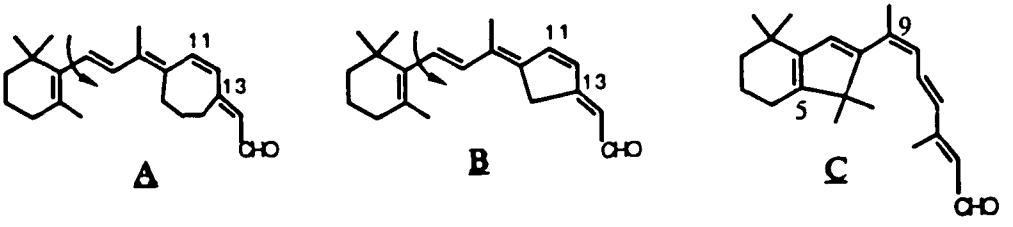

give evidence that the twisted 12-s-trans and the chirally skewed 6-s-cis conformation are present in the native pigments, and the fact that the pigment with the 11-cis locked chromophore is unbleachable supports the implication that the 11-cis to trans photoisomerization is essential for the rhodopsin bleaching process.[267]

Studies of other cis, di-cis and tri-cis analogs indicate that in addition to 13-cis and the all-trans isomers, the 7-cis and 9-cis isomers can form a visual pigment.[268-270] A recent study of 9,13-dicis rhodopsin indicates this dicis retinal reacts with opsin at a slower rate than it isomerizes to 9-cis retinal.[271]

It has been verified from the studies of demethyl-retinal analogs that

5-, 9-, and 13-methyl groups are not necessary for pigment formation,[272-275] and from the studies of the ring-modified retinal analogs, such as analog D, E and F,[276]

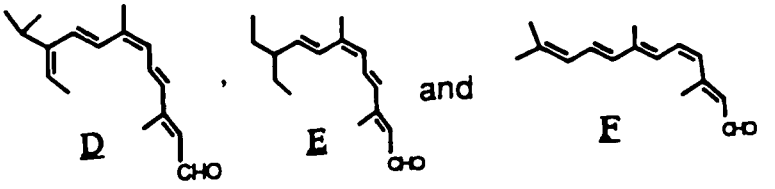

which are bound to opsin, and analog G and H,[277]

G H

which are not able to bind to opsin, that the methyl groups at C-1 and C-5 are important for retinal pigment incubation. Retinal analogs with aromatic rings instead of cyclohexyl rings are also bound to the opsin.[278]

A series of dihydro-retinal analogs, as mentioned above, have been studied by the Nakanishi group [279,280] and led to an external point charge model.

Photoaffinity labelling compounds have been used extensively to investigate the binding site of proteins.[281-283] In the case of rhodopsin, X-ray, neutron and electron diffraction methods can not provide such valuable data because crystallization of rhodopsin is very difficult.[284,285] Therefore, the photoaffinity labelling technique is a particularly valuable tool for the determination of the retinal binding site and clarification of the tertiary structure of the protein. For example, the analog I and J,

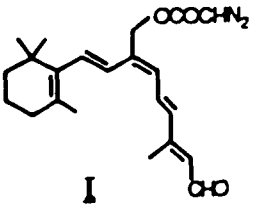

I

and

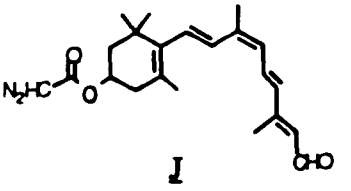

J

have been synthesized and bound to bovine opsin.[286]

Analogs For Bacteriorhodopsin

From the studies of 13-cis and 13-trans locked retinal analogs K and L,

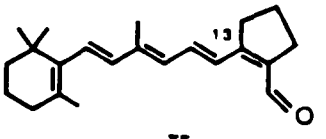

K

and

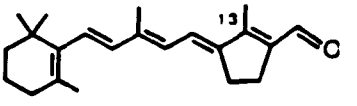

L

it is further apparent that isomerization of C_{13}-cis to C_{13}-trans is essential for the bR photocycle,[287] since no proton translocation upon irradiation of either analog was observed. Also, studies of 6-s-cis and 6-s-trans locked retinal analogs indicated the existence of a 6-s-trans conformation of the retinal moiety in the native protein.[288]

A point charge model to explain the bulk opsin shift of bacteriorhodopsin has been proposed from a study of a series of dihydro retinal analogs, as mentioned before.

The absorption maxima of aromatic bacteriorhodopsin analogs, such as M and N,[289-296] are blue shifted (440 nm to 470 nm), consistent with a point

charge at the ring site.

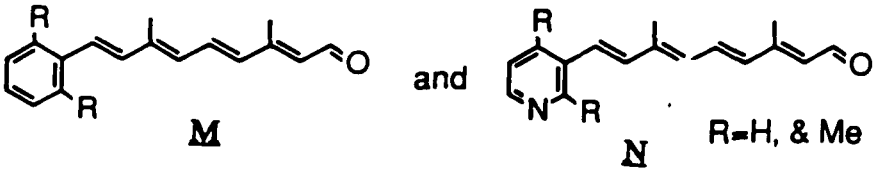

Recently, evidence of the pKa effect on the absorption maxima of the pigment:[297-300]

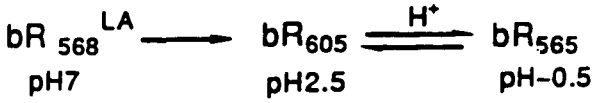

from a study of these two transition forms induced from acidification of the protein combined with a series of artificial bR pigments,[301] gave solid evidence that the formation of bR_{605} is due to changes in polyene-opsin interactions in the vicinity of the Schiff base linkage. On the other hand, the formation of bR_{565} might be associated with changes in retinal-protein interactions in the vicinity of the retinal ring, since no bR_{565} was generated in the pigment analogs bearing major changes in the ring site of the retinal, like:

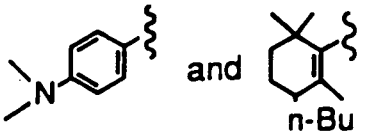

The Specific Aim

Both photoactivated forms of rhodopsin and bacteriorhodopsin: Meta II and M_{412} photointermediates, are generally thought to be very important transition states. Meta II activates visual G-protein (Gt) which lets sodium ion conductance change in the plasma membrane of photoreceptor cells during visual transduction, and M_{412} induces proton shuttling back and forth from inside to outside of the purple membrane coupled with the synthesis of ATP. In order to understand both molecular process understanding the tertiary structures of the proteins, including the ß-ionone ring site have become a more and more attractive and interesting field. Using retinal analogs with photoaffinity labelling groups is a suitable tool for the purpose, not only in the case of the visual pigment, which is difficult to crystalize, but also for bacteriorhodopsin, which gives a two-dimensional crystal lattice. Binding a highly reactive group to the active site of the proteins and using specular scattering along with a labeled atom in the chromophore can enable one to locate the chromophore binding site and to analyze the amino acid residues involved. The process is schematically included below:[302]

1) Synthesis of a suitable retinal analog with a photoactive group,

2) Formation of the pigment analog combined with opsin,

3) Irradiation of the pigment analog to obtain the linked species,

4) Bleaching or CH_2Cl_2 denaturation/extraction to study the binding site and amino acid sequencing.

The probes containing spacer arms with a variable number of carbons are thus designed 1) to determine the length from the ß-ionone ring site to the edge of the membrane, and 2) if successful, to anchor the active sites of the protein with label-bearing spacer arms through cross-linking and 3) to reveal the structural functions of bovine rhodopsin and bacteriorhodopsin at their photoactivated stages.

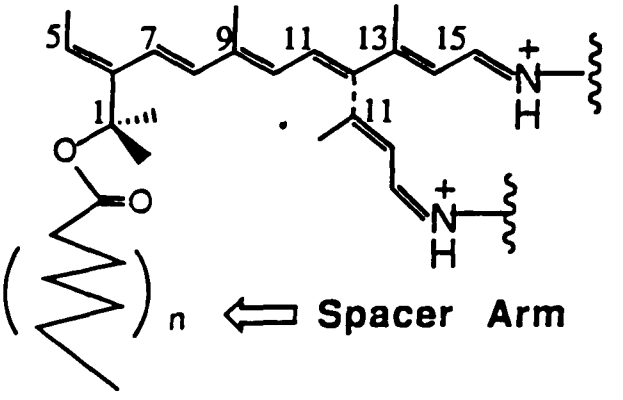
5
7
9
11
13
15
1
11
O
O
n
Spacer Arm

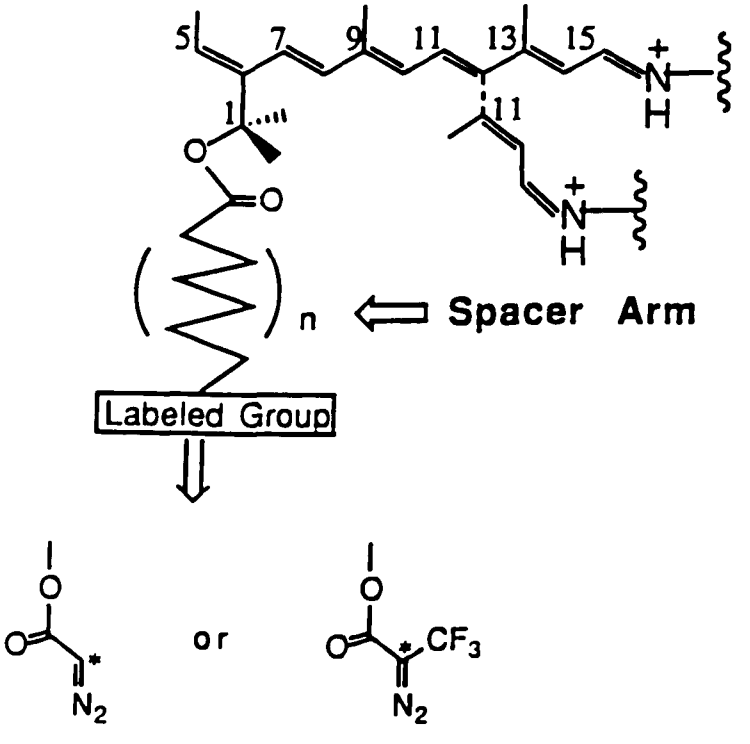
5
7
9
11
13
15
1
11
O
O
n
Spacer Arm
Labeled Group
O
O
N2
or
O
O
CF3
N2

I. Studies in the Syntheses of the Seco-Ring Retinal Analogs with Spacer Arms of Various Numbers of Carbons.

Application of Dehydration Methodology in the Synthesis of the Precursor of the Seco-Ring Retinal analogs.

The process of forming multivinyl compounds from a simple ketone in the syntheses of butenolides, carotenoids, retinals and retinoids has been successful by several approaches.[303] The synthetic route designed to obtain dodecenal 15 is based on the following heuristic sequence of events. The first route, as outlined in Scheme 1, starts with pentanones 5a and 5b,[304] both of which contain the gem-dimethyl group required for the opsin binding, plus a protected tertiary hydroxyl group which is required for introduction of a various length of a carbon chain at the final step through a esterification, and a carbonyl group required for the connection of a conjugated polyene chain.

Scheme 1:

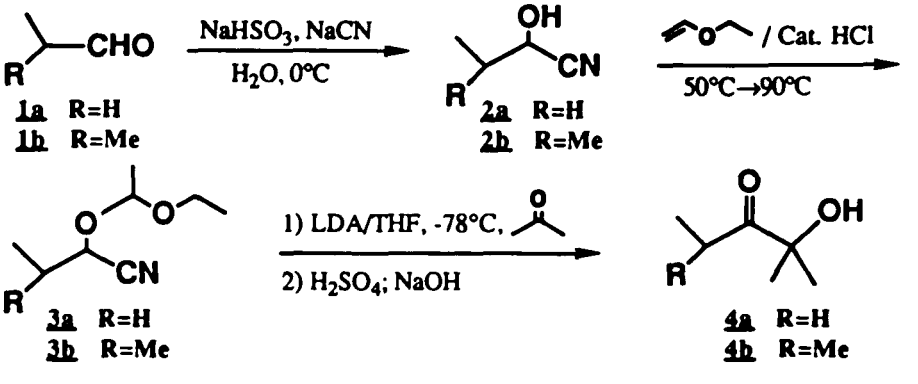

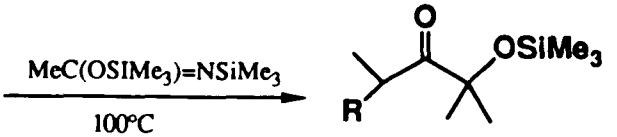

5a R=H
5b R=Me

In addition, condensation of pentanones 5a or 5b with a nine-carbon conjugated polyene chain 12, prepared as indicated in Scheme 2 [1) and 2)],[305] will allow dehydration of a newly formed tertiary hydroxyl group at C-6 in 13a or 13b, to give the desired pentene 14. Finally, stepwise reduction of the triple bond in 14a or 14b to a double bond with lithium aluminum hydride ($LiAlH_4$), oxidation of the primary hydroxyl group to the aldehyde and cleavage of the protective group can be accomplished to give all-trans-pentenal 15a or 15b.

Scheme 2:

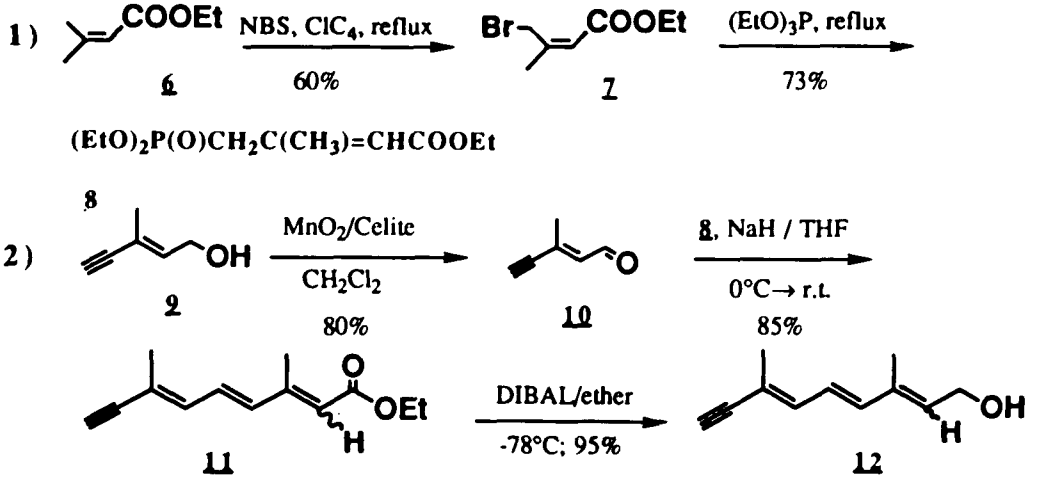

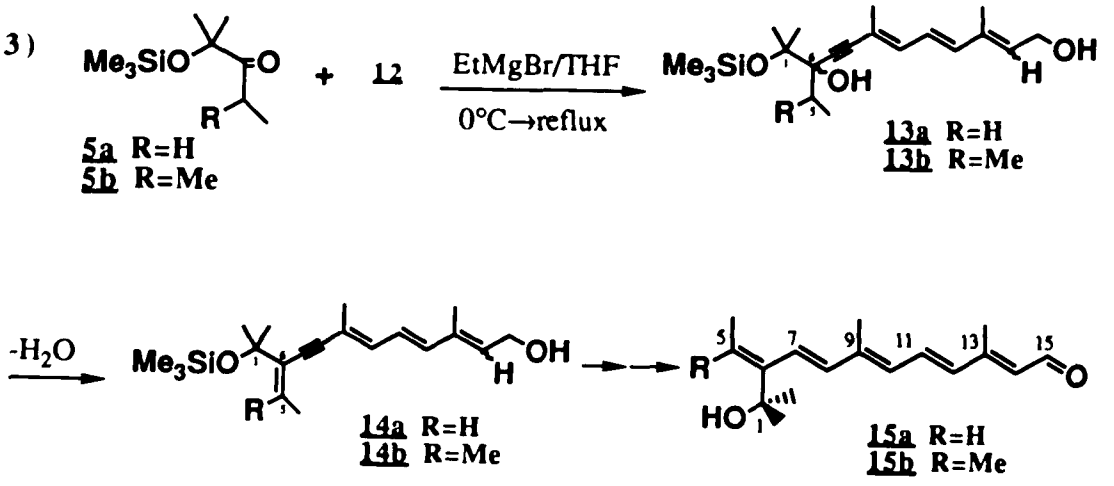

Pentanones 5a and 5b were made by the method described by S. D. Young and co-workers, outlined in Scheme 1. Propionaldehyde or isobutyroaldehyde was treated with an aqueous solution of $NaHSO_3$ and NaCN respectively, followed by a acid-catalyzed reaction with ethyl vinyl ether to give nitrile compound 3. The following aldol addition reaction of nitrile compound 3 with acetone, and subsequent acid-induced hydrolysis of the condensed product and base-induced dehydrocyanation provided α-hydroxy pentanones 4a and 4b. Protection of the tertiary hydroxyl group using N,O-bis (trimethylsilyl) acetamide gave pentanones 5a and 5b. The yield of each step is shown in Table 1.

The stepwise preparation of the nine-carbon polyene chain 12 is illustrated in Scheme 2. In the first step, the bromization of butanoate 6 with N-bromosuccinimide (NBS) in tetrachloromethane (CCl_4) at reflux

Table 1. Yields of Reactions in Scheme 1

Step	R=H (%)	R=Me (%)
a	61	64
b	64	58
c	63	50
d	68	60

temperature and subsequent treatment with triethylphosphite at reflux for three hours afforded a mixture of trans and cis phosphonosenecioate 8 in 60% and 73% distillated yield, respectively.[306] Mild oxidation of commercially available five-carbon-chain enynol 9 with manganese dioxide (MnO_2) superficially absorbed on purified Celite in methylene chloride resulted in the unsaturated aldehyde 10 in 80% of isolated yield in the step 2. This mild and efficient reagent for oxidizing allylic alcohols to conjugated aldehydes was newly developed in our group, and is easily prepared, handled and stored. The Horner-Emmons reaction of aldehyde 10 was accomplished [307-310] by the treatment of the phosphonosenecioate 8 with sodium hydride (NaH) in tetrahydrofuran (THF) in 85% yield (after silica gel column chromatography). The nine-carbon conjugated polyene chain 12 was thus readily obtained by the treatment of the ester 11 with diisobutylaluminium hydride (DIBAL-H) in ether at -78 °C in 95% isolated yield.[311]

Finally it was envisaged that dehydration reaction of the resultant tertiary alcohols 13a or 13b from the condensation reaction in step 3 would be a potentially useful to approach the eleven-carbon side-chain precursor of an acyclic system. In addition, compound 13b having one more methyl group at C-5 compared with compound 13a, could be expected to be more easily dehydrated than compound 13a. [312,313] Nucleophilic addition of a mixture of the anions of 2-trans and 2-cis-3,7,-dimethylnona-2,4,6-trien-8-yn-1-ol 12 (3:1) formed by reaction with EtMgBr to 2,5-dimethylsilyloxypentan-3-one 5b was performed in THF at reflux temperature for five hours. After the isolation by the silica gel chromatography, ^{1}H NMR spectrum showed no trace of the protective group and the yield of the reaction was nearly 40%. The trimetylsiliyl group was thought to be removed during the work-up process (saturated aqueous ammonium chloride.) The resultant diastereomers of triols 16:

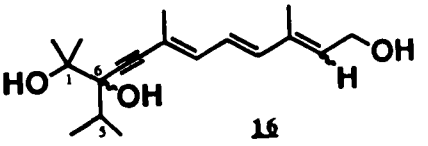

16

were expected to be regioselectively dehydrated with difficulty at C-6 even after the conversion of triols 16 to the corresponding aldehyde 17:

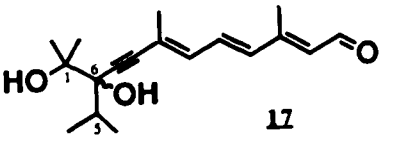

17

though MnO_2/Celite oxidation.

The reaction of 2-methyl-2-(trimethylsilyloxy)pentan-3-one 5a with trienynol 12 was performed in an identical fashion and afforded a similar result in 42% isolated yield

based upon the desilylated product (see Table 2.).

Table 2. EtMgBr-Mediated Coupling Reaction of Pentanons 5 with Nine-Carbon Polyene Chain 12

R	Isolated yield(%)	UV(λmax, in MeOH)
H	42	302
Me	40	304

In addition, the same reactions of pentanones 5a and 56 with the dianion E-3-methylpenta-2-en-4-yn-1-ol 9 were carried out respectively using H_2O instead of saturated aqueous NH_4Cl. The results of the reaction are summarized in Table 3.

It was shown that the yields were higher than with using the nine-carbon chain and only partial deprotection was achieved. This was not surprising considering that the necessity of heating during the reaction caused some decomposition in the case of the longer conjugated system. An alternative synthetic pathway to approach the desired precursor 15a or 15b was thus considered starting from diols 18 , illustrated in Scheme 3,

Table 3. EtMgBr-Mediated Coupling Reaction of Pentanones 5 with Five-Carbon Polyene Chain 9

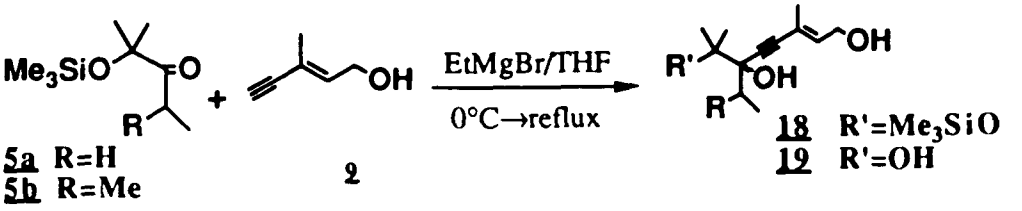

5a R=H
5b R=Me

9

18 R'=Me_3SiO
19 R'=OH

R	Isolated yield(%)	Ratio of 18:19
H	87	2:1
Me	73	4:1

consisting of the reduction of the triple bond in compound 18 using lithium aluminum hydride and subsequent MnO_2/Celite oxidation and dehydration to provide triene aldehyde 22 which could be reacted with the Wittig reagent 8. The resultant pentene ester 23 could be easily converted to 15a or 15b by DIBAL-H reduction, MnO_2/Celite oxidation and n-Bu_4N^+ F^- desilylation. The initial attempt to reduce the triple bond of 16a with $LiAlH_4$ in ether under reflux indicated 61% yield after column chromatography, but the product underwent desilylation to give triol 26:

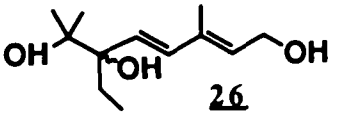

26

which was not suitable for regioselective dehydration at C-6. As with compounds 16 and 17, this is regretful because the group at C-1 would be more easily lost than the OH substituent at C-6. The final attempt to dehydrate at C-6 started from

Scheme 3:

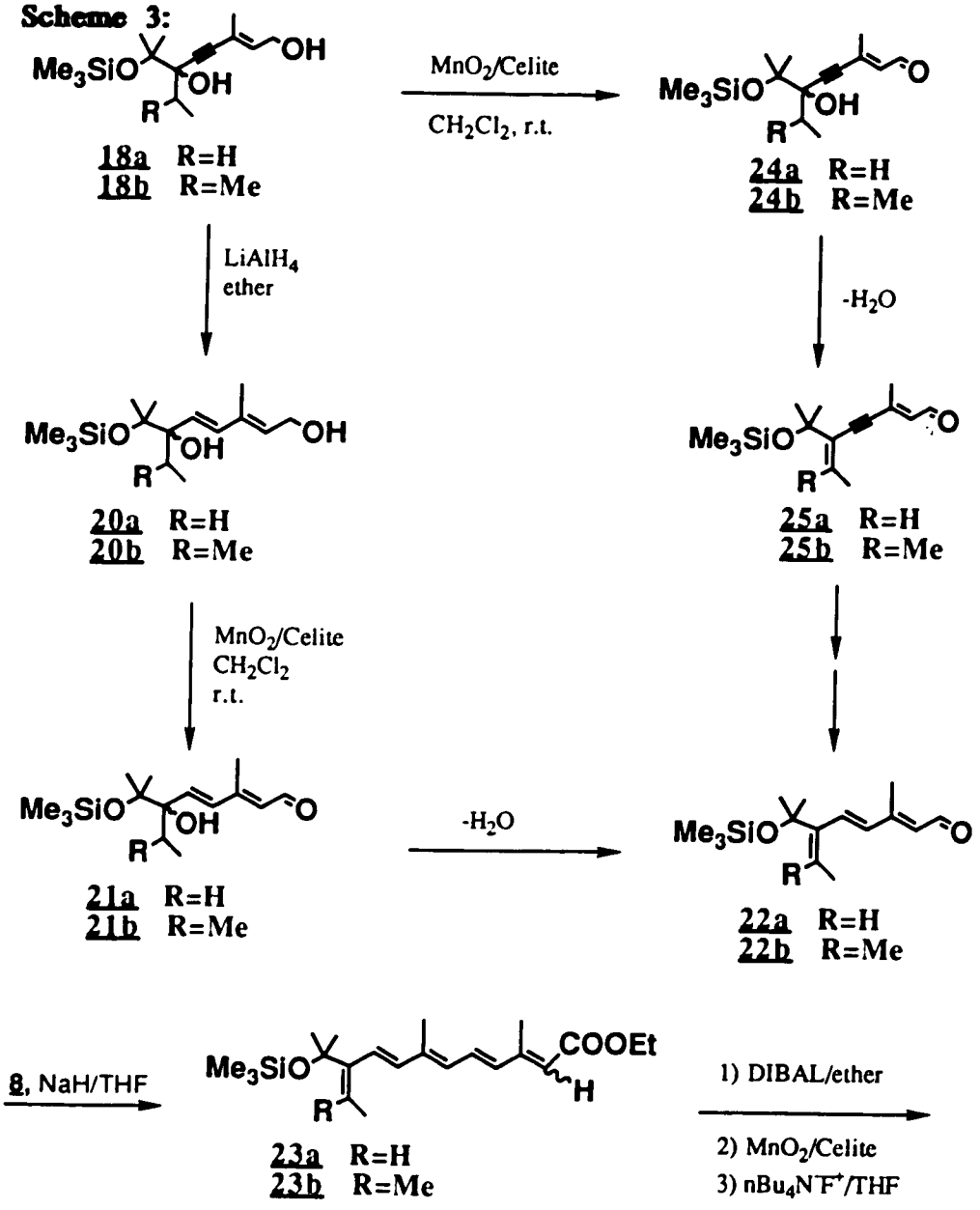

18a R=H
18b R=Me

24a R=H
24b R=Me

20a R=H
20b R=Me

25a R=H
25b R=Me

21a R=H
21b R=Me

22a R=H
22b R=Me

23a R=H
23b R=Me

15a or 15b

aldehydes 24a and 24b (see Scheme 3.) which were easily obtained from MnO_2/Celite oxidation of diols 18a and 18b in methylene chloride at room temperature in 74% and 81% yield respectively. The results of dehydration of 24a and 24b with different reagents and conditions are summarized in Table 4. In no case, however, as shown in Table 4, did dehydration afford the desired product. Dehydration of the tertiary hydroxyl group of either 24a or 24b with the acidic media (entry 1, 2) did not give the product 25 but resulted in the exclusive desilylation of both 24a and 24b. Using a mild reagent (entry 3) gave no trace of reaction, and in order to stabilize the protective group towards basic conditions and increase the strength of the reagent, acid anhydrides with triethyl amine (Et_3N) and pyridine were used (entry 4) but with no satisfactory result. Presumably, the tertiary hydroxyl group at C-6 in compounds 24 is too sterically hindered to be approached by reagents.

The attempted synthesis of pentenals 15a and 15b from pentanones 5a and 5b both by using nine-carbon and five-carbon polyene chains was unsuccessful and the troublesome aspect of both procedures was the difficulty of the dehydration. In response to this problem, a new synthetic methodology has been developed, shown in the next section.

Table 4. Dehydration of Aldehyde 24a and 24b

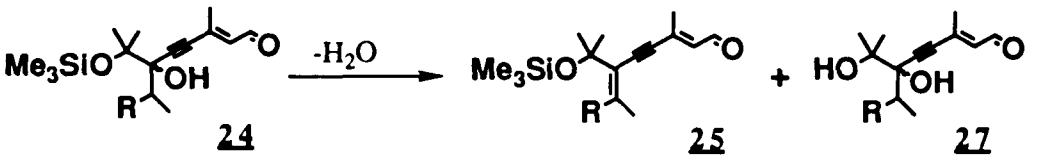

24 25 27

Entry	R	Reagent	Reaction time/temp.	Product
1	H, Me	40%HBr/HOAc[314]	4 hrs., -40°C-0°C	27
2	H, Me	p.CH_3-C_6H_4-SO_3H in C_6H_6[315]	5 min., 80°C	272
3	Me	$FeCl_3$-SiO_2/ether[316]	10 hrs., r.t.	none
4	Me	Ac_2O or $(CF_3CO)_2O/Et_3N$/ pyridine[317]	48 hrs., r.t.	25(minor) + unknown product(major)

Application of Acyclic Vinyl Triflates in the Synthesis of Pentenal 15a and 15b

In order to avoid a nucleophilic addition to the carbonyl compound followed by dehydration of the intermediate hydroxyl product to obtain the corresponding olefin, a vinyl cation generated from the corresponding ketone could be considered as an alternative to the nucleophilic addition-dehydration route. Thus, the formation of an enol derivative with a leaving group and the displacement of the leaving group by a nucleophile would attain this goal. Enol trifluoromethanesulfonates (triflates) have been much employed as a source of vinylic cations in late 70's,[318] and McMurry and Scott reported a useful method for making enol triflates from the corresponding ketone substrates, followed by various nucleophilic substitutions to complete the conversion of ketones into olefins.[319,320] However, although extensive synthetic application of this method has been directed toward almost all types of cyclic carbonyl compounds, scant examples of acyclic carbonyl compounds can be cited from references. It was envisaged that if formation of vinyl triflates from corresponding cyclocarbonyl compounds could attain 65%-95% yields, there was little doubt that the reaction could be applied to acyclic carbonyl compounds as well. This interest encouraged us to the synthesis of triflates from acyclic carbonyl compounds. The synthetic steps that were designed are outlined in general terms in Scheme 4. They involved a) generation of the enol triflates from the corresponding compounds (5 to 28) by the method

described by McMurry and Scott, b) palladium-catalyzed intermolecular coupling of the enol triflate with methyl vinyl ketone (Heck reaction) to provide the multiconjugated ketone (28 to 29), [321] c) condensation of the conjugated ketone with the anion of trimethylsilylacetaldehyde t-butylimine [322] to provide a triene aldehyde (29 to 30), and Wittig reaction of the condensation product with phosphonosenecioate. Successive reduction of the resultant multiconjugated ester 31, MnO_2/Celite oxidation of the intermediate alcohol and cleavage of the protective group would provide the desired aldehyde 15.

Scheme 4:

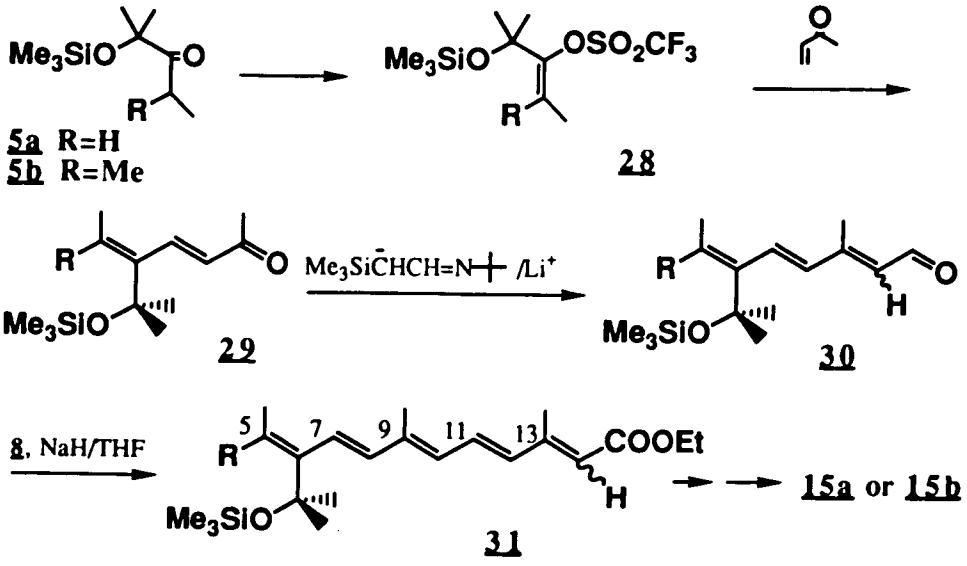

2,4-Dimethyl-4-trimethysilyoxypent-2-en-3-yl-triflate 28. R=Me, was synthesized by the trapping enolate ion generated from the corresponding pentanone 5b by two different bases with commercially available N-phenyltrifluoromethylsulfonimide [$PhN(SO_2CF_3)_2$, solid], indicated in Scheme 5.

Scheme 5:

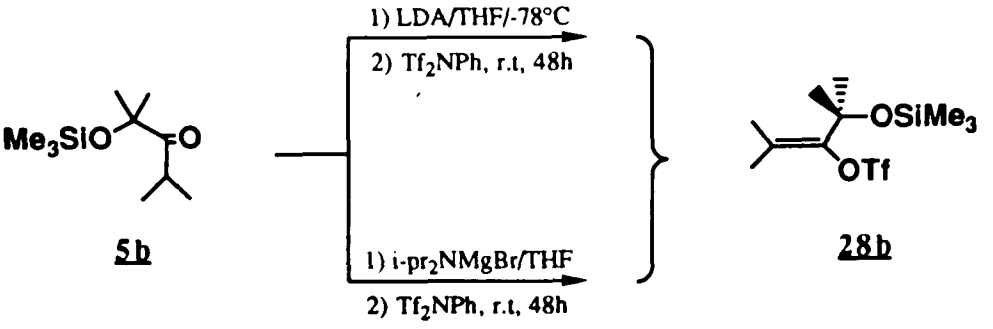

The successive treatment of a solution of lithium diisopropylamide (LDA) in THF at -78 °C with the ketone 5b for two hours and $PhN(SO_2CF_3)_2$ ($PhNTf_2$), followed by warming the reaction mixture to room temperature and stirring it for forty-eight hours, provided, after silica-gel column chromatography of the crude product, the enol triflate 28b in 1.5% yield. It could be presumed that this deprotonation under kinetic condition was less efficient because of the steric hindrance from the gem-dimethyl group at C-2. The result of the treatment of 2-methylcyclohexanone with bromomagnesium diisopropylamide ($i\text{-}pr_2NMgBr$)[323,324] followed by trapping to give the thermodynamic enol triflate as a major product (95%) encouraged us

to examine this reagent. The yieldof the formation of the enol triflate 28b was increased to 32.5% by the treatment with i-pr$_2$NMgBr, generated from the reaction of diisopropylamine with EtMgBr via one-pot process, of ketone 5b in THF at room temperature for six hours followed by trapping with PhNTf$_2$. Two vinyl methyl peaks were observed in the ^{1}H NMR spectrum of enol triflate 28b: δ_1 1.89 and δ_2 1.73, and were assigned to the methyl group syn to the triflate group, having more electropositive character, and the other anti to the triflate group, respectively. The subsequent palladium-catalyzed Heck olefination reaction [325] of enol triflat 28b with methyl vinyl ketone and bis-(triphenylphosphine) palladium(II) dichloride [Pd(PPh$_3$)$_2$Cl$_2$] was carried out at 75 °C for fifteen hours in N,N-dimetylformamide (DMF) and triethylamine, and gave trans-6-methyl-5-[(1-trimethyloxysilylethyl)]-hept-3,5-dien-2-one 29b in 53% yield after purification by chromatography. The physical properties of dienone 29b as indicated by UV and ^{1}H NMR spectra with the structural formula were shown in Figure 1. The trans configuration of the vinyl moiety was indicated by the appropriate coupling constant (J = 16 Hz) in the ^{1}H NMR spectrum.

Meanwhile, pentanone 5a was converted to the corresponding enol triflate 28a in 87% distilled yield, under kinetic reaction conditions (LDA in THF, -78 °C) and the yield of the formation of enol triflate 28a was significant, indicative of the fact that steric hindrance at the carbon position in a carbonyl compound, like ketone 5b, would cause lower reactivity. In

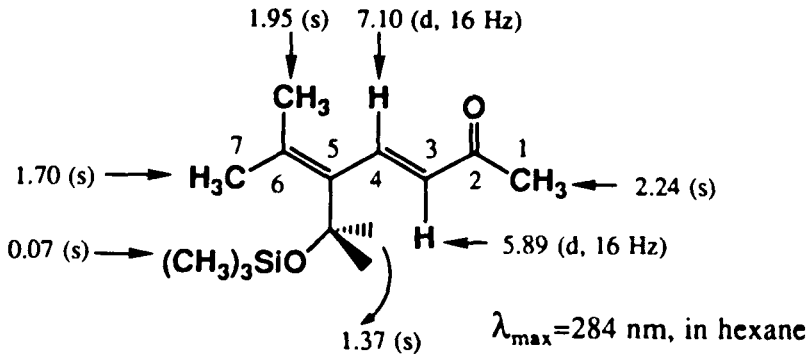

Figure 1. The Structural Formula of Dienone 29b.

addition, purification of triflate 28a by distillation could be performed although many triflates are thermally labile. The ^{1}H NMR spectrum of triflate 28a showed one vinyl proton signal at 5.55 ppm (quartet) and one vinyl methyl proton signal at 1.70 ppm (doublet) which was assigned to the vinyl proton syn to the triflate group and the vinyl methyl anti to the triflate group, as shown in Figure 2. When compared with the chemical shifts of

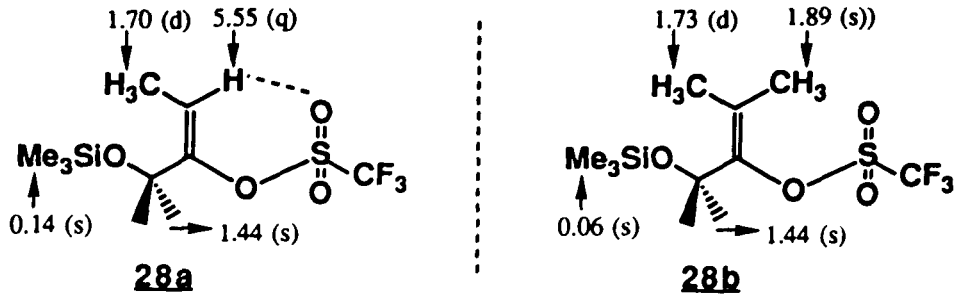

Figure 2. The Structural Formulas of Enol Triflate 28a and 28b

triflate 28b (see Figure 2.), it is found that there is small difference between the corresponding vinyl methyl groups of 28a and 28b anti to the triflate group. The same type of Heck reaction with 28a was accomplished and the yield of formation of dienone 29a differed only slightly from that of dienone 29b , indicative of the insensitivity of the Heck reaction to the steric hindrance about the enol triflate. The UV spectrum of dienone 29a showed maximum absorption at 270 nm in hexane, while the ^{1}H NMR spectrum showed three olefinic proton signals at δ 5.95 (q, J = 7.1 Hz), 6.64(d, J = 16 Hz) and 7.30(d, J = 16 Hz), illustrated in Figure 3.

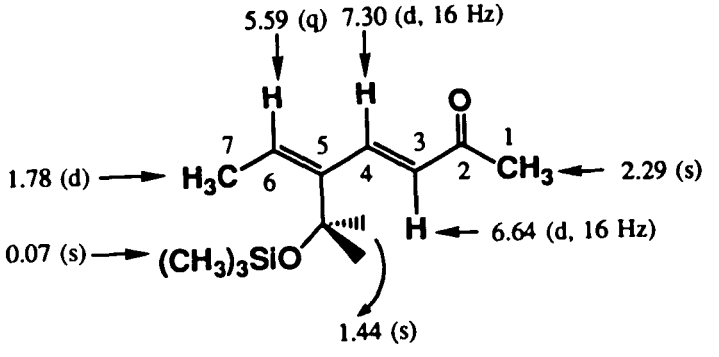

Figure 3. The Structure of Dienone 29a

Because of the success in the synthesis of the diene ketones 29a and 29b, the final desired compound 15a is now accessible via the following synthetic steps. The condensation of trans-5-[(1-trimethylsilyloxyl)-1-methylethyl]-hept-3,5-dien-2-one 29a with the anion of trimethylsilyacetaldehyde-t-butylimine

easily formed from the corresponding imine with LDA/THF at -78 °C, furnished a mixture of cis and trans triene aldehydes 30 (R=H) in 89% yield, which could be separated by a flash silica-gel chromatography [326] into a trans isomer (52%) and cis isomer (37%). The spectral data show is in Figure 4 and Table 5.

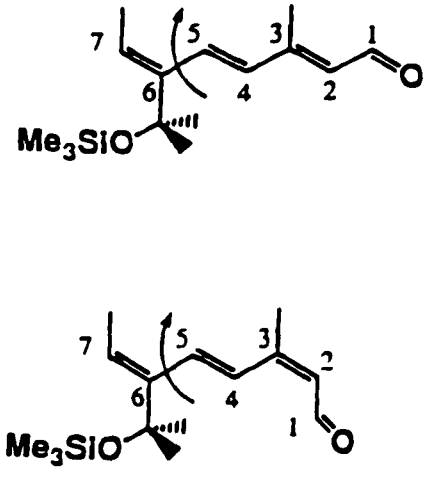

Figure 4. Trans and Cis Triene Aldehydes 30a, b

An unusual feature of the stereochemistry of both cis and trans triene aldehydes 30 near the C(5)-C(6) bond was found by Nuclear Overhauser

Table 5. ^{1}H NMR and UV Spectral Data of Cis & Trans Triene Aldehyde 30

Protons on carbon	30a trans isomer(ppm)	30b ciss isomer(ppm)
H-1	10.12 (d, J=8.2Hz)	10.11 (d, J=8.1Hz)
H-2	5.95 (d, J=8.2Hz)	5.79 (d, J=8.1Hz)
Me-3	2.31 (s)	2.05 (s)
H-4	6.81 (d, J=16.3Hz)	7.45 (d, J=16.1Hz)
H-5	6.60 (d, J=16.3Hz)	6.64 (d, J=16.1Hz)
H-7	5.81 (q, J=7.2Hz)	5.76 (q, J=7.1Hz)
H-8	1.78 (d, J=7.2Hz)	1.72 (d, J=7.1Hz)
Me_2	1.41 (s)	1.32 (s)
Me_3SiO	0.06 (s)	0.01 (s)
λ_{max}(nm) in hexane	308	304

Effect (NOE) NMR analysis. As indicated in Figure 5, irradiation of the gem dimethyl groups at 1.41 ppm (1.32 ppm) elicited a positive NOE at three vinyl-proton resonances: H-4, H-5 and H-7. Another positive NOE was observed by the irradiation of the vinyl methyl protons [Me(7)] at two vinyl-proton resonances: H-4 and H-5. These data establish that the C_6-C_7

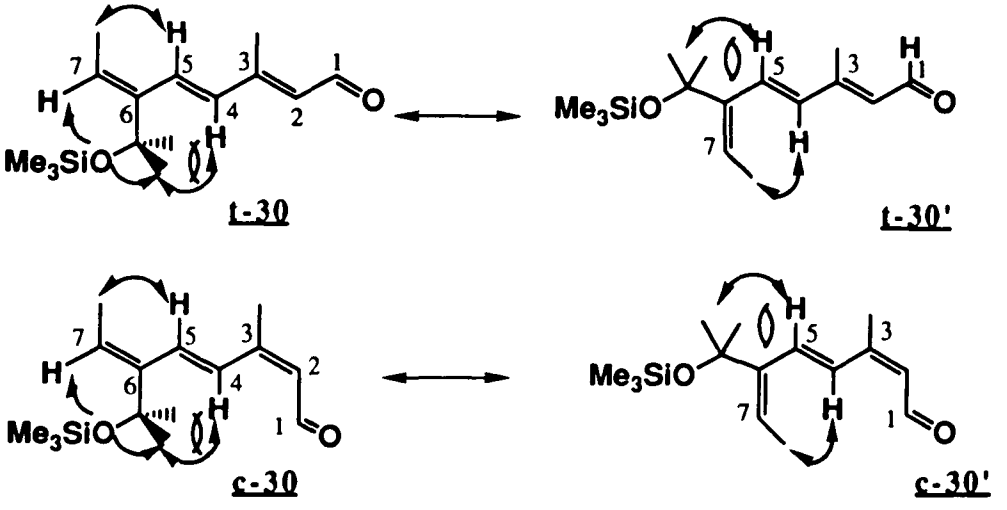

Figure 5. NOE Indication for Cis & Trans Triene Aldehydes 30

double bond is not fully coplanar (conjugated) with the rest of the polyene-side chain. Although no definite picture about the stereochemistry of both compounds is possible, the nmr data would fit some non-planar structure between t-30 and t-30' (or c-30 and c-30'), or a rapid equilibrium between the two planar structures (see Figure 5.). Due to the possible existence of steric hindrance between the bulky trimethylsilyloxy side chain and nearby H-4 and H-5 vinyl protons, the former structure is more likely.

Wittig reaction of the trans triene aldehyde 30a with the sodium salt of the phosphonosenecioate 8 in THF at room temperature for three hours afforded ester 31 in good isolated yield (92%). A mixture of C(13)-trans (74%) and C(13)-cis (18%) ester 31 was found from ^{1}H NMR analysis. Reduction of this mixture of ester 31 with DIBAL in ether at -78 °C followed by MnO_2/Celite oxidation of the resultant alcohol in CH_2Cl_2 at room temperature gave protected pentaenal 32 in 72% isolated yield.

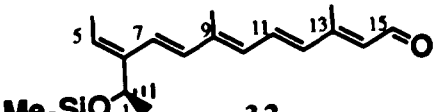

32

The protective group was easily cleaved by $nBu_4N^+F^-$ in THF at room temperature and desired product 15a [C(13)-trans and C(13)-cis isomers, 5:1] was thus obtained in seven chemical operations and 28% overall yield from pentanone 5a. The all-trans isomer of 15a was separated by High Performance Liquid Chromatography (HPLC).

The characterization of the all-trans pentene aldehyde 15a was performed in the following ways. First, the assignment of protons on the numbered carbon atoms (same as the retinal) of compound 15a, shown in Table 6, was completed by ^{1}H NMR proton-decoupling experiments and by the measurement of vicinal coupling constants of protons. After analysis of the ^{1}H NMR spectrum, the signals of vinyl protons: H-5, H-7, H-10, H-11, H-13 and H-15 were directly obtained from recognizable peak patterns and

the vicinal coupling constants. The signals for H-8 and H-12 were merged together and chemical shifts were obtained after decoupling H-7, then H-8 and H-11.

Table 6. The ^{1}H NMR Spectral Assignment of Product 15a

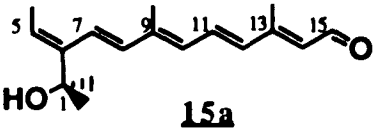

15a

Protons on carbon	All-trans(ppm)
Me-1	1.38 (s, 6H)
Me-5	1.75 (d, J = 7 Hz, 3H)
H-5	5.81 (q, J = 7 Hz, 1H)
H-7	6.46 (d, J = 16 Hz, 1H)
H-8	6.34 (d, J = 16 Hz, 1H)
Me-9	2.02 (s, 3H)
H-10	6.23 (d, J = 11 Hz, 1H)
H-11	7.11 (dd, J = 15 & 11 Hz, 1H)
H-12	6.41 (d, J = 15 Hz, 1H)
Me-13	2.31 (s, 3H)
H-14	5.96 (d, J = 8 Hz, 1H)
H-15	10.09 (d, J = 8 Hz,1H)

Second, the UV absorbance showed a maximum at 360nm in hexane and Chemical Ionization (CI) Mass spectral data (calcd. for $C_{17}H_{24}O_2$: 260.377) displayed, in addition to the $M^+ + 1$ ion of m/z 261 (30%) , the vinyl skeleton at m/z 202 (100%) formed from the cleavage of the bulky hydroxylisopropyl group, outlined in Scheme 6. Finally, the stereochemistry

Scheme 6:

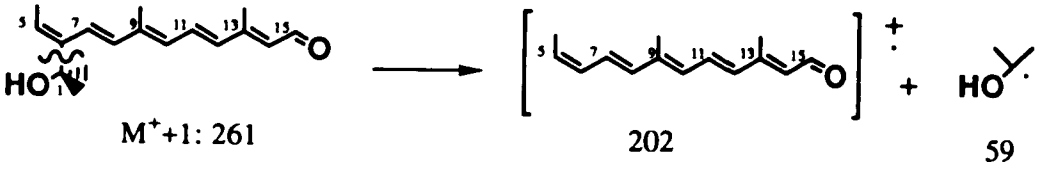

of the C(5)-C(6) double bond relative to the rest of ene system was signalled by the differential NOE spectrum of all-trans pentene aldehyde 15a. Selective saturation of the signal gem-dimethyl protons at 1.38 ppm and the signal of C-5 vinyl protons at 1.76 ppm, 12% and 14% NOE enhancements of the C(7) proton signal were observed, illustrated in Figure 6. As in compounds

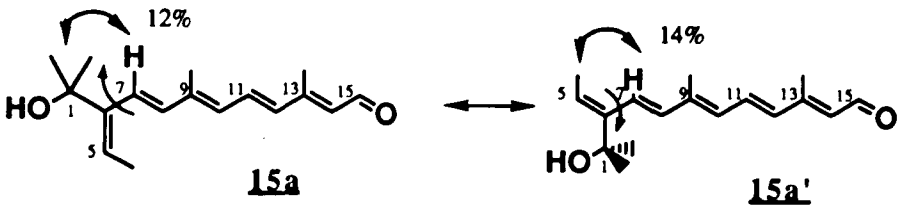

Figure 6. The NOE Indication of Pentene Aldehyde 15a

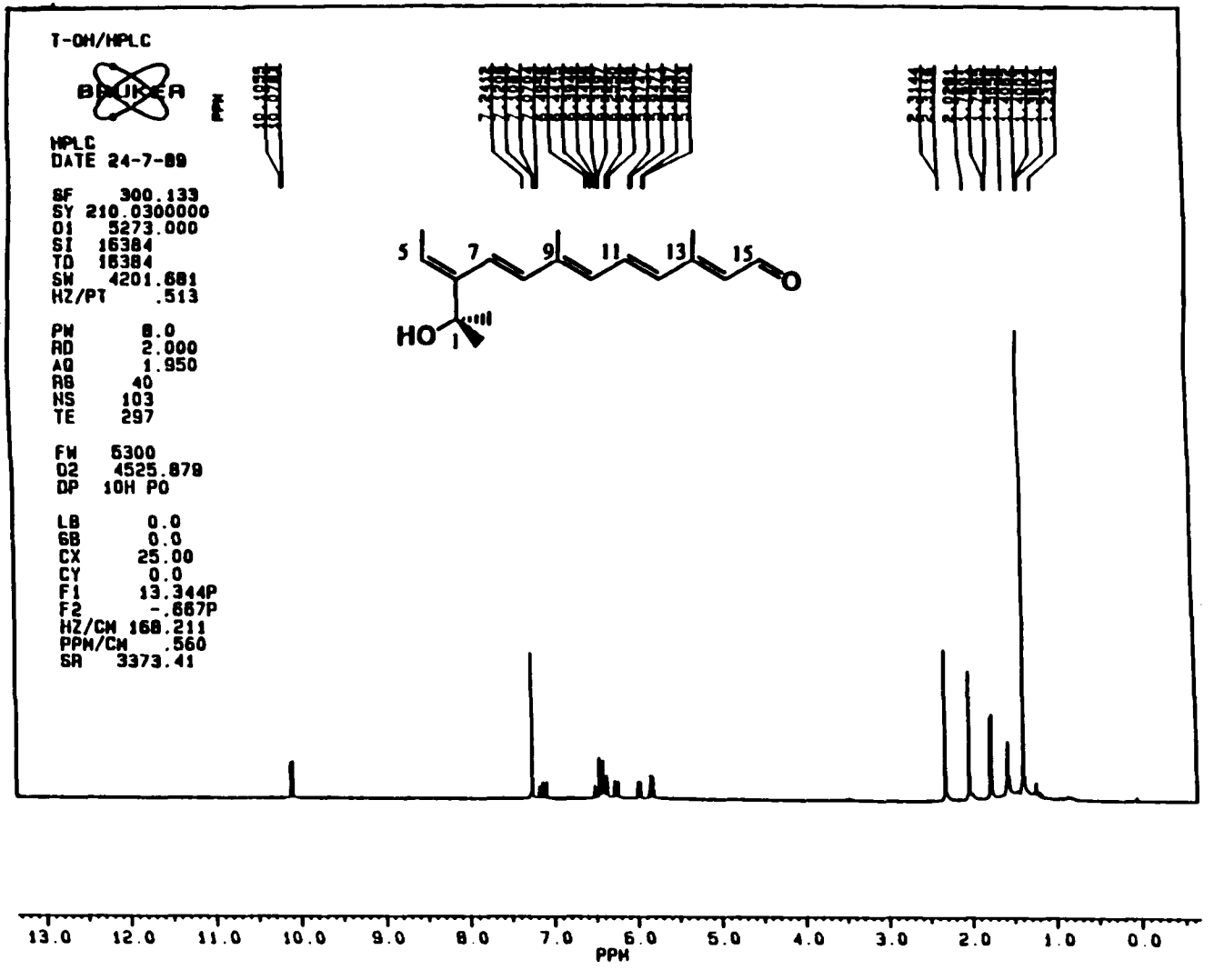
T-OH/HPLC
BRUKER
HPLC
DATE 24-7-89
SF 300.133
SY 210.0300000
O1 5273.000
SI 16384
TD 16384
SW 4201.681
HZ/PT .513
PW 8.0
RD 2.000
AQ 1.950
RG 40
NS 103
TE 297
FW 6300
O2 4525.879
DP 10H PO
LB 0.0
GB 0.0
CX 25.00
CY 0.0
F1 13.344P
F2 -.667P
HZ/CM 168.211
PPM/CM .560
SR 3373.41
HO
1
5
7
9
11
13
15
O
13.0
12.0
11.0
10.0
9.0
8.0
7.0
6.0
5.0
4.0
3.0
2.0
1.0
0.0
PPM

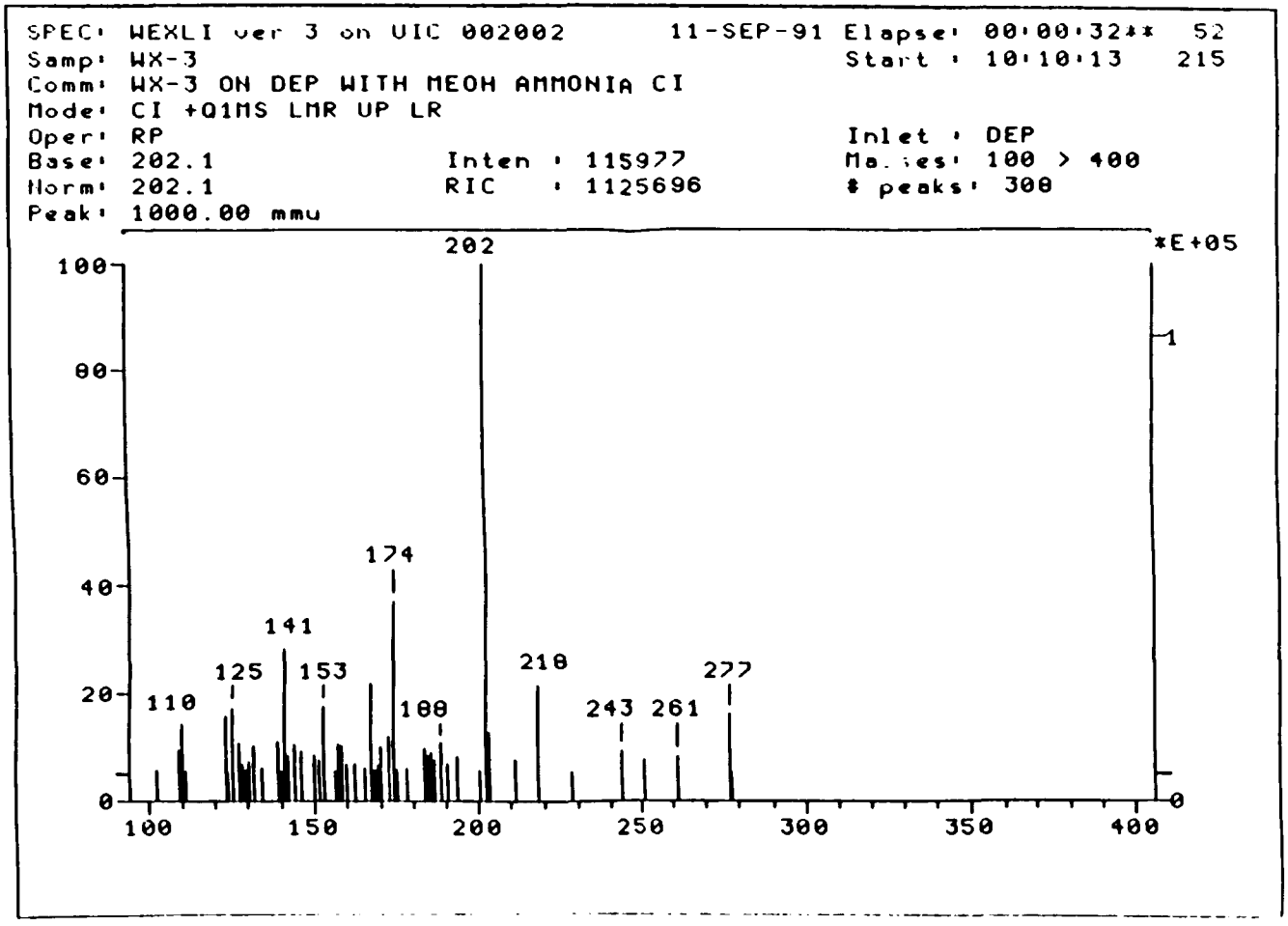
SPEC: WEXLI ver 3 on UIC 002002 11-SEP-91 Elapse: 00:00:32** 52
Samp: WX-3 Start : 10:10:13 215
Comm: WX-3 ON DEP WITH MEOH AMMONIA CI
Mode: CI +Q1MS LMR UP LR
Oper: RP Inlet : DEP
Base: 202.1 Inten : 115977 Masses: 100 > 400
Norm: 202.1 RIC : 1125696 # peaks: 300
Peak: 1000.00 mmu
*E+05
1
0
100
80
60
40
20
0
202
174
141
125
153
110
188
218
243
261
277
100
150
200
250
300
350
400

t-30 and c-30 shown in Figure 5, the C(5)-C(6) double bond in compound 15a is also not fully conjugated and planar with the rest of the polyenal chain. The structure of this pentenal could be a rotational conformer between 15a and 15a' (see Figure 6.), due to the steric interaction between the hydroxylisopropyl group and vinyl protons H(7) and H(8), or a rapidly equilibrating mixture of the two planar conformer.

Esterification of the Tertiary Hydroxyl Moiety of 15a

As mentioned in the introduction section, a series of seco-ring retinal analogs bearing various numbers of carbon-length chains have been designed to serve as a novel anchor for probing the tertiary structures of rhodopsin and bacteriorhodopsin. The completion of the total synthesis of pentene aldehyde 15a makes this proposal performable. However, in view of the structure of aldehyde 15a, mild, and neutral or basic reaction conditions for the esterification of this sterically hindered tertiary hydroxyl group should be employed due to the thermal and acidic lability of the polyene chain. The reagents we attempted to use were acetyl chlorides in the presence of a base, based on the following considerations: 1) acid chlorides are the most reactive toward nucleophilic substitution of carboxylic acids and acid derivatives, 2) bases are able to function as acid scavengers to eliminate the decomposition of products by the newly formed HCl side product.

Thus, reactions of aldehyde 15a with acid chlorides such as:

$CH_3(CH_2)_nCOCl$ (n = 2, 3, 4, 5, 6, 7 & 8) and $ClCO(CH_2)_5COCl$, were carried out in the presence of sodium acetate in CH_2Cl_2 or toluene at 0 °C to room temperature, as outlined in Scheme 7, to afford products 33 and 34.

Scheme 7:

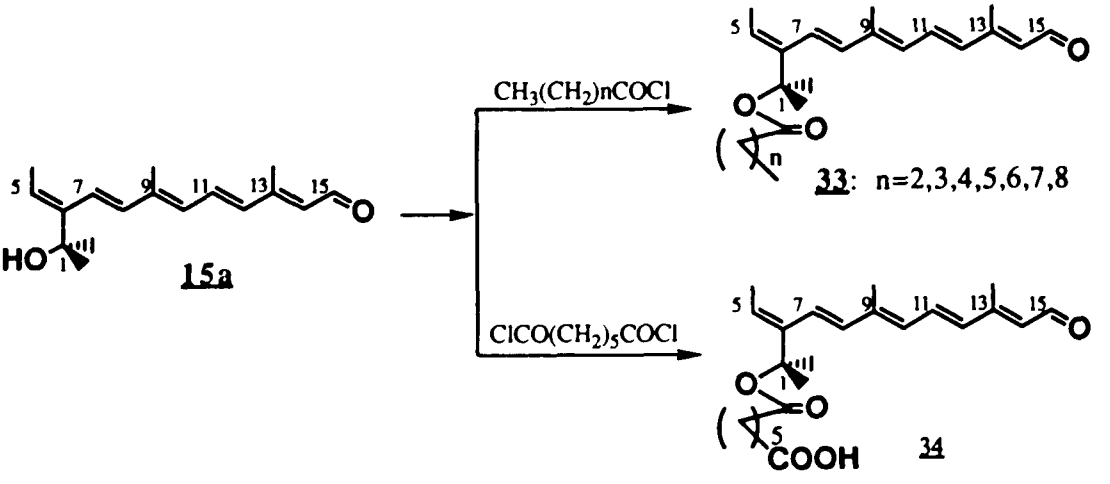

The process of acylation was easily monitored by silica-gel TLC due to the difference of polarity between the starting material (Rf = 0.2) and the product (Rf = 0.7). Isomerization occurred in the each reaction, presumably due to the sodium hydrochloride. In addition, conversion of the tertiary hydroxyl group to the corresponding ester reached only 50%. The final all-trans isomer of each product was purified by HPLC and the structure was confirmed by UV absorbance. Of particular interest is the longer wavelength maximum UV absorbance for each all-trans product compared to the aldehyde 15a in the

range from 372 nm to 374 nm, with a fine structure, suggestive of the closely full conjugation of C(5)-C(6) double bond with the side-ene chain.

II. Studies in Binding of the Seco-Ring Retinal Analogs to Opsins

Artificial pigments of both rhodopsin (Rh) and bacteriorhodopsin (bR) can be prepared by the addition of synthetic chromophores to apoproteins (bleached proteins or opsins). Rh opsin and bR opsin can be prepared by treating their proteins with hydroxylamine (NH_2OH) under illumination. Unlike rhodopsin, purple membrane needs a stronger condition and a longer time to produce its apomembrane. Regeneration can be performed with opsin in suspension or solubilized in detergent solution.[327] Usually, binding in suspension is preferred due to the stability of the structure of the pigment and the quality of the membrane (and less extent of delipidation). In addition, less than 2% to 3% ethyl alcohol in the total volume of the reconstitution mixture is recommended when used to solubilize the chromophore.[328]

In order to obtain useful information from artificial pigments, not only is the efficient regeneration of the pigment from the synthetic retinal required, but also the properties and function must be similar to those of the native pigment. In this respect, several tests for the legitimacy of the artificial pigments can be carried out as follows:

1) The bathochromatically shifted absorption maximum in the UV/VIS

region of the spectrum can be indicative of the formation of the pigment analog, and Circular Dichroism (CD) measurements of the pigment should show a characteristic absorption similar to that of the native pigment.

2) Addition of the native chromophore to a solution of the artificial pigment, called the displacement experiment, is to insure that the native chromophore binding site in the protein is actually occupied by the artificial one.[329]

3) Irradiation of the formed pigment in the dark should trigger a pigment peak shift due to the bleachability of rhodopsin, and light-dark adaptation for bacteriorhodopsin, if the pigment is formed from all-trans isomer.

4) CH_2Cl_2 Extraction of the bound chromophore, shown in Scheme 1, is necessary to check the nature of the bound chromophore in the formed pigment analog.[330]

5) The addition of hydroxylamine to the formed pigment solution is necessary to check the relative stability of the pigment.

Scheme 1:

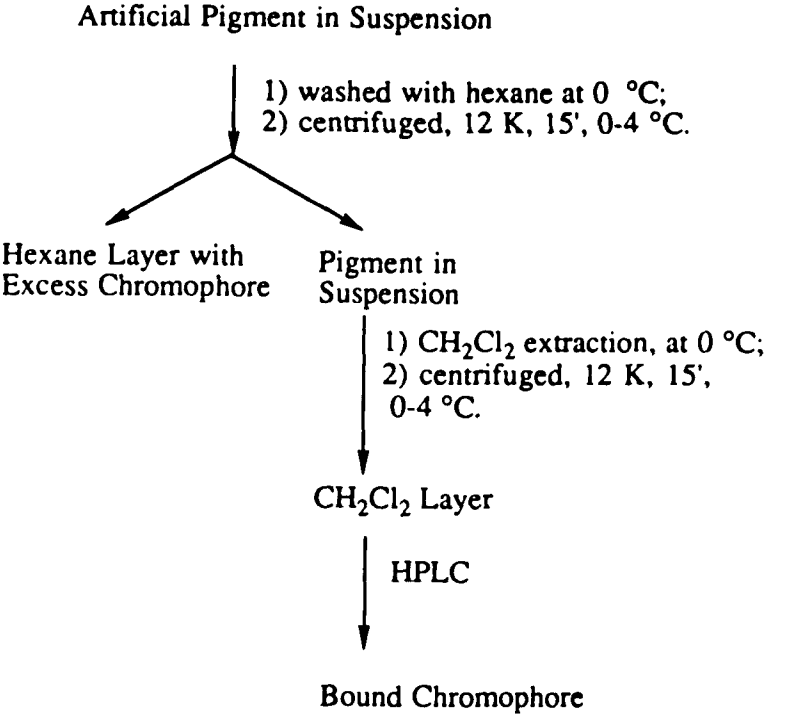
Artificial Pigment in Suspension
1) washed with hexane at 0 °C;
2) centrifuged, 12 K, 15', 0-4 °C.
Hexane Layer with Excess Chromophore
Pigment in Suspension
1) CH_2Cl_2 extraction, at 0 °C;
2) centrifuged, 12 K, 15',
0-4 °C.
CH_2Cl_2 Layer
HPLC
Bound Chromophore

Binding to Bacterioopsin

It is necessary and important to ascertain the isomeric purity of the synthetic retinal by HPLC before the binding experiment as the artificial bR pigment can be formed only from the all-trans or C(13)-cis isomer of the retinal analog. The method of bleaching purple membrane of Fodor and co-workers [331] was used with slight modification. The purple membrane was suspended in 1.0 M hydroxylamine and the pH was adjusted to 7.8 with 1.0 N NaOH. The sample was then irradiated with light from two 750 W projector lamps. The temperature of the solution was maintained by a warm bath at 25 °C to 30 °C during the irradiation until the purple color was dispelled. The entire process for the removal of the retinal chromophore to form the retinaloxime and bacterioopsin needed about fourteen to twenty hours, as outlined in Scheme 2. The bleached bR was washed six times with

Scheme 2:

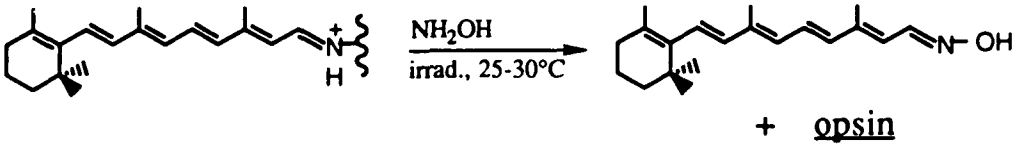

double-distilled water by centrifuging the solution. The white pellets were resuspended in 0.02 M phosphate buffers at pH 7.0.

Binding of Pentaenal 15a. The purity of hydroxyl-retinal 15a was checked by elution of the sample from the μ-Porasil column with 20% ethyl acetate in hexane at a flow rate of 1.0 ml/min. The HPLC trace in Figure 1 showed the peak of pure sample at 17.2 min and the absorption maximum in the UV spectrum of this chromophore showed at 360 nm in hexane. Hydroxyl-retinal 15a dissolved in 10 μl ethanol was added to a 0.5 ml UV sample cuvette containing the suspension of bacterioopsin at room temperature in the dark. The OD ratio of the chromophore to opsin was about one to one (1.0 OD). The formation of the pigment was monitored by the growth of a 510 nm absorption band as shown in Figure 2, in which the 380 nm absorption band was due to excess chormophore. The completion of the regeneration of the pigment only took 10 min and the efficiency is about 42% under these conditions. To the above formed pigment suspension was added an excess of all-trans retinal in ethanol. After continuous monitoring the UV/VIS absorption for four hours, no formation of the pigment at 560 nm, which is the absorption maximum of the native pigment in the dark, was observed. Light adaptation of the pigment analog at the 518 nm absorption maximum was observed by irradiation with a 750 W projector lamp filtered through a 400 nm-cut-off glass filter. The above behavior of the pigment analog, no displacement by the native chromophore and the light-dark adaptation, indicated that the same binding site was occupied by the retinal analog and that it functioned similarly to bacteriorhodopsin.

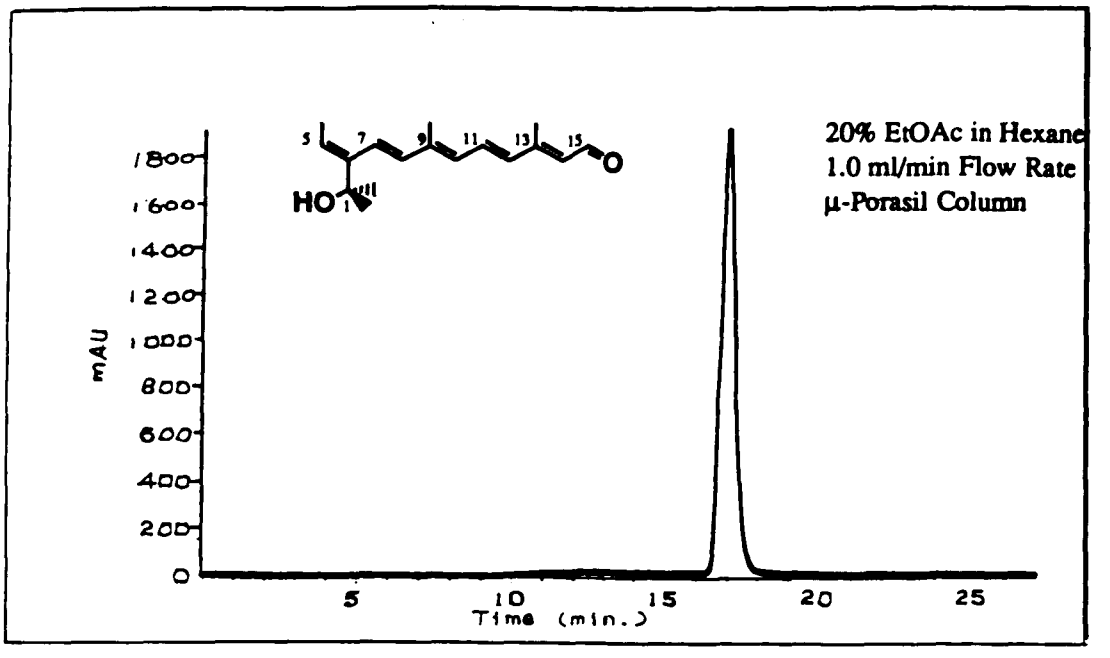

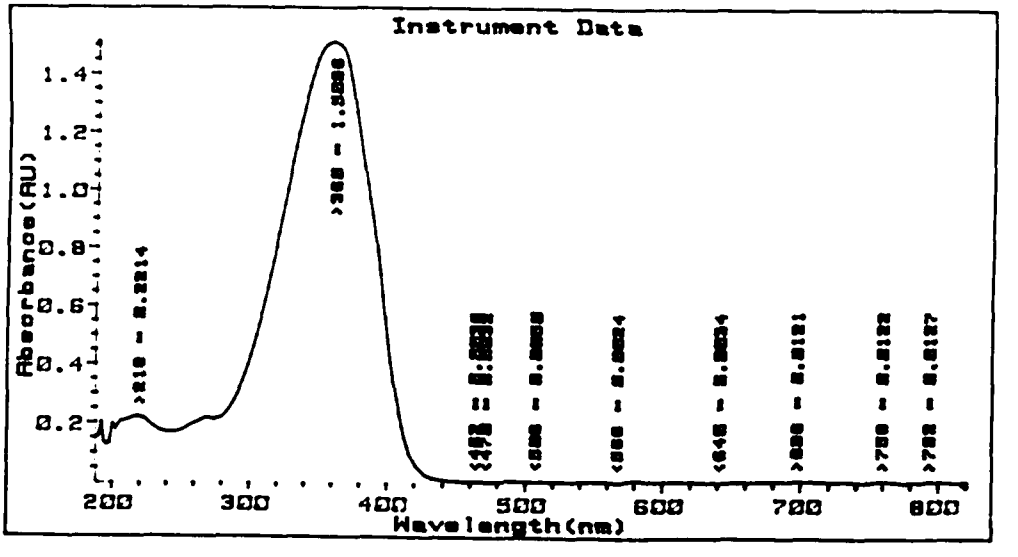

Figure 1. The HPLC profile (above) and UV spectrum (below) of the retinal 15a.

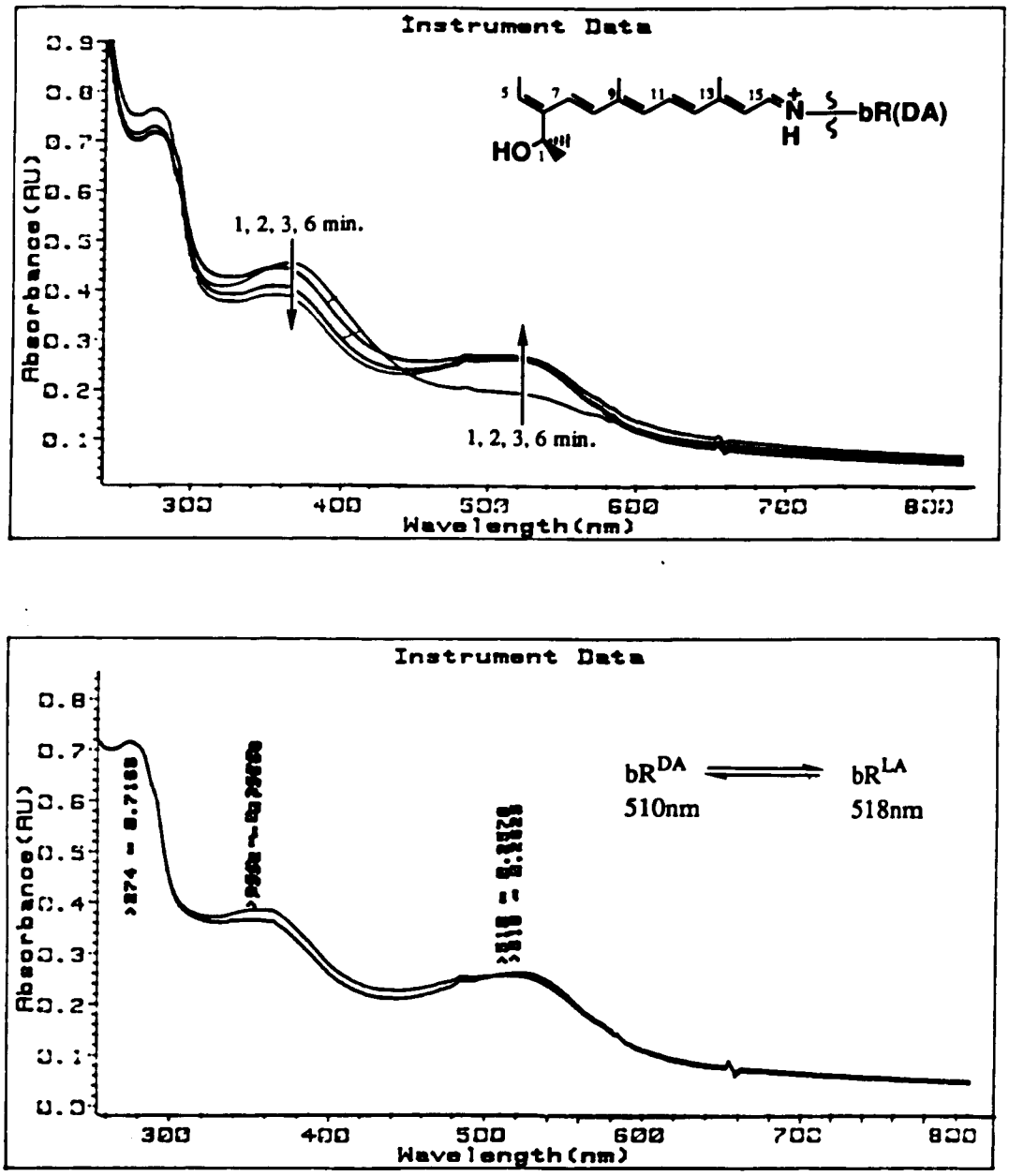

Figure 2. The formation of the bR analog from the retinal 15a (above) and its light-dark adaptation (below).

Binding of All-Trans Seco-Ring-Retinal analogs 33(n = 4-10) and 34.

The method used for the binding study of retinals 33 and 34 was identical to that described above. In Table 1, the absorption maxima of retinals 33 and 34 and their HPLC retention times are given. As seen from Table 1, the longest wavelength absorption maximum at 372-374 nm and the fine structure in the UV spectrum were observed for each of the retinals 33. On the other hand, the UV spectrum of retinal 34 showed a shorter wavelength absorption maximum than that of retinals 33 with no fine structure, but was still longer than that of retinal 15a containing no spacer arm (λ_{max} = 360 nm).

Table 1. UV Spectral and HPLC Data of Retinal 33 and 34

Chromophore	R.T.(min.)	% in hexane	UV(nm)
33, n = 2-8	14	10% ether	372-374
34	7	15% EtoAc	368

*: column: μ-porasil, flow rate: 1.0 ml/min.

The existence of the fine structure in the absorption spectra of retinals 33 could be attributed to the planarity between the 5-ene and the polyene side-chain to some extent.[332,333] The order of retinal maximum absorbance:

33 > 34 > 15a also suggested the same degree of conjugation of the 5-ene to the polyene side-chain.

The bR pigment analogs were regenerated from HPLC purified all-trans isomers of retinals 33 and 34 and their properties are detailed as follows:

1) Except for the retinal analog 33 with a ten-carbon-containing spacer arm (n = 8) no pigment regeneration was observed. However, retinals 33 (n = 2, 3, 4, 5, 6 & 7) and 34 could be bound to bR opsin with maximum absorption at 530-532 nm and complete regeneration only took less than ten minutes, as shown in Figure 3.

2) All of the bR analogs formed underwent a reversible light-dark adaptation, and none of the retinal analogs were displaced by the native retinal (all-trans retinal).

3) The CD spectrum of the pigment formed from retinal 33 n = 5 showed a positive Cotton effect at 490 nm and a negative Cotton effect at 590 nm as shown in Figure 4b, similar to that of the native pigment at different wavelength, as shown in Figure 4a.

4) Upon formation of the artificial pigments, unlike retinals 33 n = 2, 3, 4 & 5, the spectra of retinals 33 n = 6 & 7 showed the appearance of an intermediate, called pre-pigment, at 420 nm, which was then converted to the final pigment, at 530-538 nm, after several hours, while the spectrum of retinal 34 showed the intermediate at 480 nm. For these events, Figures 3,

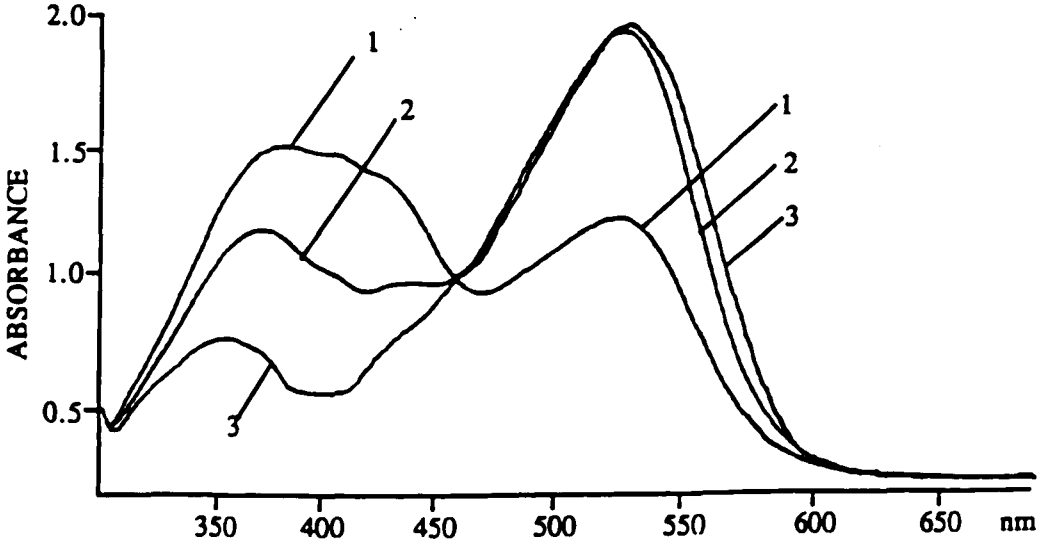

1-1min, 2-5min, 3-24hrs.

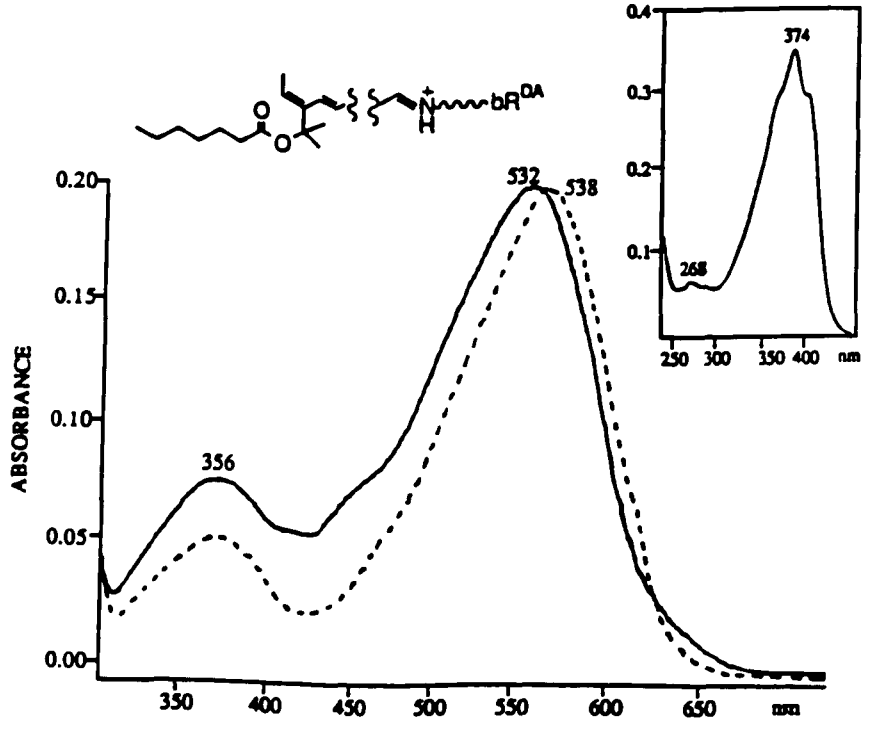

Figure 3. The formation of 33, n=5 bR pigment (above) at 1 min. (1), 5 min. (2) and 24 hrs. (3). And its Dark(solid)-Light(dash) adaption (below). The insert is the UV spectrum of the retinal.

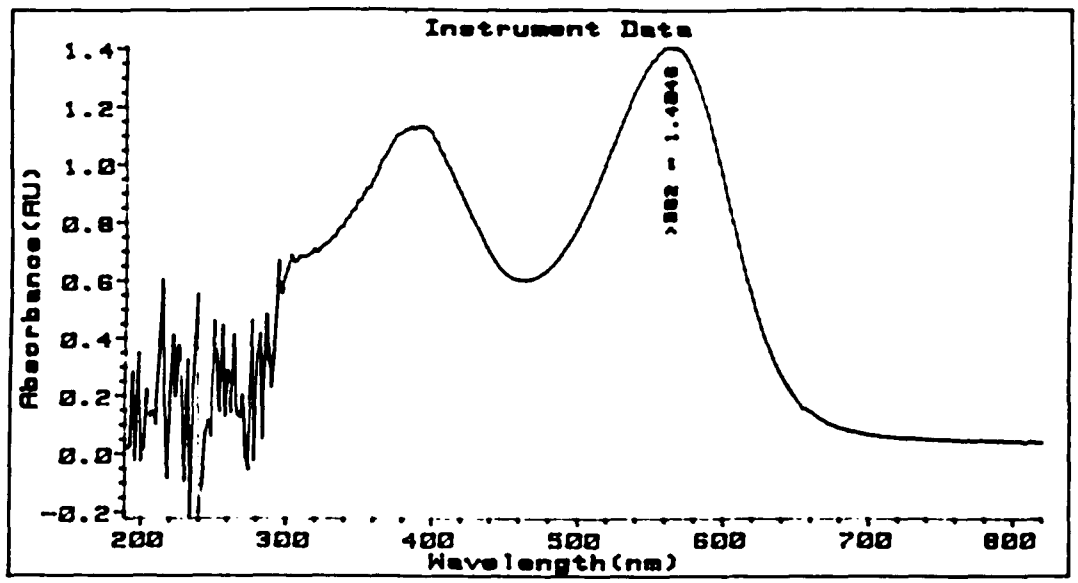

AVIV PLOT V3.2a cr T. 27.3C. data. 6-06-89 time. 08:10:50
taken 06-06-89 at 01:38:08. opl 1.005. AvT 1.0 sec
scan from 650.00 nm to 450.00 nm every 2.00 nm w/ 2.00 nm bw WX-1.SMD
y lower lim -10.0000. y upper lim 10.0000 millidegrees

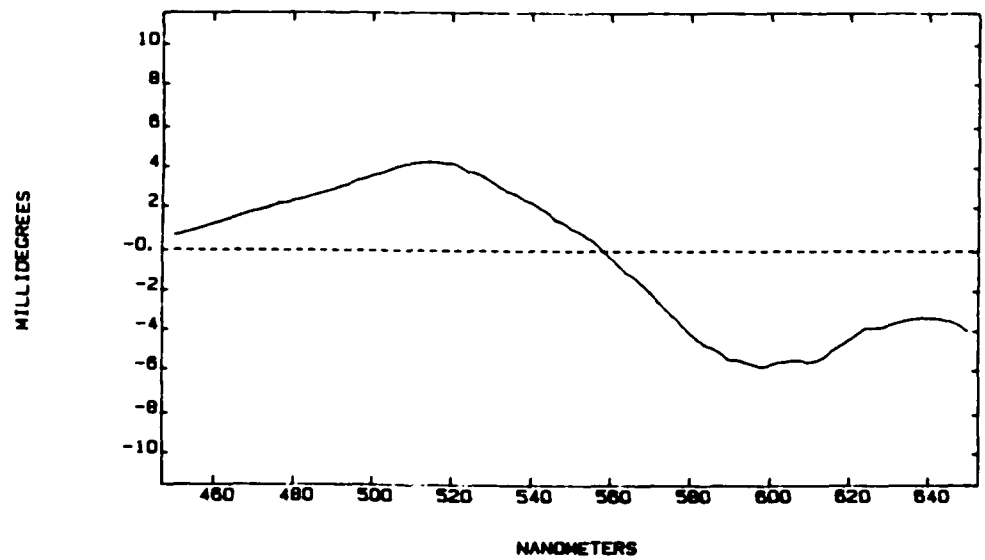

Figure 4. a) Native bR^{DA} absorption (above), and CD spectrum (below).

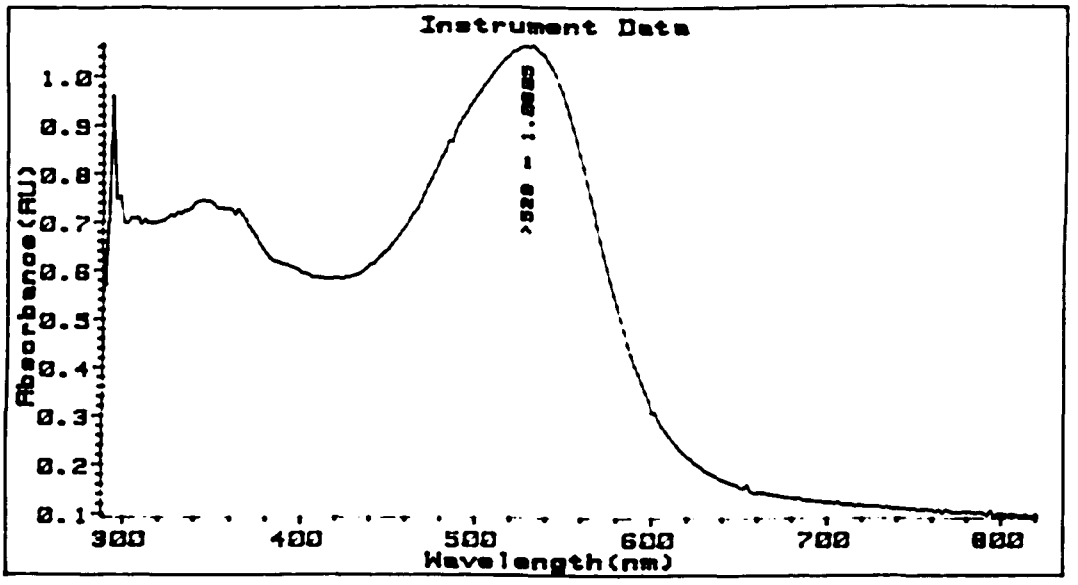

AVIV PLOT V3.2e cr T. 29.5C. date. 8-08-89 time. 07:09:25
taken 08-08-89 at 07:05:46. opl 1.005. AvT 2.0 sec
scan from 650.00 nm to 401.00 nm every 1.50 nm w/ 1.50 nm bw 7c-5
y lower lim -10.0000. y upper lim 10.0000 millidegrees

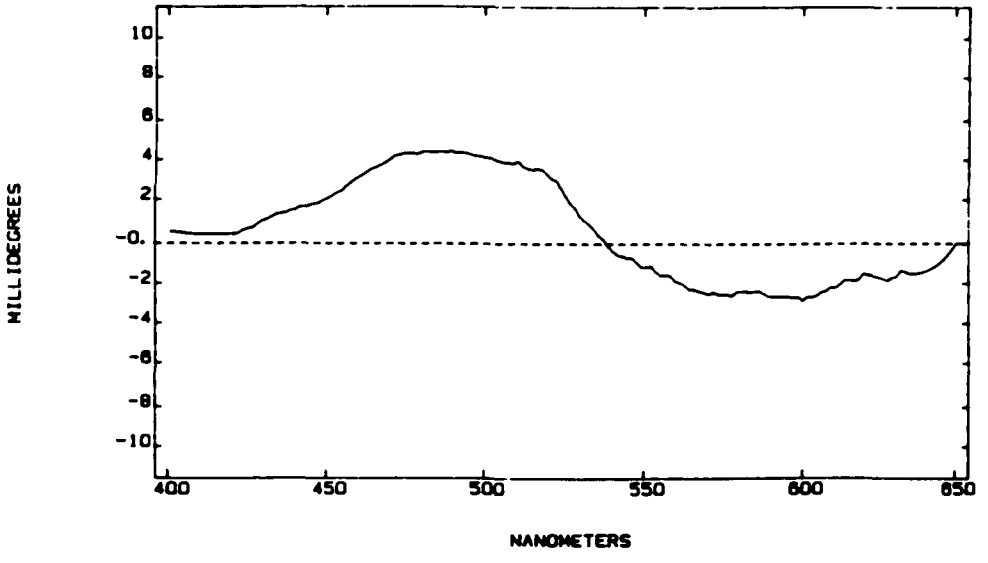

Figure 4. b) 33, n=5 bR pigment absorption (above), and CD spectrum (below).

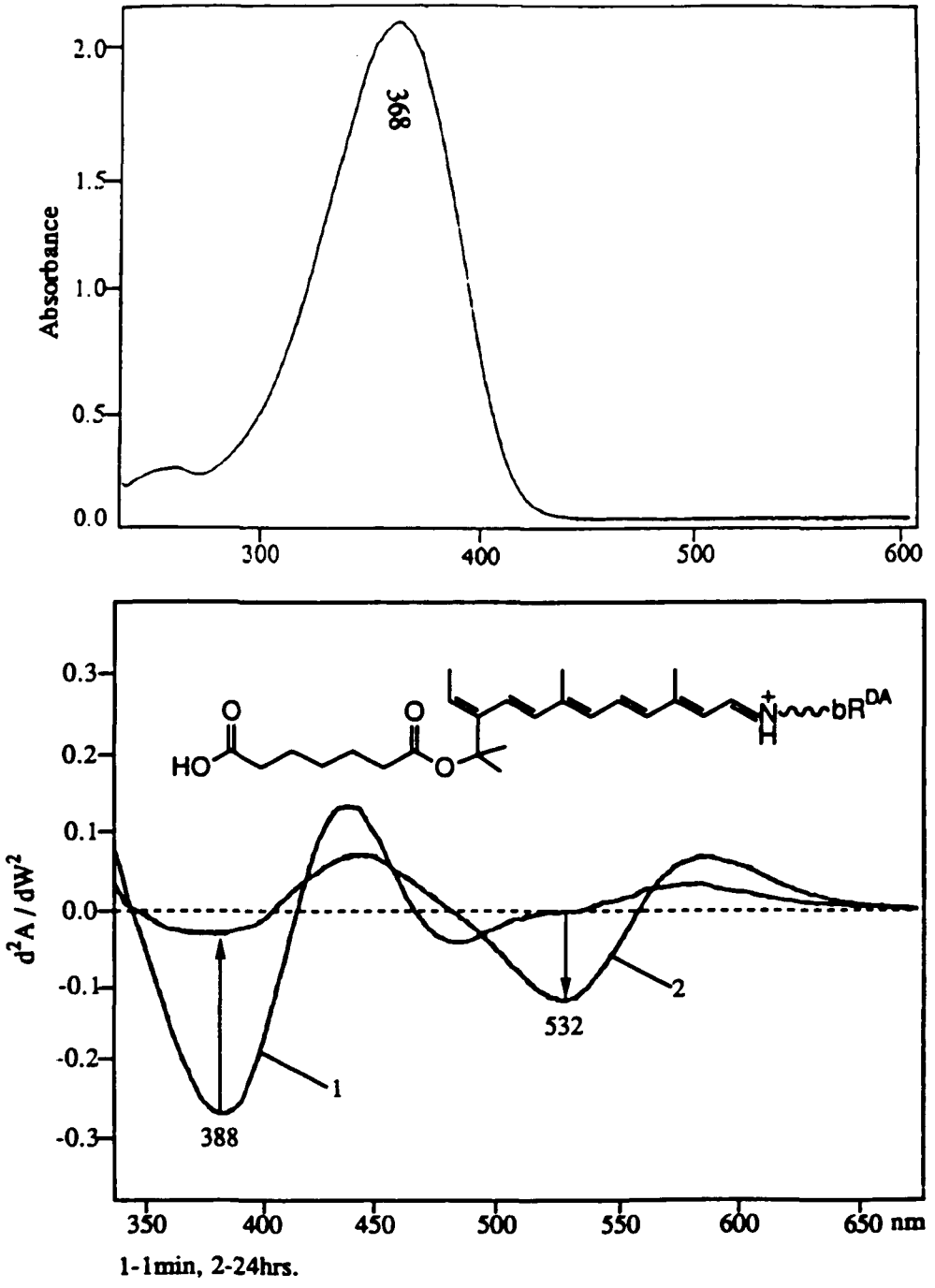

Figure 5. The UV absorption (368 nm) of retinal 34 (above), and its bR pigment formation followed by second derivative measurement (below).

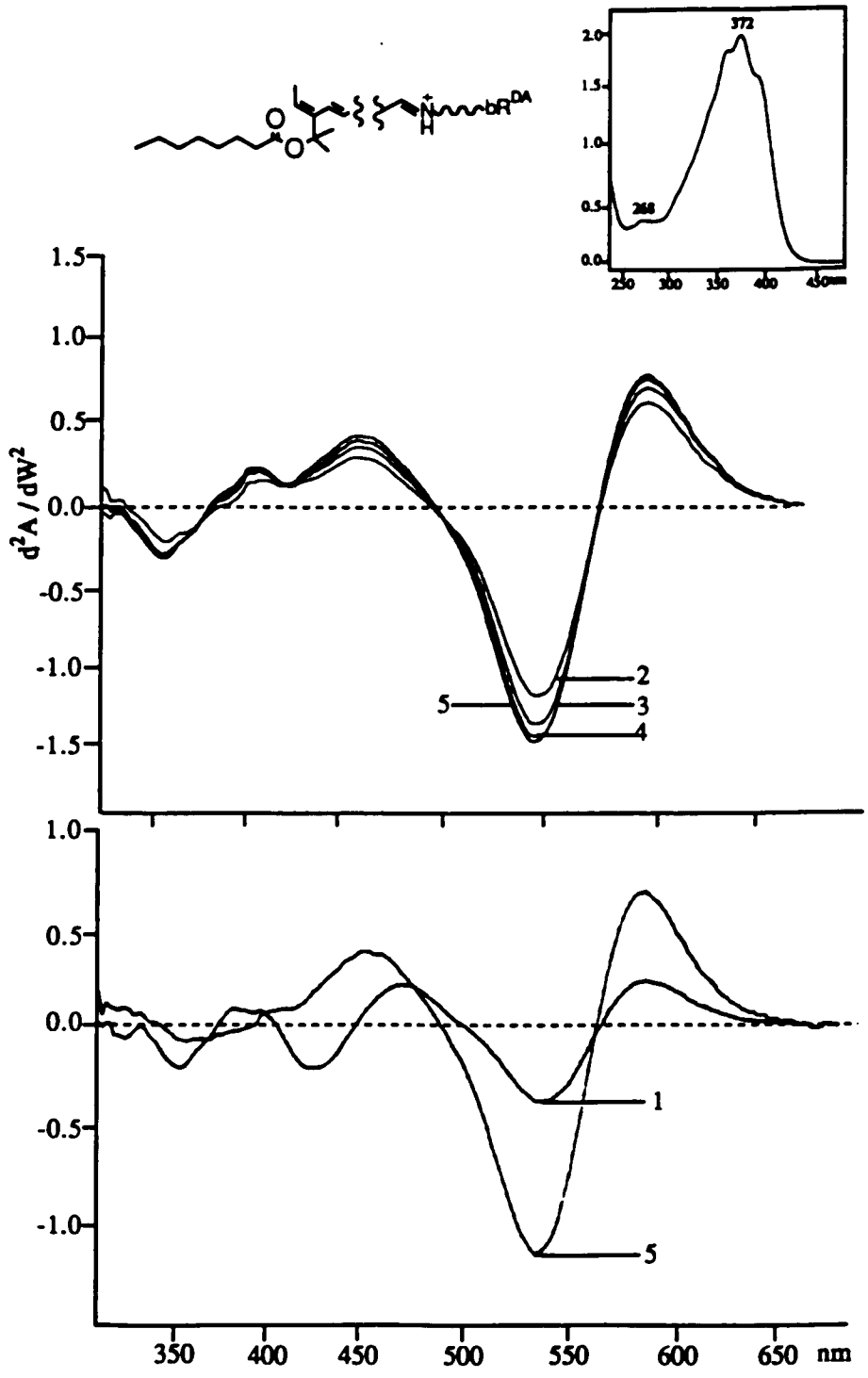

Figure 6. The 33, n=6 bR pigment formation by second derivative measurement at 1 min. (1), 3 min. (2), 10 min. (3), 20 min. (4) and 24 hrs. (5).

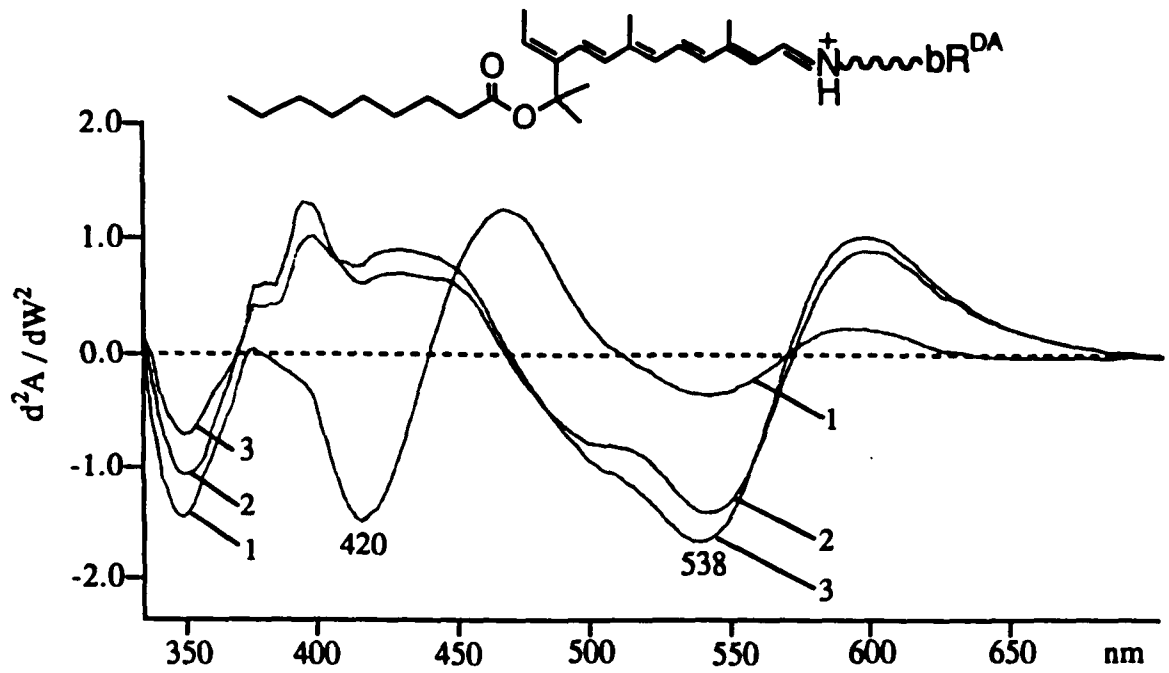

1-1min, 2-5min, 3-1hr.

Figure 7. The bR pigment formation with retinal 33, n=7 in the dark measured by second derivative absorbance at 1 min. (1), 5 min. (2) and 1 hr. (3).

5, 6 & 7 show a clear isosbestic points at 460 nm, 500 nm (34, 7C-COOH) and 480 nm (33, n = 6 & 7), respectively, after one minute of the incubation, directly correlated with the growth of the final pigment at the assigned peak. In addition, the spectrum of bR analogs with nine-carbon spacer arm retinal (33, n = 7) showed a fine structural feature at 500 nm which was stable for 24 hours.

5) Addition of 1.5 M NH_2OH to the pigment suspension in the cases of retinals 33, n = 5 and n = 7 and retinal 34 caused a slow decrease of the pigment absorption, as shown in Figures 8, 9 and 10, respectively, indicative that these spacer-armed-retinal pigments were remarkably stable in the presence of NH_2OH.

6) In the cases of retinal 33, n = 5 and retinal 34 pigments, the unbound and bound chromophores were extracted with hexane and methylene chloride respectively, as outlined in Scheme 1. During this process, the temperature of the solution was kept at 0 °C-4 °C to minimize the retinal isomerization. After concentration of the CH_2Cl_2 phase, the nature of the bound chromophore was examined by HPLC. HPLC profiles of the extracts showed that the chromophore was unchanged during the binding experiment.

Discussion. The introduction of a series of saturated carbon chains through an ester linkage to hydroxylated seco-ring retinal 15a imposed such a steric bulk at C(6) position or at the side-chain that the compound adopted the less sterically hindered geometry which 5-ene coplanation to the polyene

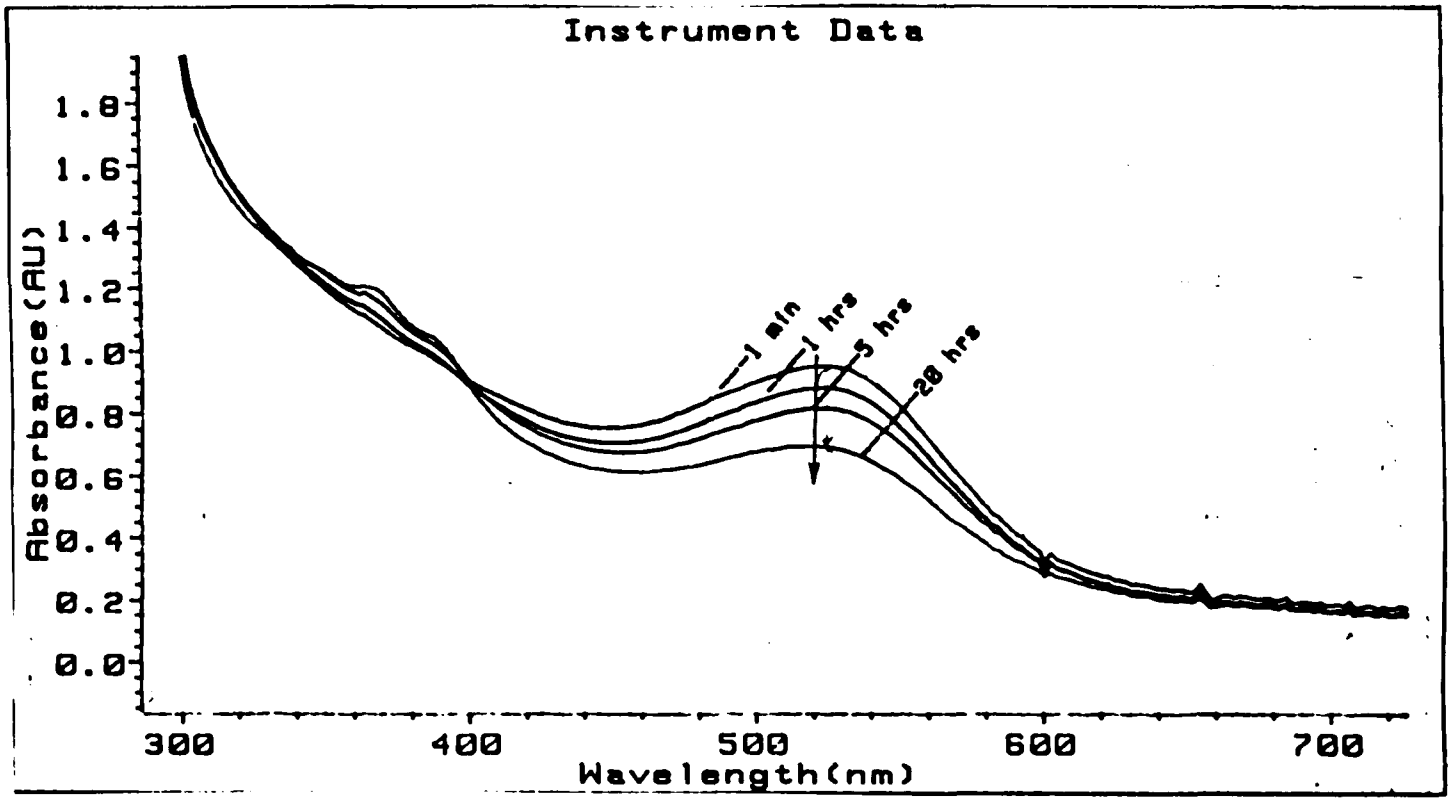

Figure 8. The stability of the 33, n=5 bR pigment in 1.5 M NH_2OH measured by the decrease of a 530 nm absorption band.

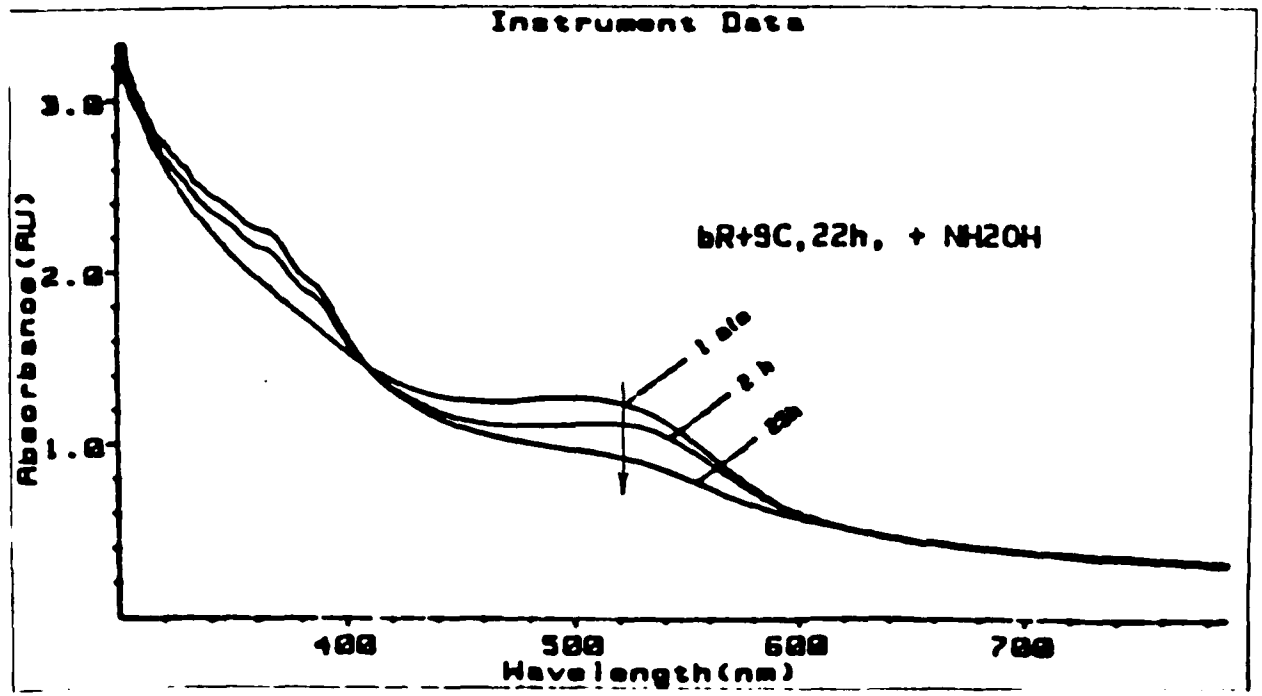

Figure 9. The stability of the 33, n=7 bR pigment in 1.5 M NH_2OH measured by the decrease of a 530 nm absorption band.

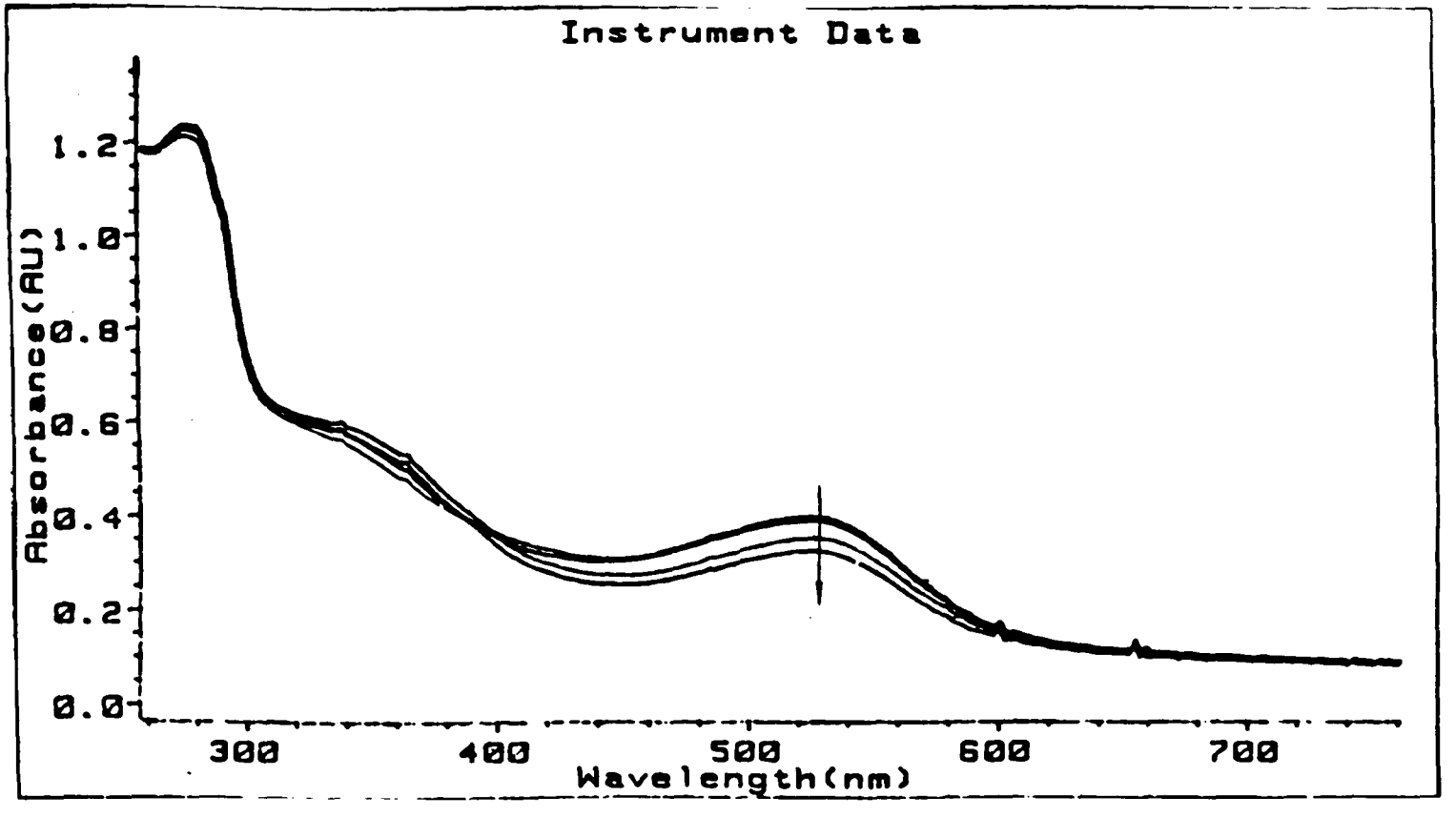

Figure 10. The stability of the 34 bR pigment in 1.5 M NH_2OH measured by the decrease of a 530 nm absorption band at 0 min., 1 min., and 2 hrs. to 5 hrs..

side-chain occur, exhibited longer absorption maximum and vibrational fine structure. However, the seven-carbon-chain retinal with a terminal carboxylic acid group 34 did not show a fine structure in the UV spectrum. Presumably, there might be a intramolecular hydrogen bonding between both terminal polar group which made 5-ene coplanar to the polyene side-chain to less extent, see Figure 11.

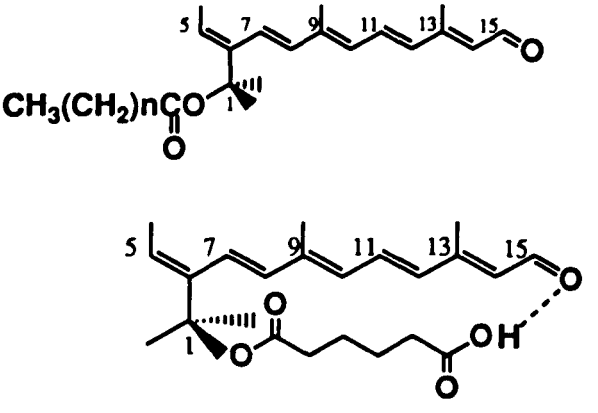

Figure 11. The Structural Formula of Retinals 33 and 34

Seco-ring retinals 15a, 33 (n = 2, 3, 4, 5, 6 & 7) and 34 were efficiently bound to bR apoprotein to form pigment analogs which absorbed

maximally at 530-536 nm, while the ten-carbon spacer arm retinal analog (33, n = 8) was not bound to bR opsin. The yields of pigment regeneration were moderate (40%-60%). The bR analogs formed from all seco-ring retinal analogs inhibited native pigment formation when the all-trans retinal was added. These results suggest that the ring-binding site in bacteriorhodopsin is very flexible, bR apoprotein can accept either planar or nonplanar ene systems, and the native binding site of the chromophore in bacteriorhodopsin is fully occupied by the seco-ring retinal analogs. Compared to native bR pigment absorption, a nearly 30 nm blue shift could be observed with these bR analogs, consistent with an external point charge near the ß-ionone ring.

The similarity in the CD spectra of the native bR pigment and the pigment formed with retinal 33, n = 5 (see Figure 4.) indicated that the additional spacer arm generated little disturbance in the structure of the purple membrane and that the protein-chromophore interactions in both cases are identical. The negative and positive Cotton effects in the observed CD spectra are attributed to the effect of a coupled oscillator type of interaction between the three retinal moieties and the three protein molecules in the bR crystalline lattice.[334] Further, that these spacer-armed pigment analogs caused little distortion of the native protein conformation is denoted by the striking stabilities of the Schiff base linkages when treated with 1.5 M NH_2OH.

Strong pigment generating efficiency of retinals 33, n = 2-7, fitting inside the membrane at the native ß-ionone-ring binding site as they do, is

consistent with the current model of bR which indicates that the orientation of the retinal in the purple membrane is tilted toward the exterior surface of the membrane.[335-337] The spacer arm appears to be situated in the interhelical space. The inhibition of binding of retinal 33, n = 8 (ten-carbons spacer arm) to bR opsin appears to indicate nine-carbons from the ester linkage is sufficient for the chromophore to reach the exterior surface of the membrane, as shown in Figure 12. A definite length of hydrocarbon chain can not be simply calculated, due to solvent effects on the conformation. [338] Theoretical calculation indicates that the gauche conformation is more acceptable in condensed phases. Further, the conformation of the spacer arm in the membrane might be even more complicated and the chain might be constricted by the helical segments of the protein. Thus, the depth of the external surface from carbon-2 of the ß-ionone ring can be estimated based on: 1) the functional similarity of be analogs generated from seco-ring-spacer-arm retinals to the native pigment; 2) the similarity in stability of the membrane structure and the binding-site structure from primary binding studies; and 3) the C-C bond length in an aliphatic chain (zigzag) is 1.25 Å.[339] For retinal 33, n = 7, this value is 11-12 Å, as outlined in Figure 13, in excellent agreement with a current 3-D model from the high-resolution electron microscopy work of R. Henderson and co-workers,[337] which has been extensively applied in the study of the protein.

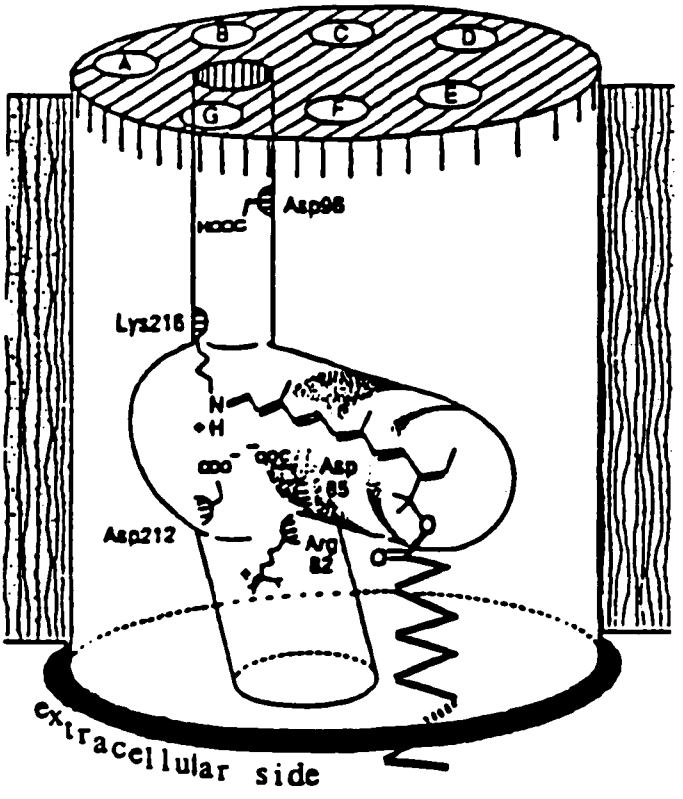

Figure 12. A three dimensional view of the retinal binding site for the pigment analog in bacteriorhodopsin, based on R. Henderson's model for the structure of bR in *J. Mol. Biol.* **1990**, *213*, 899-929.

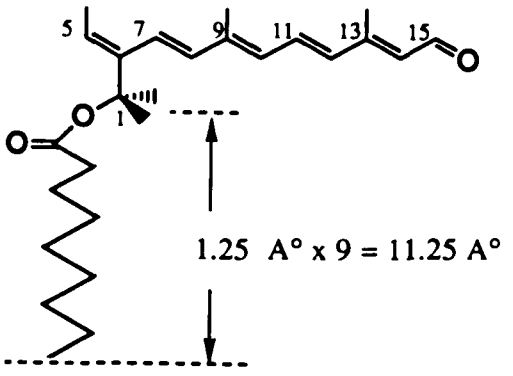

Figure 13. The Distance Between the Ring Site & the Membrane Surface

Binding to Bovine Opsin

Preparation of Opsin. Visual pigment analogs can be generated by the addition of synthetic retinal analogs to bleached rod outer segments (ROS) or opsin in suspension or in detergent solution.[340] Bovine ROS were isolated from fresh retinae by a conventional sucrose stepwise gradient method as described by Papermater [341,342], as briefly outlined in Scheme 3. The ROS thus obtained was suspended in 67 mM phosphate buffer pH 7.0 and was bleached by irradiation with a 750 W projector light beam at 0 °C in the presence of 100 mM hydroxylamine at pH 6.5, to give retinal oxime and opsin, with a color change from pink to white in five minutes. After being washed six times with 10 mM HEPES [N-(2-hydroxyethyl)piperazine-N'-2-ethanesulfonic acid] [343] buffer at pH 7.0 to remove the retinal oxime, the white pellet was dissolved in 10 mM CHAPSO/10 mM HEPES {CHAPSO: 3-[(3-cholamidopropyl)dimethylammonio-2-hydroxy-1-propanesulfonate, a non-denaturing zwitterionic detergent with a CMC (critical micelle concentration) value of 8} [344] and the opsin thus obtained was used for further experiments.

Isomerization of All-Trans Retinal. The native chromophore of bovine rhodopsin is 11-cis retinal, although the other cis isomers, such as 9-cis, 7-cis and their di-cis and tri-cis (except 13-cis) and all-trans could be

Scheme 3.

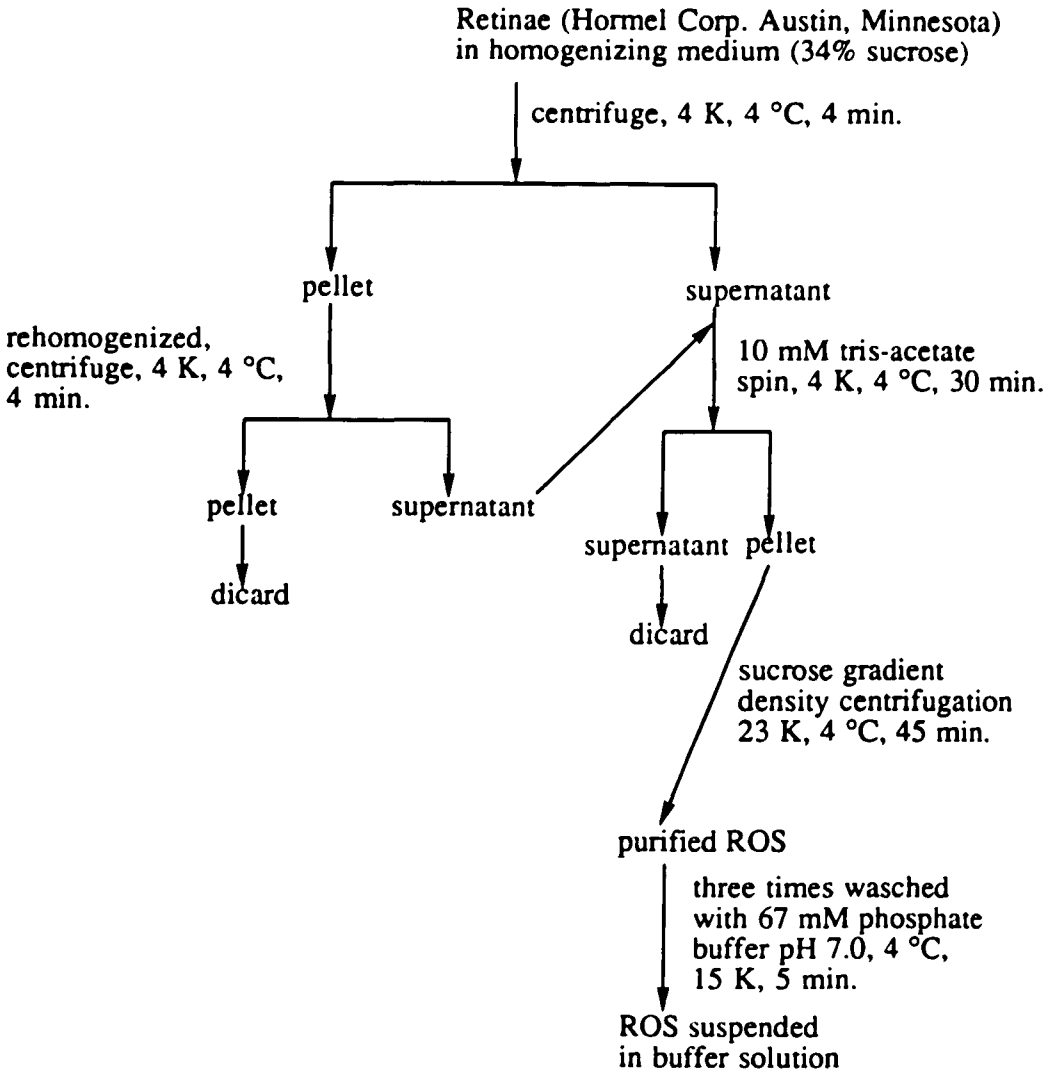
Retinae (Hormel Corp. Austin, Minnesota)
in homogenizing medium (34% sucrose)
centrifuge, 4 K, 4 °C, 4 min.
pellet
supernatant
rehomogenized,
centrifuge, 4 K, 4 °C,
4 min.
10 mM tris-acetate
spin, 4 K, 4 °C, 30 min.
pellet
supernatant
supernatant
pellet
dicard
dicard
sucrose gradient
density centrifugation
23 K, 4 °C, 45 min.
purified ROS
three times wasched
with 67 mM phosphate
buffer pH 7.0, 4 °C,
15 K, 5 min.
ROS suspended
in buffer solution

formed to pigments.[345-348] The observed geometric specificity of opsin could be explained by a two-dimensional projector map. [349,350] The majority of cis isomers of synthetic retinal analogs were obtained by direct irradiation of the corresponding all-trans chromophores, and all isomers could be isolated by HPLC. However, the distribution of the major isomers of the retinals after isomerization by light is dependent upon excitation energy, irradiation time, solvent and concentration in different cases.[351-356] Isomerization experiments with all-trans retinal, C(13)-demethyl-all-trans retinal, and 7C-seco-ring-all-trans retinal: 33 (n = 5) were carried out by using a 750 W projector light beam with a 374 nm-cut-off glass filter. The results are summarized in Table 2, and HPLC patterns of the isomerized all-trans chromophore are indicated in Figures 14, 15 and 16.

Table 2.

Retinal:	all-trans retinal				
Peak #:	1	2	3	4	5
%:	17.8	22.2	18.2	4.7	34.2
Isomer:*	13-cis	11-cis	9-cis	--	trans

Retinal:	13-demethyl retinal			
Peak #:	1	2	3	4
%:	14.9	26.6	18.5	39.7
Isomer:*	11-cis	9-cis	13-cis	trans

Retinal:	retinal 33, n=5					
Peak #:	1	2	3	4	5	6
%:	4.3	2.68	32.1	20.9	8.1	30.1
Isomer:	--	--	9-cis & 11-cis		--	trans

*: The isomers were identified from ^{1}H NMR decoupled experiments.

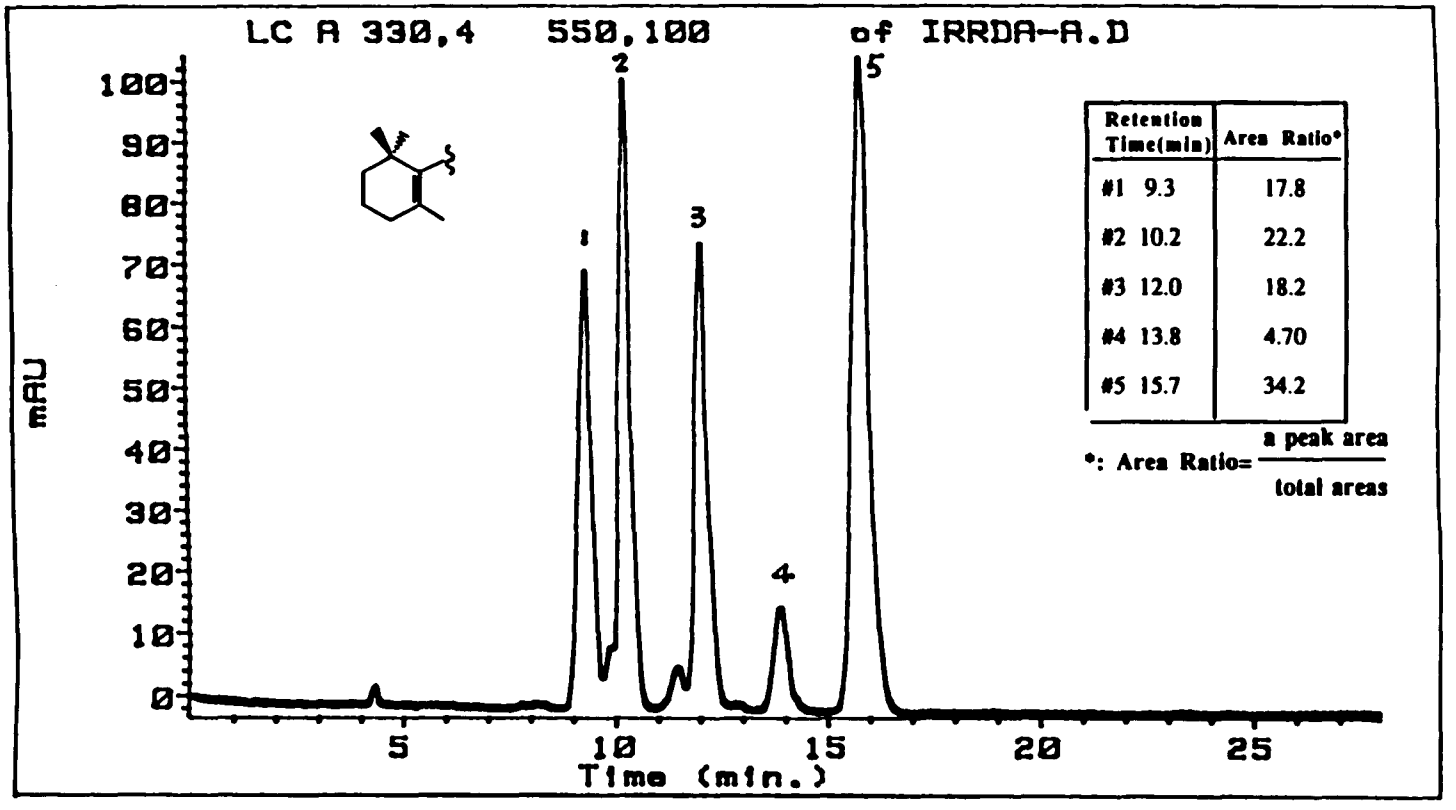

Figure 14. HPLC profile of the isomerization products of all-trans retinal in CH_3CN using a 750 W projector beam with a 374 nm cut-off glass filter. Column: μ-Porasil: solvent: 8% ether in hexane; 1 ml/min; HP 1090 Diode Array detector.

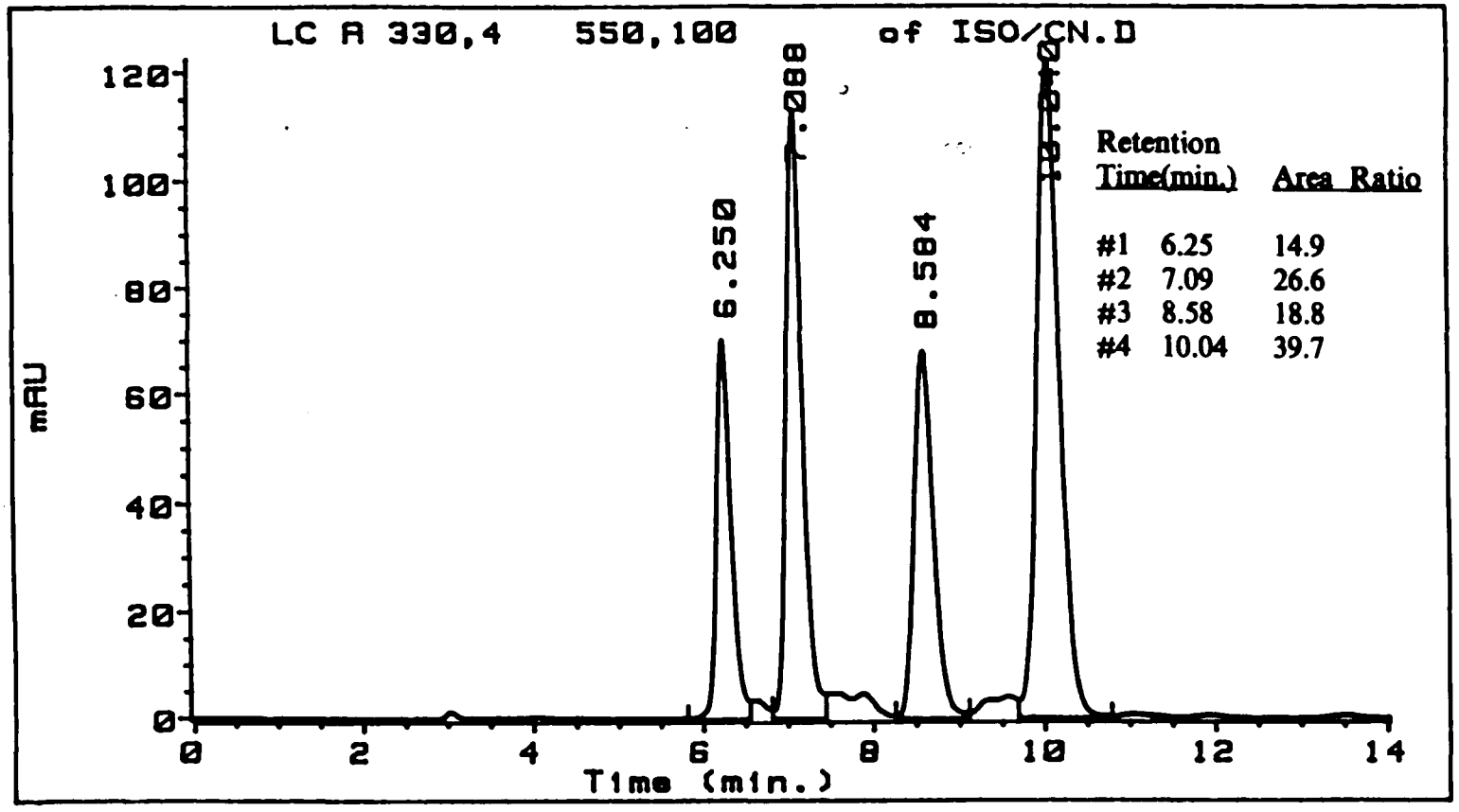

Figure 15. HPLC profile of the isomerization products of all-trans-13-demethyl retinal in CH_3CN using a 750 W projector beam with a 374 nm cut-off glass filter. Column: μ-Porasil: solvent: 10% ether in hexane; 1 ml/min; HP 1090 Diode Array detector.

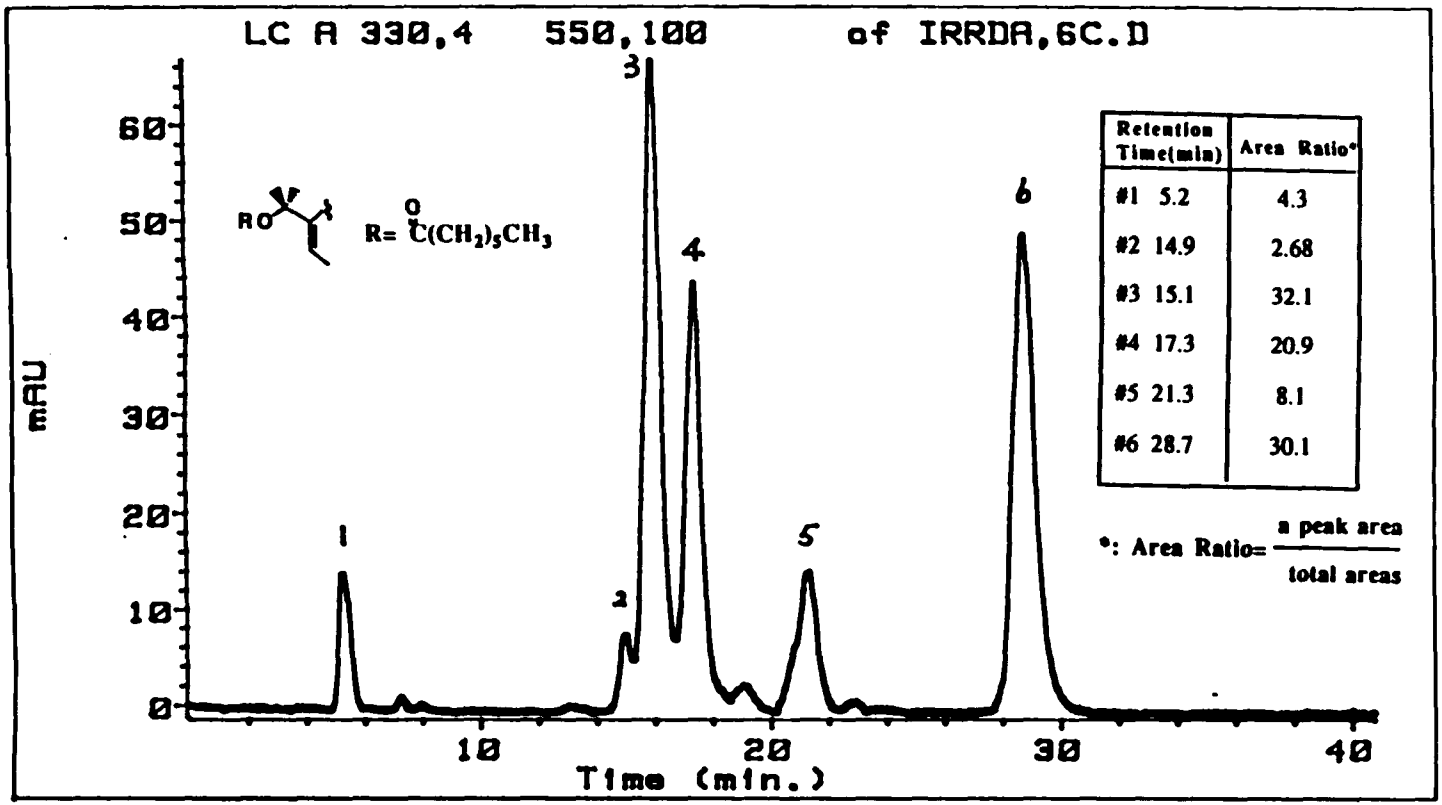

Figure 16. HPLC profile of the isomerization products of retinal 33, n=5 in CH_3CN using a 750 W projector beam with a 374 nm cut-off glass filter. Column: μ-Porasil: solvent: 5% ether in hexane; 1 ml/min; HP 1090 Diode Array detector.

Binding of Cis Isomers of 7C-Spacer-Armed Retinal 33. Two cis isomers of 7C-spacer-armed retinal 33, n = 5, from isomerization of the corresponding all-trans isomer (R.T. = 15 min. & 17 min., peaks #3 & #4) were dissolved in 10 μl of ethanol and this solution was added to a 0.5 ml UV sample cuvette containing a solution of bovine opsin in 10 mM CHAPSO/10 mM HEPES in the dark. The OD ratio of the chromophore to opsin was about one to one. The formation of the pigment was monitored by the growth of a 450 nm absorption band in the UV/VIS, as shown in Figure 17. The spectrum contained a contribution due to an excess chromophore at about 380 nm. Completion of the incubation took nearly one hour. After four hours, the native chromophore, 11-cis retinal, in 10ul of ethanol was added to the solution of the pigment analog, and no native pigment absorbance band (500 nm) was observed after twenty four hours. The above experimental results showed that cis isomers of the spacer-armed retinal analog could be efficiently bound to bovine opsin to form the visual pigment analog, and that the native binding site was fully occupied by the retinal analog.

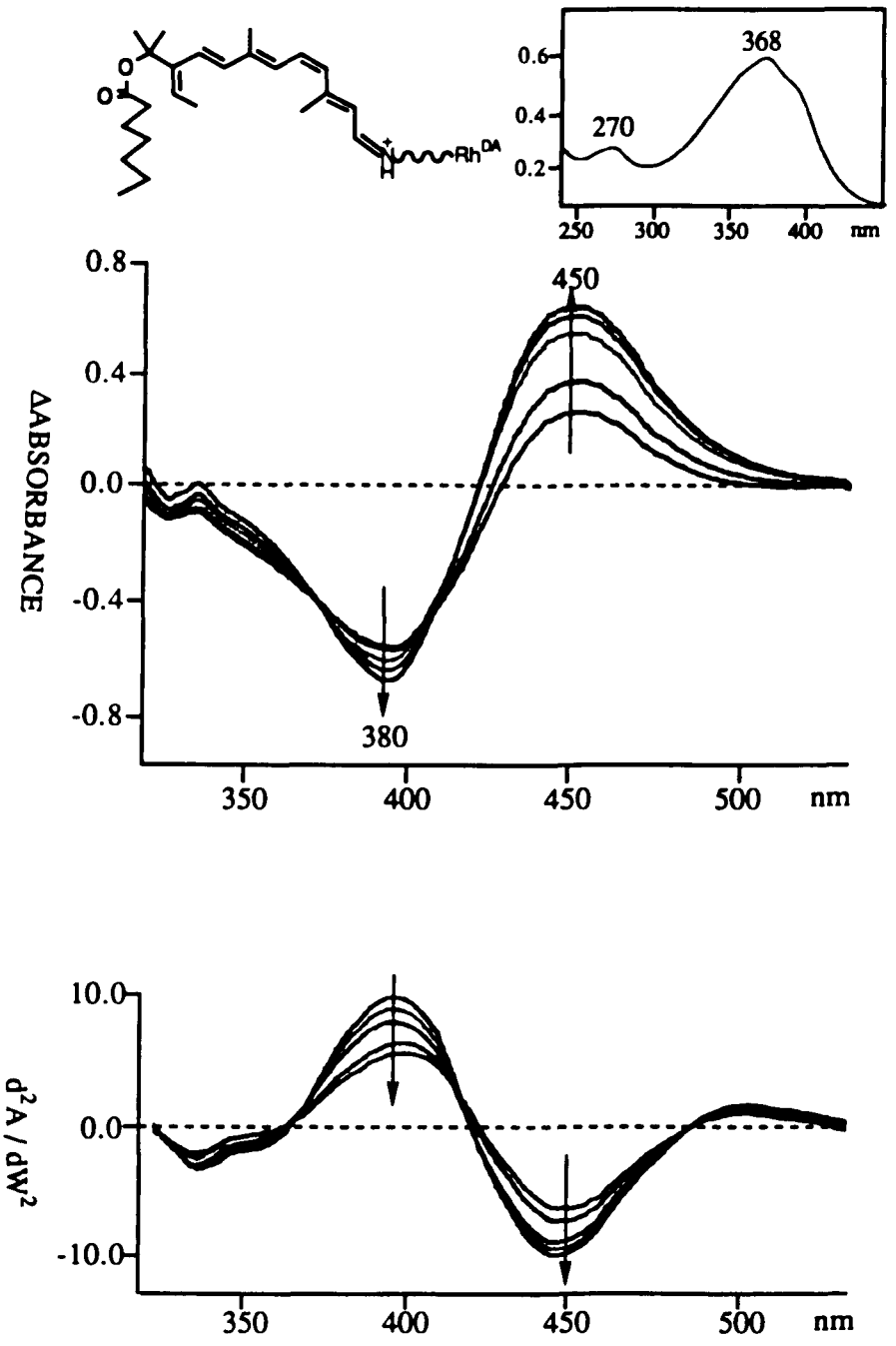

Figure 17. The UV spectrum of cis isomers of retinal 33, n=5 (up right), and their Rh pigment formation by subtraction (above) and second derivative UV/VIS measurement (below).

III. Study in the Synthesis of the Seco-Ring Retinal Analog Attached with a Terminal Photoactive Group.

Based on the study of pigment analogs containing spacer armed chromophores, it has been concluded that these seco-ring spacer armed retinal analogs can be used as a probe for the study of both opsin pigments, due to their functional and structural similarity to the native chromophore (11-cis or all-trans retinal). The binding results have also suggested an approximate distance of 10-12 Å between the ring-site and the surface of the membrane. However, several important questions have to be mentioned, such as whether or not the spacer arm really touches the end of the membrane, and what amino acid residues surround to it. Attachment of a photoactive group, such as a photoaffinity labeling group to the spacer arm would give a tool for the investigation of the tertiary structures of these membrane proteins. The photoaffinity labeling technique has been employed to study enzyme structure and function. [357-363]

Thus, the synthetic route in Scheme 1 was proposed as an approach the spacer-armed retinal analog to which is attached a diazoester group 35. The most synthetically challenging feature of compound 35 is the incorporation of the primary hydroxy aliphatic acid into the tertiary hydroxy moiety in the precursor 15a, due to steric hindrance at that C(1) position. Scriven [364] reported an acylation method in which the addition of a catalytic

amount of 4-dimethylaminopyridine (DMAP) could cause a significant increase

Scheme 1:

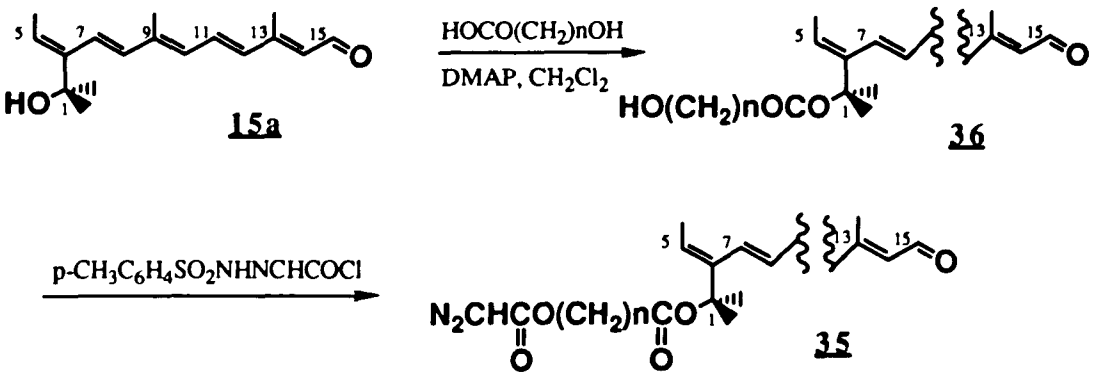

of the acylation product in the reaction of 1-methylcyclohexanol, a sterically hindered alcohol, with acetic anhydride (from 5% yield to 86% yield). In addition, it is also advantageous to utilize DMAP as a catalyst in the acylation of a sterically hindered alcohol with a carboxylic acid in the presence of dicyclohexylcarbodimide (DCC).[365] The further preparation of diazoester 35 could be performed by the method described by Corey and Myers. [366]

Synthesis of a Seco-Ring Spacer-Armed Retinal with an Attached a Diazoester Group 35 from the Precursor 15a.

δ-(t-Butyl-dimethylsilyloxy)-pentanoic acid 37 , as shown in Scheme 2, was obtained by the treatment of δ-valerolactone with lithium hydroxide (LiOH) and hydrogen peroxide (H_2O_2), followed by 2,6-lutidine and *tert*-butyldimethylsilyl triflate (t-$BuMe_2SiOSO_2CF_3$), in only 30% isolated yield. [367]

Acylation of the precursor 15a with the acid 37 was carried out in the present of DCC and DMAP at room temperature for twenty-four hours. It was found from TLC monitoring that the yield of this reaction was very low. After cleavage of the protective group by $nBuN^+F^-$ in THF, the intermediate 36, as shown in Scheme 3, was treated with glyoxylic acid chloride p-toluenesulfonylhydrazone in the presence of triethylamine and N,N-dimethylaniline give a new compound, in very low yield, assumed to be diazoester 35.

Scheme 2:

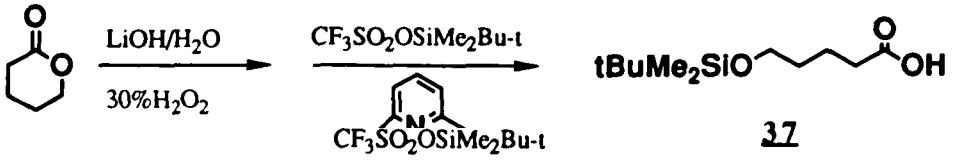

37

Scheme 3:

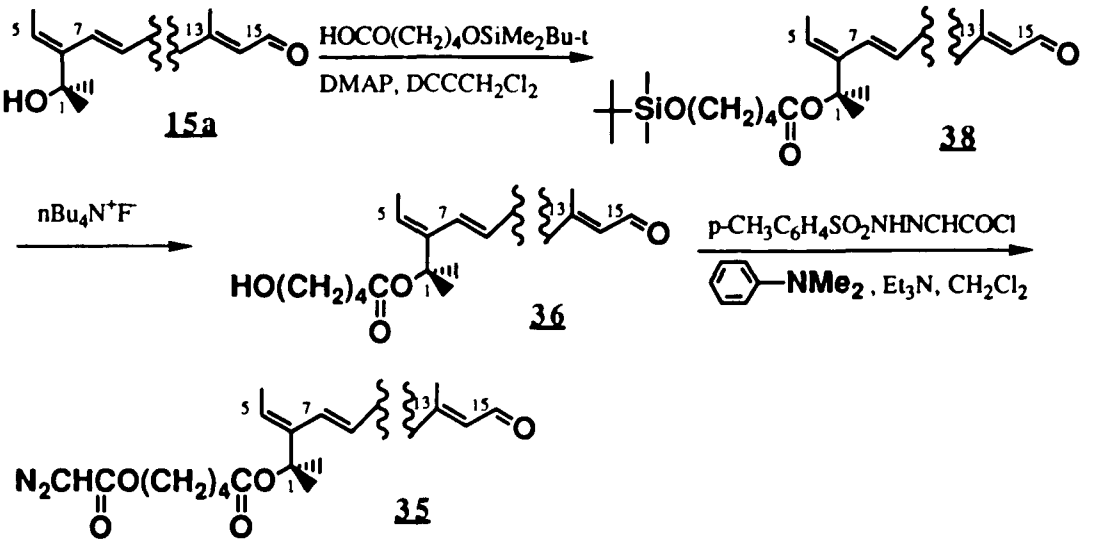

The same acylation reaction was performed on 31 as described in Scheme 4. Again, the yield of the new compound, assumed to be 41, was very low.

Scheme 4:

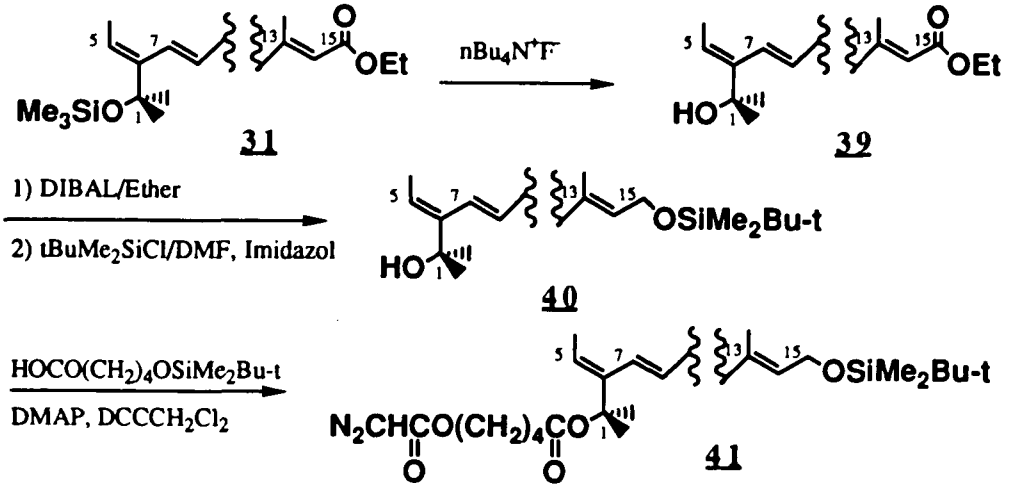

According to Scriven, the reaction mechanism is illustrated in Scheme 5.

Scheme 5:

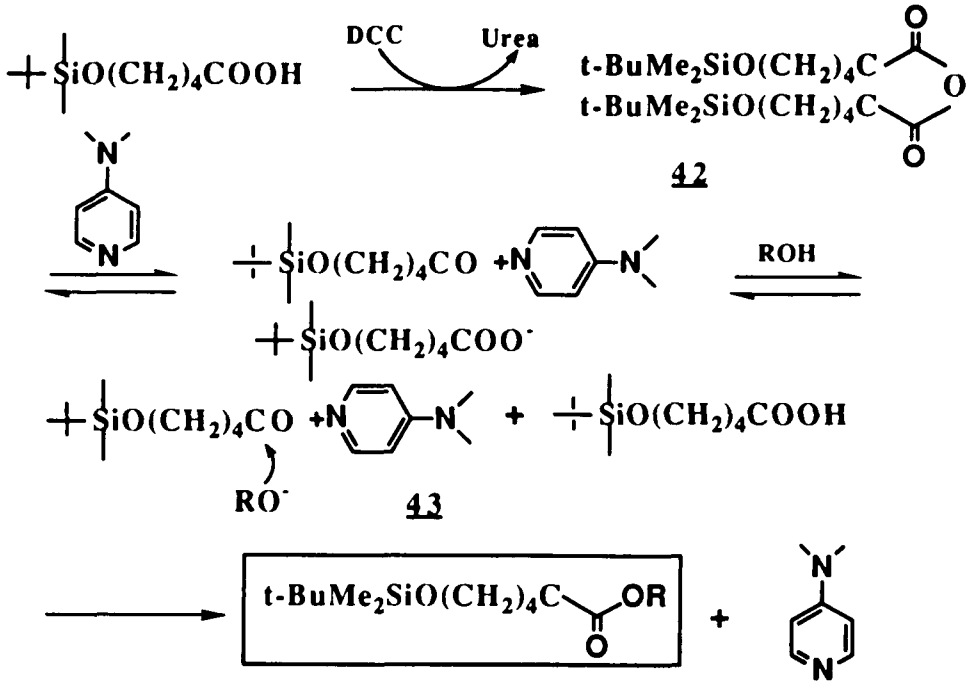

It is likely that the anhydride 42 was formed during the reaction, based the mechanism in Scheme 5, due to the observation of a urea precipitated. It is not clear why acylation of the tertiary hydroxyl group in the precursor 15a was inefficient. It is tentatively assumed that this sterically hindered alcohol could not easily approach the acylpyridinium species 43. Nevertheless, the HPLC purified compounds, assumed to be 35 and 36, was bound to bR opsin, as shown in Figure 1.

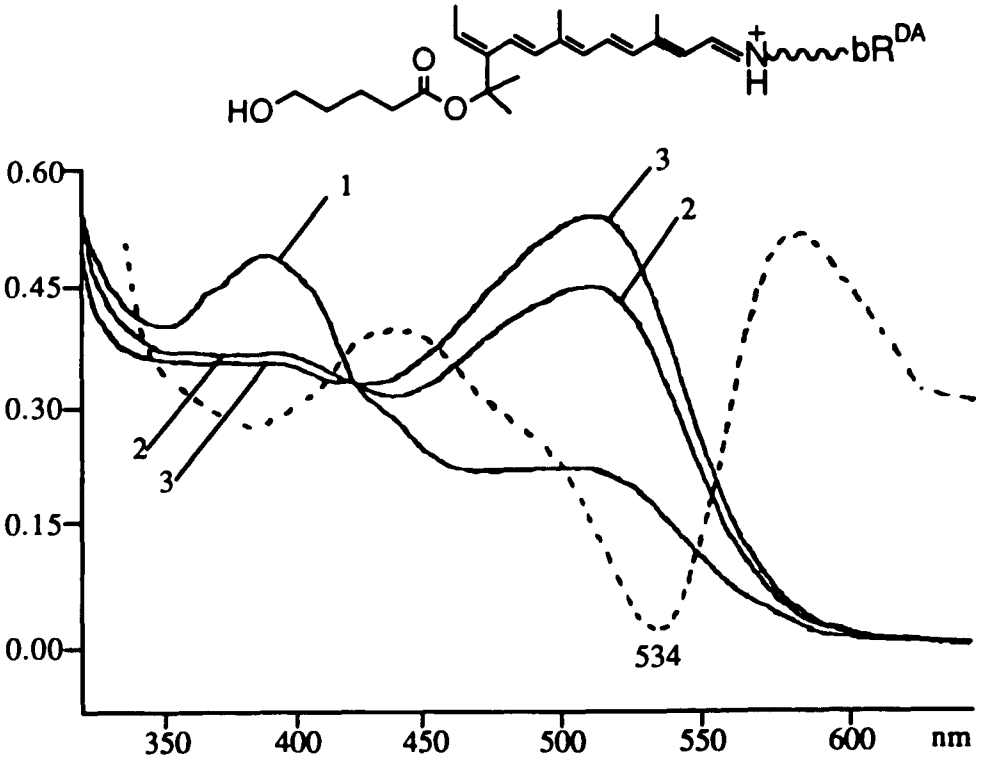

Figure 1. a. The 36 bR formation, as measured by 530 nm UV/VIS band absorption (solide) at 1 min (1), 4 min (2) and 4 hrs (3), and its second derivative spectrum (dash) at 534 nm.

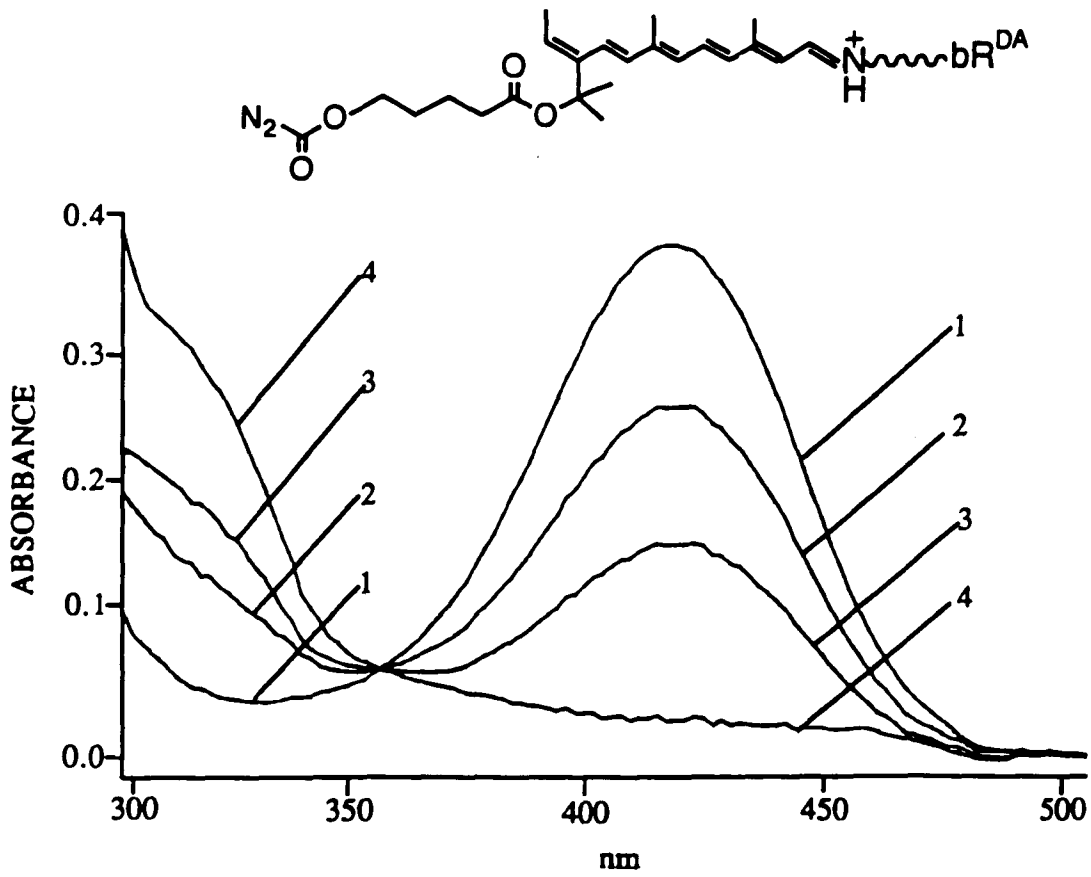

Figure 1. b. The bR analog formed from the diasoester 35 with bR opsin at 1 min (1), 25 min (2), 1 hr (3) and 24 hrs (4).

In order to circumvent the acylation the problem, other approaches have been investigated such as acylation using a lactone, as shown in Scheme 6.

Scheme 6:

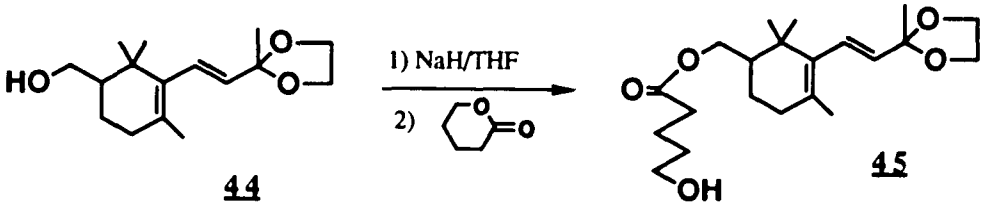

44 45

Compound 44 was treated with sodium hydride (NaH) in THF at 0 °C, and then after two hours at room temperature, the δ-valerolactone was added to the reaction mixture at 0 °C. Work-up provided a 16% yield of compound 45 and 80% recovery of unreacted compound 44. It was assumed that the yield of the reaction could be increased under different reaction conditions The same type of reaction was attempted with compound 40, as outlined in Scheme 7. Unfortunately, the reaction of compound 40 with sodium hydride or n-butyllithium and the lactone produced a mass of products which were hard to isolate and identify.

Scheme 7:

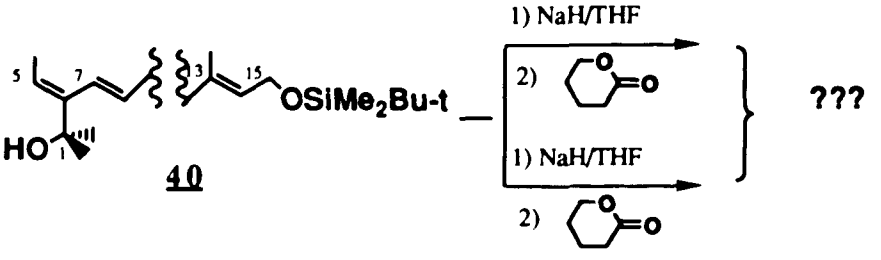

40

Another Approach to a Spacer Armed Retinal Bearing A Terminal Diazoester.

The introduction of an alkyl chain via an ester linkage to an effective precursor containing a primary instead of a tertiary hydroxyl group as in compound 15a, might be considered as an alternative way to accomplish the synthesis of a spacer-armed retinal bearing a terminal diazoester substituent. The synthetic route to the key precursor 48 was designed as outlined in Scheme 8, based on the following considerations.

Scheme 8:

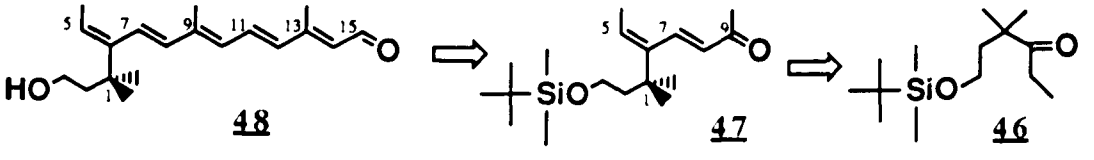

48 47 46

First, 1-*tert*-butyldimetylsilyloxy-3-dimethylhexan-4-one 46 should be readily converted to a useful vinyl triflate and followed by the Heck-olefination sequence, as discussed in Part I of this section, should afford key

intermediate 47. Second, the conjugated ketone 47 should be efficiently coupled with a lithium salt of trimethylsilylacetaaldehyde t-butylimine, followed by Wittig reagent from phosphonosenecioate 8. Then DIBAL reduction and MnO_2/Celite oxidation would provide 1-hydroxypropyl-seco-ring retinal 48 which would be readily acylated by the method of Scriven.

Preparation of Hexanone 46. 4,4-Dimethyl-5-hexen-3-one 49 in

Scheme 9:

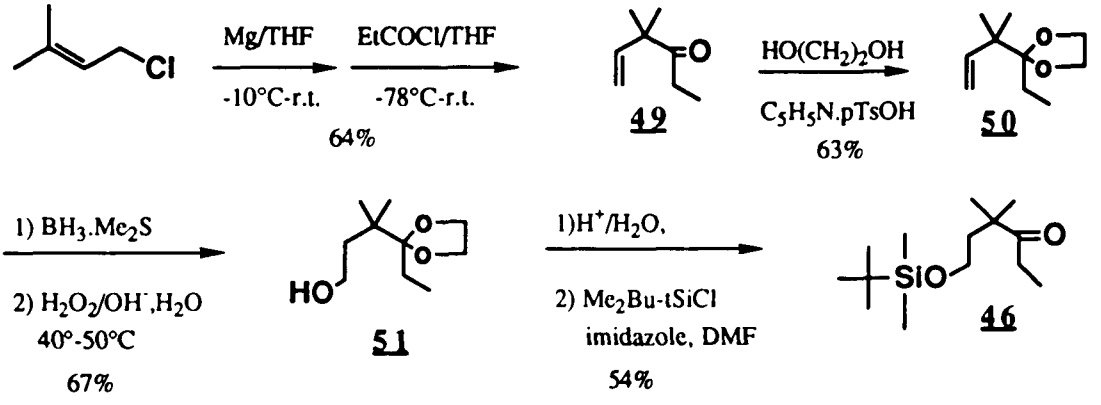

Schemer 9 was obtained in 64% yield by coupling the Grignard reagent of prenyl chloride with propanoyl chloride in THF.[368] The protection of ketone 49 was accomplished in 63% yield after distillation by treatment with ethylene glycol [$HO(CH_2)_2OH$] in benzene, using pyridinium *p*-toluenesulfonate ($C_5H_5N.p$-TsOH) as a catalyst.[369] The transformation of the double bond in

ketal alkene 50 to the primary alcohol 51 was performed by hydroboration with $BH_3{\cdot}Me_2S$ followed by H_2O_2 oxidation in aqueous NaOH in 67% yield after distillation. The ketal was hydrolyzed by treatment with acidic aqueous acetone and protected ketone 46 was obtained in 54% yield by treatment with Me(t-Bu)SiCl-Imidazole in DMF. Thus the total synthesis of hexanone 46 was achieved in four chemical steps and in 14.6% overall yield from prenyl chloride.

Synthesis of All-Trans Dieneheptanone 47. Following the success in the synthesis of the dienones 29a and 29b from the corresponding enol triflates 28a and 28b, followed by palladium-catalyzed coupling (Heck-reaction) with methyl vinyl ketone, we predicted that the preparation of the heptenone 47 could be performed in the same reaction fashion, as outlined

Scheme 10:

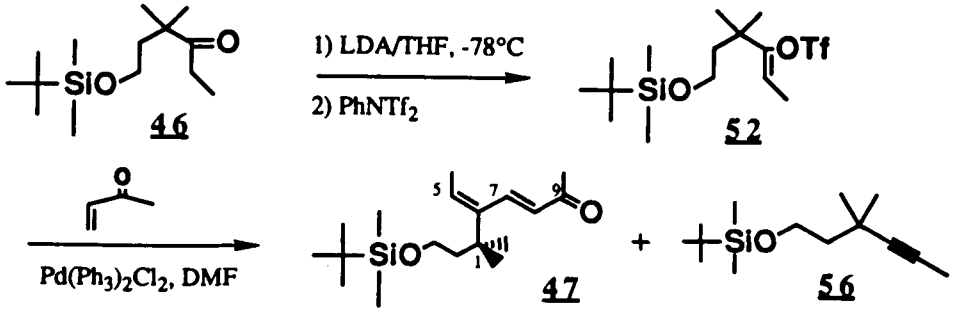

in Scheme 10. Thus, ketone 46 was treated with LDA in THF at -78 °C followed by the addition of $PhNTf_2$. The reaction mixture was stirred for 48 hours at room temperature. Several points regarding the reaction leading to enol triflate 52 deserve explicit mention. First, enol triflate 52 decomposed during purification by distillation, due to a high boiling point (>100 °C / 0.0 mmHg), indicative that this enol triflate is thermally labile. Secondly, purification of enol triflate 52 could be accomplished by silica gel column chromatography, but unexpectedly, the yield of compound 52 was only reached 50% based on the recovery of starting ketone 46 and another unknown product 56 which was present in the reaction mixture in the same amount as enol triflate 52. ^1H NMR analysis of enol triflate 52 and the structure of product 56 are indicated in Figure 2. ^1H NMR analysis of the

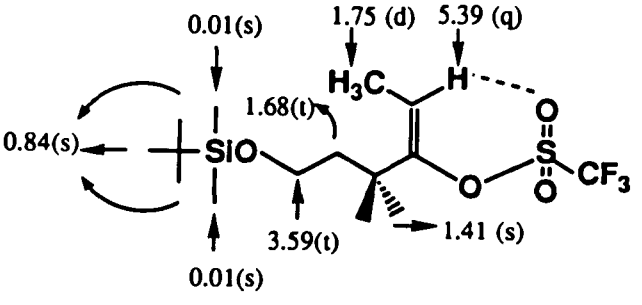

52

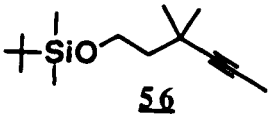

56

Figure 2. ^1H NMR of enol triflate 52, and the structure 56.

unexpected product 56 showed notrace of vinyl proton (5.39 ppm, q) or the doublet pattern of the vinyl-methyl group was observed. Instead, the resonance of the $\underline{OCH_2}$ moved down field to 3.78 ppm and a singlet 1.75 ppm was clearly observed. In addition, compound 56 was surprisingly found as the major product in the further Heck-reaction enol triflate 52 with methyl vinyl ketone catalyzed by $Pd(PPh_3)_2Cl_2$ in DMF at 75 °C.

The normal Heck-reaction occurs though a mechanism described by Scott and McMurry,[370] as shown in Figure 3. The Heck reaction starts

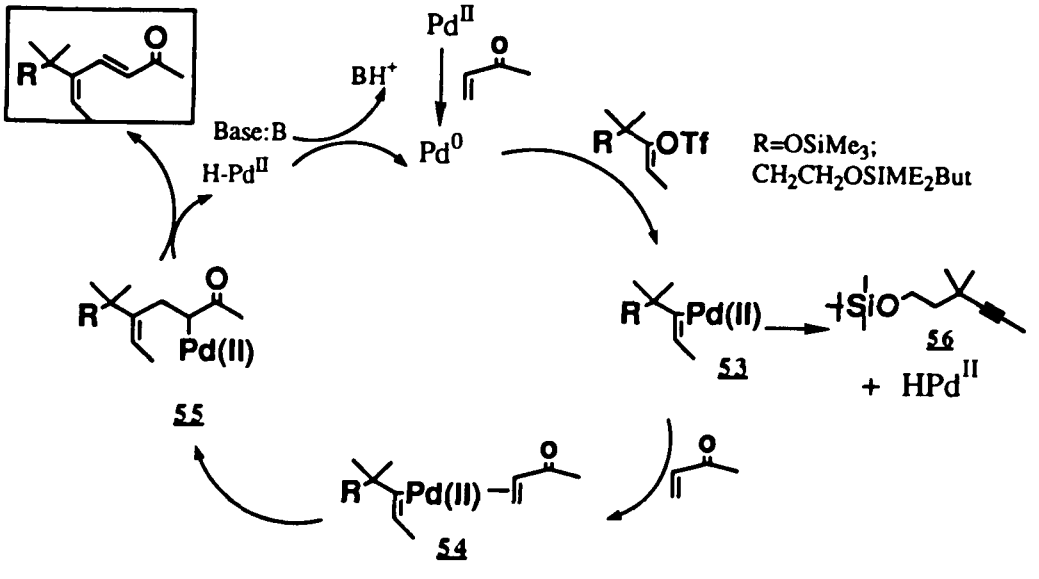

Figure 3. The mechanism of the Heck reaction.

from the reduction of the palladium(II) ($Pd(Ph_3)_2Cl_2$) catalyst to a palladium(0) species by the olefin, methyl vinyl ketone in this case. The oxidative addition of the triflate as an electrophile affords a palladium(II) species, 53, which is coordinated with methyl vinyl ketone to give the species 54. Successive intermolecular insertion of the carbon-carbon double bond of methyl vinyl ketone into the carbon-palladium bond in the vinyl palladium intermediate 54 and dehydropalladium ($-HPd^{II}$) from the palladium(II) species 55 afford the desired dienone product. Unfortunately, the coupling reaction of the enol triflate 52 with methyl vinyl ketone gave 56 as the major product, indicated in Scheme 11, and a tiny amount of the coupling product 47. Presumably, the oxidative-addition product 53 from the enol triflate 52 gave 56 by

Scheme 11:

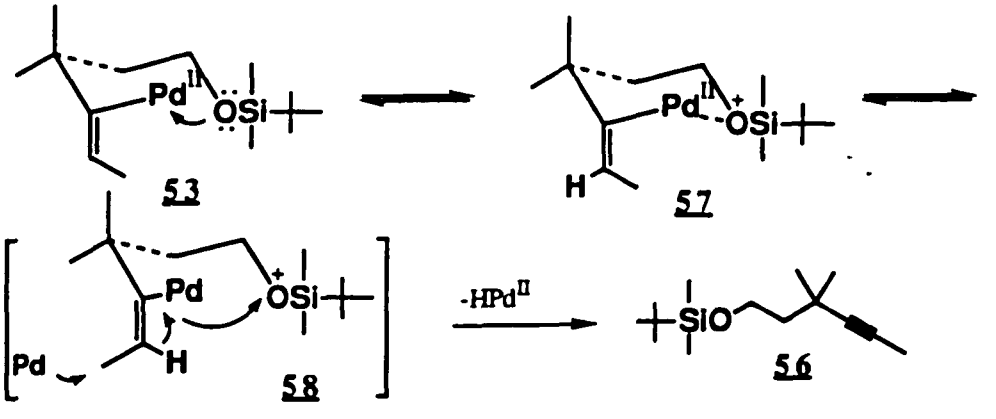

reductive elimination, perhaps with the assistance of the neighboring siloxy oxygen. In addition, the same compound 56 was a by product in the

formation of triflate 52.

The same results were achieved from the similar reaction shown in Scheme 12.

Scheme 12:

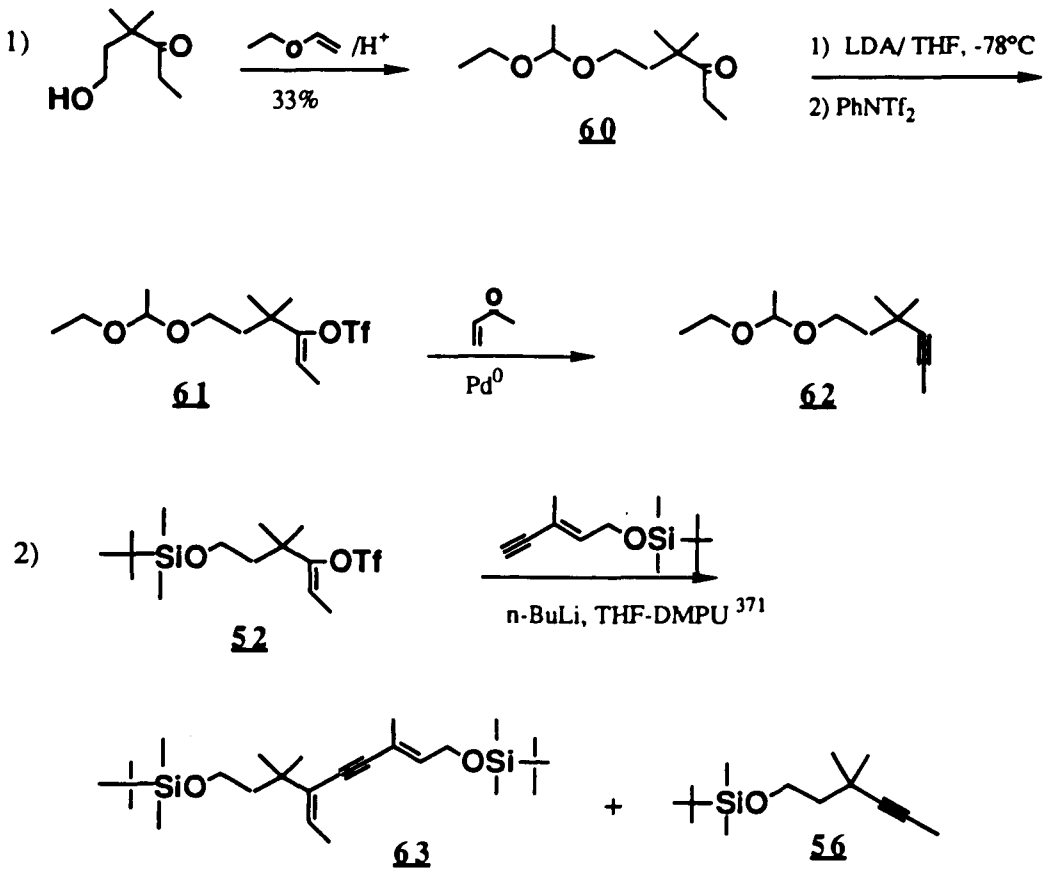

The attempted preparation of dienone 47 by the Heck reaction was impractical due to the formation of the undesired major product 56. In order to circumvent this problem, a different synthetic approach was tried, described in Scheme 13.

Scheme 13:

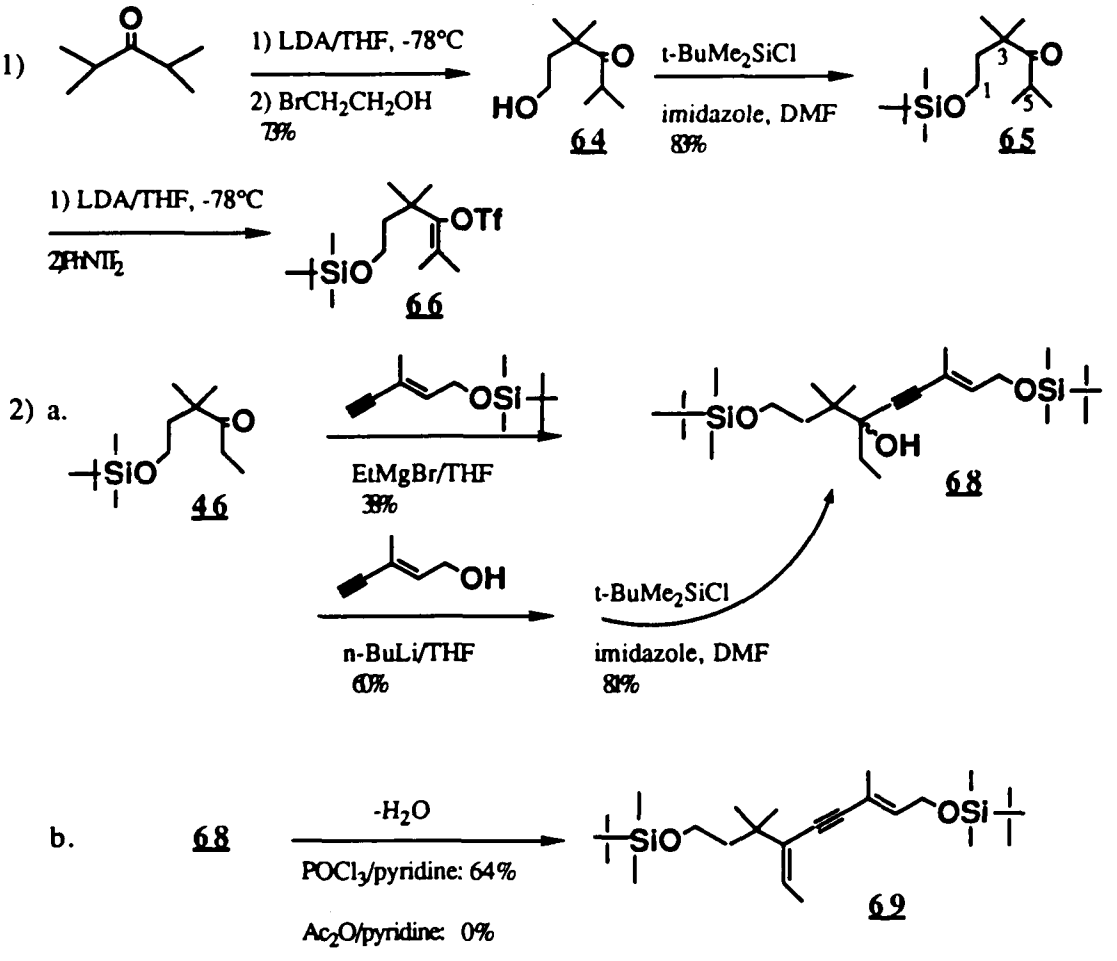

2,4-Dimethylpentan-3-one in Scheme 14 was selected as a starting material containing one more methyl group at C(1) than the ketone 46, so as to prevent dehydro-palladation before coordination with methyl vinyl ketone in the Heck reaction. The ketone 65 was readily obtained from two chemical steps in 73% and 83% yield respectively, as shown in the scheme. The preparation of triflate 66 was carried out under the same reaction conditions as described before. Unfortunately, the majority of the starting ketone was reisolated, presumably due to the steric bulk of the methyl groups.

However, examination of the dehydration methodology required the double bond at C(5) (numbering as in retinal) showed that this method might be considered as an alternative way to overcome the problem encountered in the Heck reaction, despite the fact that the choice of dehydration reagent and reaction conditions were very critical in this conjugated system, based on previous experiences.

The key intermediate 68 as shown in Scheme 14(2) was obtained by the condensation o hexanone 46 with the magnium or lithium salts of the enynol in 38% and 48%, respectively. The subsequent dehydration was performed with two different reagents. The use of $POCl_3$ /pyridine gave a single isolated desired product 69 in 64% yield, whereas Ac_2O/pyridine failed.

It is clear that the seco-ring retinal analog with a spacer arm bearing a terminal diazoester substituent could be elaborated from the dehydrated

product 69 by successive $LiAlH_4$ reduction of the triple bond, cleavage of the protective group and oxidation, Wittig reaction with compound 8, DIBAL reduction and oxidation, and final acylation, as illustrated in Scheme 14.

Scheme 14:

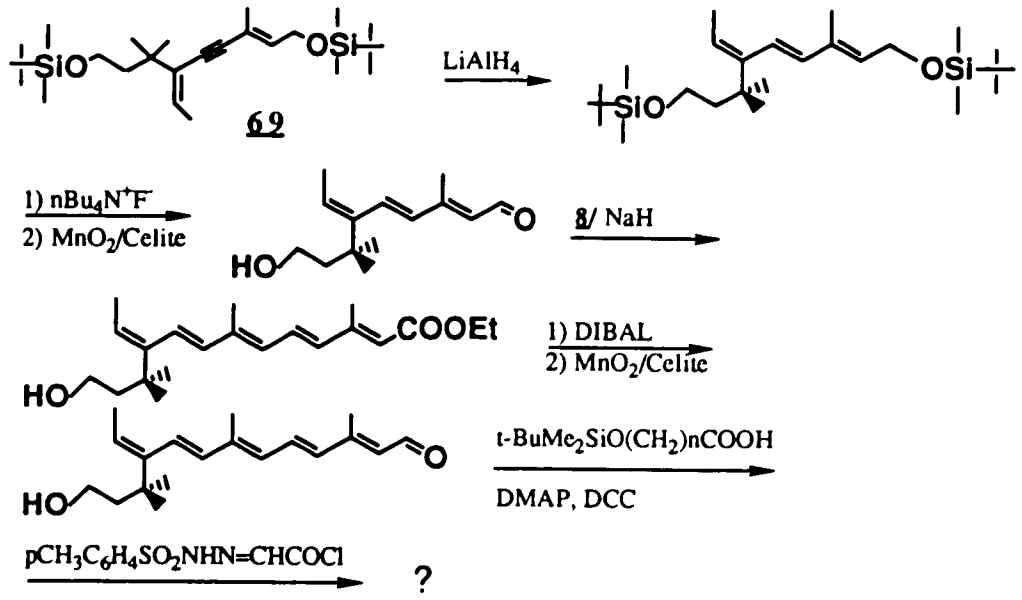

Synthesis of Seco-Ring Retinal 72 from the Ketone 47. The continuation of the full-chain synthesis was carried out by using a tiny amount of the dienone 47 (see Scheme 10), as shown in Scheme 15. The ester 71 was produced by conventional Wittig reaction in 95% yield and, followed by DIBAL reduction and MnO_2/Celite oxidation afforded the corresponding aldehyde 72. Unfortunately, the aldehyde 72 could not be characterized due

to decomposition during the final TLC purification.

Scheme 15:

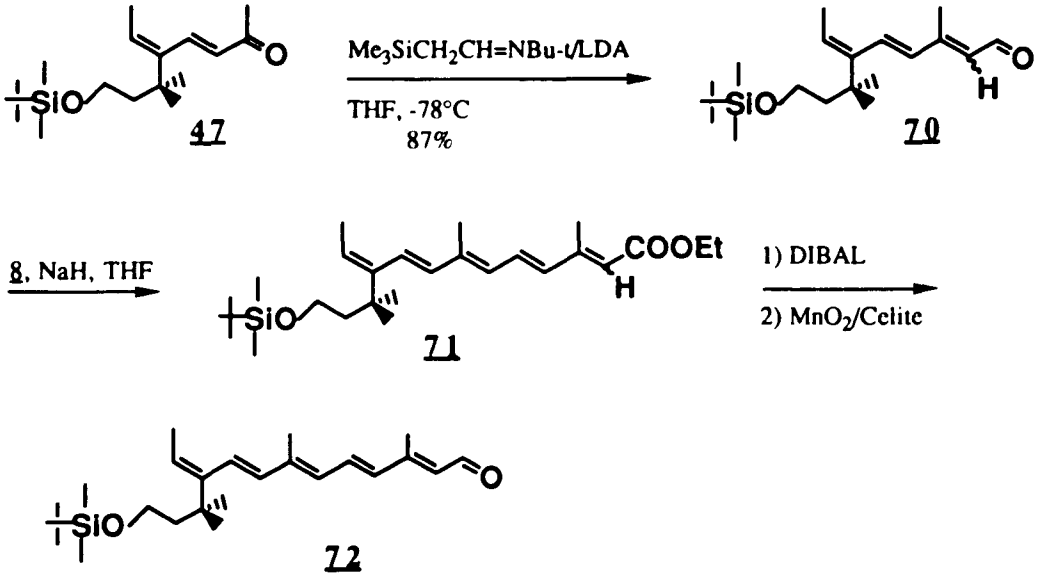

In summary, although it has been shown that the attempted synthesis of seco-ring retinal with a spacer arm bearing a terminal diazoester group was unsuccessful because of the difficulty of acylating a tertiary hydroxyl and the unexpected formation of compound 56, it is clear that a judicious application of the synthetic route outlined in Scheme 14 might give access to the desired retinal analog.

General Data. All air and / or moisture-sensitive reactions were carried out under an atmosphere of nitrogen or argon using flame-dried glassware and standard syringe / septa techniques. Reactions were monitored by thin layer chromatography (TLC) on Polygram O Silg / UV-254 plates. All anhydrous solvents, such as ether, tetrahydrofuran, methylene chloride and N,N-dimethylamine, and most standard chemicals were purchased from Aldrich Chemical Company. Unless otherwise noted, compounds were purified by flash chromatography using Merk Grade 60, 230-400 mesh silica gel, eluting with the indicated solvent system. Boiling points are uncorrected. A Hewlett-Packard HP 1099 high performance liquid chromatography (HPLC) equipped with a μ-proasil column and a Diode Array Detector (DAD) were employed for the purification of retinal analogs. ^{1}H NMR spectra were recorded using a Bruker NMR-300 MHz instrument with $CHCl_3$ (7.24 ppm) as an internal reference in the solutions. ^{13}C NMR spectra were recorded at 75.5 MHz referenced to the central line of the $CDCl_3$ solvent (77.00 ppm). All coupling constants are presented in Hertz (Hz). For ^{1}H NMR spectra, multiplicity is denoted by s (singlet), d (doublet), t (triplet), q (quartet), m (multiplet) and br (broad). For both nuclei, chemical shifts are reported in parts per million (ppm). Ultraviolet-Visible (UV/VIS) spectra were scanned by using a Hewlett-Packard HP UV 8452A fast-scan UV/VIS spectrophotometer and Circular Dichroism (CD) spectra were obtained from an AVIV 60 DS Circular Dichroism spectrophotometer. The preparations of compounds containing more

than two double bonds were performed in the dark room with a dim light.

2-Hydroxyl-3-methylbutyronitrile (2b). To the solution of sodium bisulfite (57.7 g, 0.555 mol) in distilled water (194 mL) at 0 °C was added in one portion precooled isobutyrnaldehyde (40.0 g, 0.555 mol). After additional stirring at 0 °C for 0.5 h, the precooled solution of sodium cyanide (27.2 g, 0.555 mol) in water (84 mL) was added in one portion. The reaction mixture was stirred at 0 °C for 2 h. The resultant white precipitate of sodium sulfite was filtered out and washed with ice water (150 mL). The filtrate was extracted with ethyl ether (3 x 100 mL) and the extracts were dried over $MgSO_4$. The 35.1 g (64%) of the product was obtained by distillation after the pH in mixture was adjusted to 5 with concentrated hydrochloric acid. bP: 113-120 °C (33 mmHg). IR (neat): 3450, 2950, 2250, 1460 cm^{-1}. ^1H NMR: δ 1.03 (d, J = 6.0 Hz, 3H), 1.08 (d, J = 6.0 Hz, 3H), 2.05 (m, J = 6.0, 5.4 Hz, 1H), 2.55 (s, 1H), 4.28 (t, J = 5.4 Hz, 1H). ^{13}C NMR: δ 16.7, 17.2 32.6, 66.5, 118.8.

2-Hydroxybutyronitrile (2a). Yield: 61%. bP: 108-114 °C (30 mmHg). IR (neat): 3420, 2960, 2310, 1460 cm^{-1}. ^1H NMR δ 1.09 (t, J = 7.3 Hz, 3H), 1.88 (td, J = 7.3, 6.3 Hz, 2H), 2.67(s, 1H), 4.43 (t, J = 6.3 Hz, 1H).

2-(1'-Ethoxylethoxy-3-methylbutyronitrile (3, R=Me). To 2-hydroxy-3-methylbuyronitrile (35.1 g, 0.355 mol) and a few drops of

concentrated hydrochloric acid was added dropwise ethyl vinyl ether (38.2 g, 0.531 mol) at a constant temperature of 50 °C. After being stirred at 90 °C for 4 h, the resultant mixture was distilled to give 35.2 g (58%) of the product. bp: 106-108 °C (30 mmHg). IR (neat): 2950, 1460, 1390 cm^{-1}. ^1H NMR δ 1.02 (d, J = 6.8 Hz, 3H), 1.08 (d, J = 6.8 Hz, 3H), 1.18 (t, J = 6.9 Hz, 3H), 1.38 (d, J = 5.3 Hz, 3H), 1.96-2.07 (m, 1H), 3.66 (q, J = 6.9 Hz, 2H), 4.21 (d, J = 6.8 Hz, 1H), 4.88 (q, J = 5.3 Hz, 1H).

2-(1'-Ethoxylethoxy)-butyronitrile (3, R=H). Yield: 64%. bp: 85-87 °C (30 mmHg). IR (neat): 2970, 1425, 1385 cm^{-1}. ^1H NMR δ 1.06 (t, J = 7.5 Hz, 3H), 1.20 (t, J = 6.9 Hz, 3H), 1.36 (d, J = 5.3 Hz, 3H), 1.80-1.90 (m, 2H), 3.66 (q, J = 6.9 Hz, 2H), 4.22 (t, J = 6.5 Hz, 1H), 4.83 (q, J = 5.3 Hz, 1H).

2,4-Dimethyl-2-hydroxypentan-3-one (4, R=Me). To a solution of redistilled diisopropylamine (21.3 g, 0.210 mol) in dry tetrahydrofuran (100 mL) at -10 °C was added dropwise through an additional funnel 1.6 M n-Butyllithium in hexane (128.3 mL, 0.205 mol) under an N_2 atmosphere. The mixture was then cooled to -75 °C and 2-(1'-ethoxylethoxy-3-methylbutyronitrile (35.2 g, 0.205 mol) was added dropwise. After being stirred for an additional 10 min at -70 °C, dry acetone (13.3 g, 0.231 mol) was added dropwise to the reaction mixture. After the completion of addition, the resultant mixture was warmed to 0 °C and poured into water (150 mL). Removal of the volatile organic compounds, extraction of the residue with

methylene chloride (3 x 100 mL) and concentration of the extracts gave a yellow oil. This crude oil was stirred with methanol (88 mL) and aqueous 5% sulfuric acid (44 mL) overnight at room temperature. After removal of methanol, the yellow residue was extracted with ether (3 x 100 mL) and the extracts were shaken in a separatory funnel with 10 N aqueous sodium hydroxide (30 mL) for 15 min. The organic layer was washed with brine (100 mL) and dried over $MgSO_4$. After concentration, the yellow residue was distilled to give 13.4 g (50%) of the product. bp: 60-65 °C (15 mmHg). IR (neat): 3450, 2960, 1700, 1460 cm^{-1}. ^1H NMR δ 1.11 (d, J = 6.7 Hz, 6H), 1.39 (s, 6H), 3.07 (m, J = 6.7 Hz, 1H), 3.84 (br, 1H). ^{13}C NMR δ 19.84, 26.19, 33.91, 76.54, 218.6.

2-Hydroxy-2-methylpentan-3-one (4, R=H). Yield: 63%. bp: 57-65 °C (15 mmHg). IR (neat): 3450, 2960, 1705 cm^{-1}. ^1H NMR δ 1.11 (t, J = 7.2 Hz, 3H), 1.36 (s, 6H), 2.56 (q, J = 7.2 Hz, 2H), 3.77 (br, 1H). ^{13}C NMR δ 7.61, 15.90, 28.56, 76.01, 215.6.

2,4-Dimethyl-2-trimethylsilyoxypentan-3-one (5b). A mixture of 2,4-dimethyl-2-hydroxypentan-3-one (13.4 g, 0.103 mol) and N,O-bis(trimethylsilyl) acetamide (10.5 g, 0.0515 mol) was stirred at 100 °C for 12 h with a reflux condenser under an N_2 atmosphere. Water (8 mL) was added to the resultant semisolid mixture at room temperature and after being stirred for 1 h, hexane (25 mL) was added to the above mixture. The aqueous layer was extracted with hexane (2 x 20 mL). After the combined organic layer was

washed with water (4 x 20 mL), dried over $MgSO_4$ and concentrated, the residue was distilled to give 12.5 g (60%) of the product. bp: 71-82 °C 15 mmHg). IR (neat): 2960, 1710, 1460 cm^{-1}. ^1H NMR δ 0.14 (s, 9H), 1.04 (d, J = 6.5 Hz, 6H), 1.32 (s, 6H), 3.34 (m, J = 6.5 Hz, 1H). ^{13}C NMR δ 2.31, 19.34, 27.53, 33.94, 80.44, 218.6.

2-Methyl-2-trimethylsilyoxypentan-3-one (5a). Yield: 68%. bp: 71-75 °C (15 mmHg). IR (neat): 2960, 1710, 1460 cm^{-1}. ^1H NMR δ 0.14 (s, 9H), 1.01 (t, J = 7.3 Hz, 3H), 1.32 (s, 6H), 2.66 (q, J = 7.3 Hz, 2H). ^{13}C NMR δ 2.23, 7.82, 27.37, 29.18, 76.58, 220.0.

Ethyl 4-bromo-3-methylbutanoate (7). A mixture of ethyl 3-methyl-2-en-butanoate (cis/trans mixture, from Aldrich Chemical Co.) (30.0 g, 0.23 mol) and N-bromosuccinimide (NBS) (30.5 g, 0.17 mol) in dry CCl_4 (60 mL) was heated to reflux in a period of 30 min and after 3 h of reflux and solvent removal, distillation of the crude oil gave 28.6 g of bromobutanoate 7 in 60% yield. bP: 66-70 °C (0.0 mmHg). ^1H NMR (one isomer) δ 1.26 (t, J = 7.2 Hz, 3H), 2.25 (s, 3H), 3.92 (s, 2H), 4.15 (q, J = 7.2 Hz, 2H), 5.93 (s 1H).

Phosphonosenecioate (8). Bromobutanoate 7 (28.6 g, 0.138 mol) was added to triethylphosphite [$(EtO)_3P$] (22.9 g, 0.138 mol) at 100-110 °C in a period of 1 h. The mixture was heated to reflex. After 3 h, distillation gave 26.6 g of cis/trans mixture of phosphonosenecioate 8 in 73% yield. bp: 136-145 °C (0.0 mmHg). ^1H NMR (one isomer) δ 1.34-1.24 (m, 9H), 2.04 (s, 3H),

2.67 (d, J = 23.4 Hz, 2H), 4.18-4.05 (m, 6H), 5.78 (s, 1H).

E 3-methylpenta-3-en-4-yn-1-al (10). E, 3-methylpent-2-en-1-yn-1-ol 9 (1.00 g, 10.4 mmol) in methylene chloride (5 mL) was added to an suspension of MnO_2/Celite (10.0 g, 31.2%, 35.9 mmol) in methylene chloride (25 mL) at room temperature under N_2 atmosphere in a dim light. The completion of the reaction was monitored by TLC [SiO_2, EtOAc/$CHCl_3$ = 1/10] during a 30 min-1 h period. Filtration, solvent removal and purification by a flash chromatography column on silica gel (eluent: EtOAc/$CHCl_3$) gave 0.78 g (80%) of enynal 10, Rf = 0.94. ^{1}H NMR δ 2.28 (s, 3H), 3.46 (s, 1H), 6.23 (d, J = 7.9 z, 1H), 10.03 (d, J = 7.9 Hz). ^{13}C NMR δ 18.26, 85.02, 85.95, 134.9, 139.1, 190.1.

All-trans (and cis) ethyl 3,7-dimethylnona-3,5,7-trien-1-ynoate (11). Phosphonosenecioate 8 (1.97 g, 7.45 mmol) in anhydrous THF (10 mL) was added dropwise to 80% NaH in mineral oil (0.224 g, 7.45 mmol) washed with dry THF three times, and suspended in anhydrous THF (10 mL) at 0 °C. After 30 min at room temperature, the enynal 10 (0.700 g, 7.45 mmol) in anhydrous THF (5 mL) was added dropwise at -10 °C. The mixture was stirred for 3 h at room temperature and was diluted with ether (20 mL). The solution was poured into ice-cooled water (20 mL) and the aqueous phase was extracted with ether (3 x 10 mL). The combined organic phase was washed with brine (20 mL), dried over $MgSO_4$, and concentrated. Flash chromatography on silica gel, eluting with a solution of hexane/ether = 4:1,

gave 1.22 g (85%) of ester 11 , including 65.2% trans and 34.8% cis isomers. Rf = 0.65. UV (λ_{max}, hexane) 330 nm. ^{1}H NMR for trans isomer: δ 1.27 (t, J = 7.1 Hz, 3H), 1.98 (s, 3H), 2.31 (s, 3H), 3.06 (s, 1H), 4.16 (q, J = 7.1 Hz, 2H), 5.81 (s, 1H), 6.28 (d, J = 15.2 Hz, 1H), 6.25 (d, J = 11.7 Hz, 1H), 6.78 (dd, J = 15.2, 11.7 Hz, 1H); for cis isomer: δ 1.27 (t, J = 7.1 Hz, 3H), 1.98 (s, 3H), 2.03 (s, 3H), 3.06 (s, 1H), 4.16 (q, J = 7.1 Hz, 2H), 5.70 (s, 1H), 7.77 (d, J = 15.2 Hz, 1H), 6.61 (d, J = 11.8 Hz, 1H), 6.78 (dd, J = 15.2, 11.7 Hz, 1H).

All-trans (and 2-cis)-3,7-dimethylnona-2,4,6-trien-11-yn-1-ol (12). To a solution of ester 11 (0.90 g, 4.69 mmol) in dry ether (50 mL) was added dropwise 1.0 M DIBAL (10.3 mL, 10.3 mmol), in hexane at -70 °C. After additional 5 min, wet ethyl acetate (5 mL) was added to the reaction mixture and then water (10 mL) at -70 °C, Filtration through a Celite pad at room temperature, extraction of the aqueous phase with ether (3 x 10 mL), drying the combined organic phase and purification by chromatography (SiO_2, eluent; ether/hexane = 1:3) gave 0.724 g of ynol 12 in 95% yield. Rf = 0.56. ^{1}H NMR for trans: δ 1.81 (s, 3H), 1.92 (s, 3H), 3.01 (s, 1H), 4.29 (d, J = 6.3 Hz, 2H), 5.72 (t, J = 6.3 Hz, 1H), 6.27 (d, J = 14.2 Hz, 1H), 6.38 (d, J = 10.8 Hz, 1H), 6.50 (dd, J = 14.2, 10.8 Hz, 1H). ^{13}C NMR δ 12.52, 17.54, 20.21, 30.29, 59.45, 77.36, 123.6, 125.5, 1303, 132.2, 137.3, 138.5.

General Procedure for the Synthesis of Compounds 13a and 13b Resulting in Triols 16 (R=H, Me), and Compounds 18 and 19. To a solution of 4 mole equivalent amount of 3.0 M EtMgBr in THF was added dropwise 2 mole equivalent amount of ynol 12 or ynol 9 at 0 °C. The resulting solution was warmed to reflex. After additional 1 h of reflux, a solution of 1.0 mole equivalent amount of pentanone 5a or 5b in THF was added at refluxing temperature. The reaction mixture was stirred under refluxing temperature until no starting material was reacted as judged by TLC (usually 5 h)). The solution was cooled to 0 °C, and a saturated aqueous NH_4Cl solution was added followed by ether for diluting. After filtration through a Celite pad and the extraction of the aqueous phase with three times, the combined organic phase was washed with brine and dried over $MgSO_4$. The pure product was obtained from chromatography.

1,1,5,9,13-Pentamethyl-dodeca-7-yn-9,11,13-trien-1,6,15-triol (16, R=H). ^{1}H NMR δ 1.10 (t, J = 7.5 Hz, 3H), 1.24 (s, 3H), 1.37 (s, 3H), 1.62 (q, J = 7.5 z, 2H), 1.80 (s, 3H), 1.91 (s, 3H), 4.28 (d, J = 6.0 Hz, 2H), 5.70 (t, J = 6.0 Hz, 1H), 6.29-6.43 (m,3H).

1,1,5,5,9,13-Hexamethyl-dodeca-7-yn-9,11,13-trien-1,6,15-triol (16, R=Me). ^{1}H NMR δ 1.01 (d, J = 6.4 Hz, 3H), 1.05 (d, J = 6.4 Hz, 3H), 1.31 (s, 3H), 1.45 (s, 3H), 1.81 (s, 3H), 1.95 (s, 3H), 2.00 (m, J = 6.4 Hz, 1H), 4.29 (d, J = 6.0 Hz, 2H), 5.72 (t, J = 6.0 Hz, 1H), 6.30-6.44 (m, 3H).

1,1,5,9-Tetramethyl-1-trimethylsilyoxy-octa-7-yn-9-en-6,11-diol (18, R=H). ^{1}H NMR δ 0.13 (s, 9H), 1.09 (t, J = 7.3 Hz, 3H), 1.27 (s, 3H), 1.40 (s, 3H), 1.60 (q, J = 7.3 Hz, 2H), 1.81 (s, 3H), 4.21 (d, J = 5.7 Hz, 2H), 5.95 (t, J = 5.7 Hz, 1H).

1,1,5,5,9-Pentamethyl-1-trimethylsilyoxy-octa-7-yn-9-en-6,11-diol (18, R=Me). ^{1}H NMR δ 0.14 (s, 9H), 1.04 (d, J = 6.5 Hz, 3H), 1.08 (d, J = 6.5 Hz, 3H), 1.31 (s, 3H), 1.45 (s, 3H), 1.82 (s, 3H), 1.98 (m, J = 6.5 Hz, 1H), 4.22 (d, J = 7.5 Hz, 2H), 5.95 (t, J = 7.5 Hz, 1H).

1,1,5,9-Tetramethyl-octa-7-yn-9-en-1,6,11-triol (19, R=H). ^{1}H NMR δ 1.09 (t, J = 6.9 Hz, 3H), 1.24 (s, 3H), 1.35 (s, 3H), 1.60 (m, J = 6.9 Hz, 2H), 1.81 (s, 3H), 4.19 (d. J = 6.5 Hz, 2H), 5.97 (t, J = 6.5 Hz, 1H).

1,1,5,5,9-Pentamethyl-octa-7-yn-9-en-1,6,11-triol (19, R=Me). ^{1}H NMR δ 1.03 (d, J = 6.9 Hz, 3H), 1.08 (d, J = 6.8 HZ, 3H), 1.28 (s, 3H), 1.40 (s, 3H), 1.83 (s, 3H), 2.00 (m, J = 6.8 Hz, 1H), 3.70 (br, 1H), 4.22 (d, J = 7.0 Hz, 2H), 5.99 (t, J = 7.0 Hz, 1H).

General Procedure of MnO_2/Celite Oxidation Reaction of Allylalcohol. Celite was purified by a 10% HCl solution in MeOH, and followed by washing with water to neutralize the filtrate, and dried by vacuum at 100 ^{0}C. $KMnO_4$ (38.4 g) was dissolved in H_2O (600 mL) at room temperature and the solution was stirred for one hour. The purified Celite (120 g) was added to the above solution, after an additional 30 min., the

suspension was cooled to 0 °C. Then a 40% NaOH aqueous solution (48.8 mL) and a solution of $MnSO_4.H_2O$ (60.8 g) in H_2O (108 mL) were added to the suspension. The resulting mixture was stirred for another 30 min. at 0 °C, and was filtered and washed with H_2O until the filtrate was neutralized. MnO_2/Celite was dried by vacuum at 100 °C, giving 174.36 g (31.2% MnO_2 content).

To a solution of allylalcohol in methylene chloride was added MnO_2/Celite at room temperature until no starting material was shown as judged by TLC (usually 10-20 fold excess amount needed). The suspension was filtrated and the filtrates were concentrated. The pure conjugated aldehyde was obtained from chromatography purification.

1,1,5,9-Tetraethyl-1-trimethylsilyoxy-octa-6-ol-7-yn-9-en-10-al (24a). ^{1}H NMR δ 0.14 (s, 9H), 1.09 (t, J = 7.3 Hz, 3H), 1.26 (s, 3H), 1.39 (s, 3H), 1.65 (q, J = 7.3 Hz, 2H), 2.28 (s, 3H), 2.93 (br, 1H), 6.15 (d, J = 7.7 Hz, 1H), 10.00 (d, J = 7.7 Hz, 1H).

1,1,5,5,9-Pentamethyl-1-trimethylsilyoxy-octa-6-ol-7-yn-9-en-10-al (24b). ^{1}H NMR δ 0.04 (s, 9H), 1.01 (d, J = 6.4 Hz, 3H), 1.06 (d, J = 6.4 Hz, 3H), 1.31 (s, 3H), 1.45 (s, 3H), 2.00 (m, J = 6.4 Hz, 1H), 2.29 (s, 3H), 3.42 (br, 1H), 6.17 (d, J = 8.2 Hz, 1H), 10.00 (d, J = 8.2 Hz, 1H).

1,1,5,9-Tetramethyl-octa-7,9-dien-1,6,11-triol (26). To a suspension of lithium aluminum hydride (195.7 mg, 4.90 mmol in anhydrous

ether (60 mL) was added dropwise a solution of diols 18 (R=H) (656.0 mg, 2.45 mmol) in anhydrous ether (15 Ml) at room temperature. The resulting mixture was heated to reflex and after 3 h, was quenched with an saturated aqueous NH_4Cl solution (20 mL) at 0 °C. The organic phase was dried over $MgSO_4$ and concentrated. The product was purified through a column chromatography (SiO_2, eluent: hexane/ether = 1:1), 300 mg, 61%. ^1H NMR δ 1.10 (t, J = 7.6 Hz, 3H), 1.25 (s, 3H), 1.36 (s, 3H), 1.62 (q, J = 7.6 Hz, 2H), 1.82 (s, 3H), 4.21 (d, J = 6.0 Hz, 2H), 5.61 (d, J = 16.2 Hz, 1H), 5.98 (t, J = 6.0 Hz, 1H), 6.33 (d, J = 16.2 Hz, 1H).

2,4-Diimethyl-4-trimethylsilyloxy-3-trifluoromethanesulfonyloxy-pent-2-ene (28b).

a. To a stirred solution containing diisopropylamine (258 mg, 2.55 mmol) in anhydrous THF (5 mL) was added 1.6 M n-Butyllithium (1.6 mL, 2.55 mmol) in hexane at -10 °C. The resulting solution was stirred for 10 min and then a solution of pentanone 5b (500 mg, 2.48 mmol) in dry THF (5 mL) was added at -78 °C. The reaction mixture was stirred for an additional 2 h and then $PhNTf_2$ (887 mg, 2.50 mmol) was added as a finely ground solid at 0 °C to it. The resulting brown solution was warmed to room temperature and stirred for 24 h. Pentane (15 mL) was added to dilute the mixture and the organic phase was washed with saturated aqueous $NaHCO_3$ solution (20 mL), and then dried over K_2CO_3. After solvent removal at reduced pressure, the resultant oil was purified by chromatography on silica gel, eluting with

hexane, to yield enol triflate 28b 8.5 mg (1.5%).

b. To a stirred solution containing diisopropylamine (258 mg, 2.55 mmol) in dry THF (5 mL) was added 1.6 M n-Butyllithium (1.60 mL, 2.55 mmol) in hexane at -10 °C. Then 2.0 M EtMgBr (1.27 mL, 2.55 mmol) in ether was added at 0 °C. The resulting mixture was warmed to room temperature and stirred for 18 h. After the mixture was cooled to 0 °C, hexamethylphosphoramide (929 mg, 5.18 mmol) was added, followed by a solution of pentanone 5b (500 mg, 2.48 mmol) in dry THF (5 mL). Stirring was continued for 6 h at room temperature, then solid $PhNTf_2$ (1.30 g, 3.70 mmol) was added at 0 °C. The mixture was stirred for an additional 48 h at room temperature, then worked-up as described in procedure a., giving enol triflate 28b 208 mg (32%). ^1H NMR δ 0.06 (s, 9H), 1.44 (s, 6H), 1.73 (s, 3H), 1.89 (s, 3H). ^{13}C NMR δ 1.89 (3C), 20.12, 20.93, 29.61, 29.73, 75.48, 124.2 (q, J = 317 Hz), 129.9, 147.5.

4-Methyl-4-trimethylsilyloxy-pent-3-trifluoromethanesulfonyloxy-2-ene (28a). The procedure was followed as described in method a. for enol triflate 28b to provide enol triflate 28a in 87% distilled yield. bp: 96-109 °C (15 mmHg). ^1H NMR δ 0.14 (s, 9H), 1.44 (s, 6H), 1.73 (d, J = 7.0 Hz, 3H), 5.55 (q, J = 7.0 Hz, 1H). ^{13}C NMR δ 0.90 (3C), 28.38 28.75, 51.06, 73.48, 113.0 (q, J=318 Hz), 120.9, 154.3.

Trans 5-[1-(trimethylsilyloxy)-1-metylethyl]-hepta-3,5-dien-2-one (29a). A solution of enol triflate 28a (10.30 g, 31.9 mmol), triethylamine

(11.10 g, 110 mmol) and methyl vinyl ketone (4.94 g, 70.5 mmol) in DMF (25 mL) was added to a slurry of $Pd(PPh_3)_2Cl_2$ (0.487 g, 2.2 mol%) in DMF (25 mL). The resulting mixture was heated to 75 °C and stirred for 16 h, and then cooled to room temperature. The reaction was worked up by addition of water (20 mL) and a 1:1 ether/hexane solution (20 mL). The aqueous layer was extracted with a 1:1 ether/hexane solution (2 x 20 mL). The combined organic phase was washed with water (10 mL) and brine (20 mL), and dried over $MgSO_4$. After filtration and concentration, the residue was passed through a silica gel-packed column, and eluted with a 3:1 hexane/ether solution to afford 4.21 g (55%)of dienone 29a. ^1H NMR δ 0.07 (s, 9H), 1.44 (s, 6H), 1.78 (d, J = 7.3 Hz, 3H), 2.29 (s, 3H), 5.59 (q, J = 7.3 Hz, 1H), 6.64 (d, J=16.4 Hz, 1H), 7.30 (d, J=16.4 Hz, 1H). ^{13}C NMR δ 2.13 (3C), 14.00, 14.73, 22.55, 30.53, 75.64, 126.9, 131.4, 139.1, 143.5, 198.7.

3E,5Z-6-Methyl-5-(1-methyl-1-trimethylsilyloxyethyl)-hepta-3,5-dien-2-one (29b). The procedure was followed as described for 29a. Yield 53%. ^1H NMR δ 0.07 (s, 9H), 1.37 (s, 6H), 1.70 (s, 3H), 1.95 (s, 3H), 2.24 (s, 3H), 5.89 (d, J = 16.4 Hz, 1H), 7.10 (d, J = 16.4 Hz, 1H). ^{13}C NMR δ 1.81 (3C), 20.04, 22.91, 27.00, 31.39, 43.71, 76.00, 115.9, 132.2, 133.8, 145.6, 198.4.

2Z,4E,6E and 2E,4E,6E-3-methyl-6-(1-trimethylsilyloxy-1-methylethyl)-octa-2,4,6-trienal (30).

Preparation of Acetaldehyde t-Butylimine. To cooled (0 °C) t-

butylamine (36.6 g, 0.5 mol) was added acetaldehyde (14.8 g, 0.34 mol) in a 1.5 h period. To the mixture was added enough potassium hydroxide pellets (20 g) to form an aqueous layer, which was then removed. The organic layer was dried over potassium hydroxide overnight in a refrigerator, then distilled under nitrogen, giving acetaldehyde t-butylimine (27.0 g, 80%). bp: 70-82 °C. ^{1}H NMR δ 1.14 (s, 9H), 1.92 (d, J = 5.1 Hz, 3H), 7.65 (d, J = 5.1 Hz, 1H).

Preparation of Silylated Acetaldehyde t-Butylimine. To a solution of lithium diisopropyl amide (100 mL, 10 wt% in hexane, 0.070 mol) in dry THF (100 mL) was added dropwise a solution of the above acetaldehyde t-butylimine (6.31 g, 0.064 mol) in dry THF (10 mL) at -78 °C. After an hour, the mixture was treated with a solution of trimethylchlorosilane (7.40 g, 0.067 mol) in dry THF (10 mL) at -78 °C. The reaction mixture was warmed to 0 °C during a 3.5 h period of time, and then poured into water (150 mL). The aqueous phase was extracted with ether (3 x 50 mL), and the combined organic extracts were washed with brine (20 mL), dried over K_2CO_3 and concentrated. The residual oil was distilled at 95-105 °C (104 mmHg) to afford 9.30 g (85.3%) of colorless silylated acetaldehyde t-butylimine. ^{1}H NMR δ 0.04 (s, 9H), 1.14 (s, 9H), 1.82 (d, J = 6.4 Hz, 3H), 7.62 (t, J = 6.4 Hz, 1H).

General Procedure of Synthesis of Triene aldehyde 30. To a stirred solution of diisopropylamine (1.52 g, 15.00 mmol) in anhydrous THF

(10 mL) was added 1.6 M nBuLi (9.40 mL, 15.00 mmol) in hexane at -10 °C. The resulting LDA solution was cooled to -78 °C and treated with a solution of the above described silylated acetaldehyde t-butylimine (2.50 g, 14.50 mmol) in anhydrous THF (10 mL). After an hour at -78 °C, a solution of the conjugated ketone, such as 29a (3.00 g, 12.5 mmol) in dry THF (10 mL) was added to the above mixture. The resulting mixture was allowed to warm to 0 °C in a 3 h period of time and quenched with water (25 mL). The aqueous phase was extracted with ether (3 x 20 mL), and the combined extracts were washed with brine (20 mL), dried over $MgSO_4$, and concentrated. Chromatography of the residue (SiO_2, eluent hexane/ether = 3:1) gave 2.985 g (89%) of a mixture of cis and trans isomers of the conjugated aldehyde 30. The cis and trans isomer could be further separated by flash chromatography, 58.5% of trans and 42.5% of cis isomer. ^1H NMR spectra for cis and trans isomer of triene aldehyde 30 were given in the text. ^{13}C NMR for cis isomer: δ 2.04 (3C), 14.56 (2C), 20.67, 30.53, 75.68, 123.8, 127.4, 128.2, 132.7, 144.4, 154.8, 189.7; for trans isomer: δ 2.25 (3C), 14.60 (2C), 22.50, 30.71, 75.93, 117.3, 124.0, 129.4, 131.9, 135.6, 155.1, 191.0. MS m/z CI MS (relative intensity): 267 (M^+ + 1, 20), 194 (100), 177 (95).

Trans (and 13-cis) ethyl 6-(1-trimethylsilyloxymethylethyl)-9,13-dimethylundecapent-5,7,9,11,13-enoate (31, numbering as retinal). The Wittig reaction of trans triene aldehyde 30 (1.73 g, 6.50 mmol) with phosphonosenecioate 8 was performed, as described for the

ester 11, to afford 2.24 g (92%) of the ester 31 through chromatographic purification (SiO_2, eluent hexane/ether = 4:1), including 74% of the C_{13}-trans and 18% of the C_{13}-cis isomers. Spectra for the trans isomer: ^{1}H NMR δ 0.07 (s, 9H), 1.25 (t, J = 7.1 Hz, 3H), 1.37 (s, 3H), 1.75(d, J = 7.1 Hz, 3H), 1.99 (s, 3H), 2.33 (s, 3H), 4.16 (q, J = 7.1 Hz, 2H), 5.68 (q, J = 7.1 Hz, 1H), 5.75 (s, 1H), 6.17 (d, J = 11.4 Hz, 1H), 6.27 (d, J = 15.1 Hz, 1H), 6.33 (d, J = 16.4 Hz, 1H), 6.51 (d, J = 16.4 Hz, 1H), 6.97 (dd, J = 15.1, 11.4 Hz, 1H). ^{13}C NMR δ 2.28 (3C), 12.71, 13.81, 14.33, 14.78, 30.81, 59.72, 75.62, 118.7, 120.8, 130.4, 131.3, 135.5, 137.3, 139.6, 145.1, 152.6, 167.2. UV (λ_{max} in hexane) 358 nm. MS m/z CI MS (relative intensity) 377 (M^++1, 5), 304 (40), 287 (100). ^{1}H NMR for the cis isomer: δ 0.08 (s, 9H), 1.27 (t, J = 7.1 Hz, 3H), 1.41 (s, 6H), 1.75 (d, J = 7.1 Hz, 3H), 2.05 (s, 3H), 2.25 (s, 1H), 4.15 (q, J = 7.1 Hz, 2H), 5.63 (s, 1H), 5.68 (q, J = 7.1 Hz, 1H), 6.17 (d, J = 11.4 Hz, 1H), 6.34 (d, J = 16.4 Hz, 1H), 6.51 (d, J = 16.4 Hz,1H), 6.95 (dd, J = 15.1, 11.4 Hz, 1H), 7.77 (d, J = 15.1 Hz, 1H). UV (λ_{max} in hexane) 354 nm.

All trans (and C13-cis) pentaene aldehyde (15a). The DIBAL reduction followed by MnO_2/Celite oxidation of the above described isomeric ester 31 (95 mg, 0.239 mmol) to 9,13-dimethyl-6-(1-trimethylsilyloxymethylethyl)-undecpenta-5,7,9,13-en-15-al 32 (60 mg, 72% yield) was performed as described for ynol 12 and the general procedure of MnO_2/Celite oxidation, respectively.

The alkyl siliane protective group on the hydroxyl group was cleaved by the addition of $nBu_4N^+F^-$ (2.00 mol equivalent) into a solution of an appropriate silylated compound (1.00 mol equivalent) in THF at room temperature. The completion of the reaction was judged by TLC when no starting material was shown. The mixture was diluted with ether and washed with water and brine, and dried over $MgSO_4$. After solvent removal, the crude oil was passed through a column packed with silica gel. ^1H NMR, MS and UV spectra for all trans pentaene aldehyde 15a are indicated in the text. ^{13}C NMR δ 12.91, 13.12, 14.81, 30.33 (2C), 70.12, 121.3, 126.0, 129.3, 130.7, 132.2, 135.2, 137.6, 141.9, 144.5, 154.5, 191.1. ^1H NMR for C_{13}-cis isomer: δ 1.39 (s, (H), 1.77 (d, J = 6.8 Hz, 3H), 2.03 (s, 3H), 2.13 (s, 3H), 5.81 (q, J = 6.8 Hz, 1H), 5.83 (d, J = 8.0 Hz, 1H), 6.27 (d, J = 11.4 Hz, 1H), 6.37 (d, J = 16.4 Hz, 1H), 6.47 (d, J = 16.4 Hz, 1H), 7.01 (dd, J = 11.4, 15.1 Hz, 1H), 7.28 (d, J = 15.1 Hz, 1H), 10.17 (d, J = 8.0 Hz, 1H). UV (λ_{max} in hexane) 360 nm.

General Procedure of Esterification with Acetyl Chloride.

To a solution of the pentene aldehyde 15a (1.00 mol equivalent) in anhydrous methylene chloride containing base (sodium acetic acid or triethyl amine, 3.00 mol equivalent) was added an appropriate acid chloride (2.00 mol equivalent) at 0 °C. The mixture was allowed to warm to room temperature and after stirring for about 30 min (usually TLC shown no more product was formed), diluted with ether. The solution was washed with water and

brine, and dried over $MgSO_4$. After concentration, the desired product was purified by a preparative TLC plate (SiO_2, eluent ether/hexane = 1:3) and by HPLC.

7C-Seco-ring spacer armed retinal (33, n = 5). ^1H NMR δ 1.00 (t, J = 7.0 Hz, 3H), 1.23 (s, 6H), 1.50-1.60 (m, 8H), 1.80 (d, J = 7.0 Hz, 3H), 2.03 (s, 3H), 2.31 (t, J = 7.0 Hz, 2H), 2.32 (s, 3H), 5.61 (q, J = 7.0 Hz, 1H), 5.95 (d, J = 8.0 Hz, 1H), 6.23 (d, J = 11.4 Hz, 1H), 6.30 (d, J = 16.4 Hz, 1H), 6.37 (d, J = 15.1 Hz, 1H), 6.59 (d, J = 16.4 Hz, 1H), 7.10 (dd, J = 15.1, 11.4 Hz, 1H), 10.09 (d, J = 8.0 Hz, 1H).

7C-COOH-Seco-ring spacer armed retinal (34). ^1H NMR δ 1.30 (s, 6H), 1.62-1.58 (m, 2H), 1.82 (d, J = 7.0, 3H), 1.96-2.01 (m, 4H), 1.99 (s, 3H), 2.31 (s, 3H), 2.35-2.40 (m, 4H), 5.75 (q, J = 7.0 Hz, 1H), 5.93 (d, J = 8.0 Hz, 1H), 6.13 (d, J = 11.4 Hz, 1H), 6.30 (d, J = 16.4 Hz, 1H), 6.37 (d, J = 15.1 Hz, 1H), 6.59 (d, J = 16.4 Hz, 1H), 7.10 (dd, J = 15.1, 11.4 Hz, 1H), 10.09 (d, J = 8.0 Hz, 1H), 12.12 (s, 1H).

δ-(t-Butyldimethylsilyloxy)-pentanoic acid (37). To a solution of lithium hydroxide (0.462 g, 19.6 mmol) in water (4.5 mL) was added a solution of δ-valerolactone (1.00 g, 10.0 mmol) in THF (35 mL) at room temperature followed by 30% hydrogen peroxide (26.5 mL). After 2.5 h at room temperature, the mixture was cooled to 0 °C and acidified with 1 N aqueous hydrochloride acid to pH 1-2. It was extracted with methylene chloride (4 x 50 mL) and the combined extracts were dried over $MgSO_4$.

After concentration to 20 mL, to the mixture was added 2,6-lutidine (4.65 mL, 39.7 mmol) at 0 °C under nitrogen atmosphere. After 10 min at 0 °C, *tert*-butyldimethylsilyltriflate (5.00 g, 29.7 mmol) was added dropwise. The resulting mixture was stirred at room temperature for 45 min, quenched with water (20 mL) and extracted with methylene chloride (3 x 50 mL). The extracts were washed with 1 N aqueous HCl (20 mL) at 0 °C, brine (50 mL), dried over $MgSO_4$ and concentrated. The crude oil was dissolved into MeOH (48 mL) and THF (16 mL) and the solution was treated with K_2CO_3 (1.0 g) in water (10 mL). After 45 min at room temperature, the organic solvent was removed and brine (40 mL) was added. The mixture was cooled to 0 °C and acidified with 1 M aqueous $NaHSO_4$ to pH 3-4. The mixture was extracted with methylene chloride (4 x 50 mL), and extracts were washed with brine (50 mL), dried over $MgSO_4$ and concentrated to yellow oil. The isolation was performed on a preparative TLC plate (SiO_2, eluent benzene/HAc/MeOH = 5.6:1:1 to afford 0.129 g (30% yield) of the acid 37. ^1H NMR δ 0.02 (s, 6H), 0.88 (s, 9H), 1.79-1.87 (m, 4H), 2.43 (t, J = 7.2 Hz, 2H), 3.65 (t, J = 6.0 Hz, 2H).

Trans 15-(t-butyldimethylsilyloxy)-penten-15-ol (40). After DIBAL reduction of ester 39 (1.765 g, 5.81 mmol), the crude oil was dissolved in dry DMF (50 mL). The solution was cooled to 0 °C and *tert*-butyldimethylchloro silicane (0.874 g, 5.81 mmol) and imidazole (1.02 g, 14.5 mmol) were added to it. After stirring for 24 h at room temperature, the

quenched by water (50 mL) and the mixture was extracted with a solution of ether/hexane = 1:1 (3 x 20 mL). After drying and concentration of the extracts, the crude oil was purified by a flash chromatography, eluted with 30% EtOAc in hexane to give 1.97 g (90% yield) of the protected alcohol 40. ^{1}H NMR δ 0.04 (s, 6H), 0.90 (s, 9H), 1.44 (s, 6H), 1.72 (d, J = 6.9 Hz, 3H), 1.92 (s, 3H), 1.99 (s, 3H), 4.31 (d, J = 6.2 Hz, 2H), 5.58 (t, J = 6.2 Hz, 1H), 5.73 (q, J = 6.9 Hz, 1H), 6.10 (d, J = 11.4 Hz, 1H), 6.25 (d, J = 15.1 Hz, 1H), 6.37 (d, J = 16.4 Hz, 1H), 6.54 (d, J = 16.4 Hz, 1H), 6.55 (dd, J = 15.1, 11.4 Hz, 1H). UV (λ_{max} in hexane) 330 nm. MS m/z CI MS (relative intensity) 377 (M^+ + 1, 20), 245 (100).

Esterification of the Ketal 44 Through Lactone Opening.

To a stirred solution of NaH in mineral oil (25.5 mg, 0.637 mmol), washed with anhydrous THF, in THF (5 mL) was added dropwise a solution of the ketal 44(170 mg, 0.637 mmol) in dry THF (5 mL) at 0 °C. The resulting mixture was allowed to warm to room temperature and after 2 h, cooled to 0 °C and a solution of δ-valerolactone (76.4 mg, 0.764 mmol)in dry THF (5 mL) was added to it. After additional 3 h at room temperature, the reaction was quenched with water (5 mL). The aqueous phase was acidified with 0.5 N aqueous HCl to pH 5-6 and then extracted with ether (3 x 10 mL). The combined extracts were dried over $MgSO_4$ and concentrated. The esterified product 45 was provided through a flash chromatography on silica gel, eluted with a solution of hexane/ether = 2:1 in 16 % yield (37 mg of 45). Recovered

starting material 44: 145 mg, 85%. ^{1}H NMR δ 0.846 (s, 3H), 1.03 (s, 3H), 1.16-1.24 (m, 4H), 1.60 (s, 3H), 1.60-1.69 (m, 3H), 2.23 (t, J = 7.1 Hz, 2H), 3.61 (t, J = 6.2 Hz, 2H), 3.59 (t, J = 6.1 Hz, 2H), 3.80-3.97 (m, 4H), 5.30 (d, J = 16.4 Hz, 1H), 6.13 (d, J = 16.4 Hz, 1H).

4,4-Dimethyl-5-hexen-3-one (49). Prepared according to reference [369].

4,4-Dimethyl-5-hexen-3-(ethylene)-ketal (50). The mixture of hexenone 49 (9.20 g, 73.0 mmol), ethylene glycol (6.1 mL, 109.5 mmol) and pyridinium-*p*-toluenesulfonate (139 mg, 1% mmol)in benzene (200 mL) was heated to reflex under a Pyrex Barrett distilling receiver overnight. The resulting solution was washed with 10% aqueous NaOH solution (100 mL) and water (100 mL), and then dried over K_2CO_3. After concentration, the crude oil was distilled to provide 7.82 g (63% yield) of the ketal 50. bp: 90-95 °C (40 mmHg). ^{1}H NMR δ 0.83 (t, J = 7.4 Hz, 3H), 1.02 (s, 6H), 1.69 (q, J = 7.4 Hz, 2H), 4.00-4.02 (m, 4H), 5.10 (dd, J = 10.5, 0.7 Hz, 1H), 5.12 (dd, J = 17.5, 0.7 Hz, 1H), 5.98 (dd, J = 17.5, 10.5 Hz, 1H).

6-(t-Butyldimetylsilyloxy)-4,4-dimethylhexan-3-one (46). To a stirred solution of the hexene ketal 50 (16.8 g, 98.8 mmol) in dry THF (100 mL) was added dropwise 2.0 M $BH_3.Me_2S$ (74 mL, 148 mmol) in THF at 0 °C. After additional 30 min at 0 °C, the mixture was allowed to warm to room temperature and after 3.5 h, sufficient water was added to destroy the excess reagent. Then 3.0 M aqueous NaOH solution (49 mL, 148 mmol)

was added dropwise followed by 30% aqueous hydrogen peroxide solution (50 mL, 435 mmol) at 0 °C. The resulting solution was heated to 40-50 °C for 1 h and a solution of saturated aqueous NH_4Cl solution (100 mL) and ether (200 mL) were added at room temperature. The aqueous phase was extracted with ether (3 x 25 mL). The combined organic phases were washed with water (50 mL) and brine (50 mL), dried over $MgSO_4$ and concentrated. The product 51 (12.4 g, 67 % yield) was obtained from distillation. bp: 95-100 °C (0.00 mmHg). ^{1}H NMR δ 0.88 (t, J = 7.3 Hz, 3H), 0.97 (s, 6H), 1.60 (t, J = 6.4 Hz, 2H), 1.75 (q, J = 7.3 Hz, 2H), 3.67 (t, J = 6.4 Hz, 2H), 4.00-4.07 (m, 4H).

The mixture of the above described compound 51 (12.4 g, 65.6 mmol), water (50 mL) and pyridinium *p*-toluenesulfonate (5.06 g, 20.1 mmol)in acetone (200 mL) was reflexed for 24 h. The solvent was removed and ether (200 mL) was added to the residue. The solution was washed with saturated aqueous $NaHCO_3$ solution (100 mL) and brine (100 mL), dried over $MgSO_4$ and concentrated. ^{1}H NMR spectrum of the crude material showed the reaction was not completed. The crude mixture was dissolved into acetone (200 mL) and 3.0 N aqueous HCl solution (2 mL). The resultant mixture was stirred at room temperature for 30 min and treated with K_2CO_3. After filtration, the solution was concentrated. The residue was dissolved into ether (100 mL).The solution was washed with saturated aqueous $NaHCO_3$ (50 mL), brine (25 mL) and dried over $MgSO_4$. The crude oil from concentration was

dissolved in DMF (100 mL). Imidazole (9.70 g, 138 mmol) and t-BuMe$_2$SiCl (10.7 g, 71.3 mmol) were added to the solution. After stirring for 24 h, the reaction was quenched with water (100 mL) and treated with a solution of hexane/ether = 1:1 (3 x 50 mL). The organic phase was washed with water (20 mL) and brine (20 mL), and dried over $MgSO_4$ and concentrated. The crude oil was distilled to afford the hexanone 46 (9.20 g, 54% yield). bp: 95-102 °C (0.00 mmHg). ^{1}H NMR δ 0.02 (s, 3H), 0.77 (s, 9H), 1.04 (t, J = 7.3 Hz, 3H), 1.83 (t, J = 7.0 Hz, 2H), 2.50 (q, J = 7.3 Hz, 2H), 3.55 (t, J = 7.0 Hz, 2H).

6-(t-Butyldimethylsilyloxy)-4,4-dimethyl-2-en-3-yl-triflate (52). Prepared according to the procedure for enol triflate 28a. The pure enol triflate 52 was obtained from a flash chromatography (SiO_2, eluent hexane/EtOAc = 5:1), in 50% yield. Rf = 0.8. ^{1}H NMR δ 0.01 (s, 3H), 0.84 (s, 9H), 1.41 (s, 6H), 1.68 (t, J = 7.0 Hz, 2H), 1.75 (d, J = 7.0 Hz, 3H), 3.95 (t, J = 7.0 Hz, 2H), 5.39 (q, J = 7.0 Hz, 1H).

Preparation of All Trans Heptenone 47. The Heck reaction was performed according to the procedure for dienone 29a. A minor desired product 47 was obtained by a preparative TLC plate (SiO_2, eluent ether/hexane = 1/3). Rf = 0.45. ^{1}H NMR δ 0.00 (s, 6H), 0.85 (s, 9H), 1.06 (s, 3H), 1.07 (s, 3H), 1.63 (t, J = 7.3 Hz, 2H), 1.72 (d, J = 7.0 Hz, 3H), 2.29 (s, 3H), 3.38 (t, J = 7.3 Hz, 2H), 5.63 (t, J = 7.0 Hz, 1H), 6.10 (d, J = 16.4 Hz, 1H), 7.15 (d, J = 16.4 Hz, 1H).

6-(t-Butyldimethylsilyloxy)-4,4-dimethylhept-2-yne (56).

Produced from the preparation of enol triflate 52 and diene ketone 47. ^{1}H NMR δ 0.02 (s, 6H), 0.88 (s, 9H), 1.05 (s, 6H), 1.62 (t, J = 7.4 Hz, 2H), 1.75 (s, 3H), 3.78 (t, J = 7.4 Hz, 2H).

6-(t-Butyldimethylsilyloxy)-2,4,4-trimethyl-hexa-3-one (65).

To a stirred solution of diisopropylamine (4.34 g, 42.9 mmol) in anhydrous THF (20 mL) was added dropwise 1.6 M n-BuLi (26.8 mL, 42.9 mmol) in hexane at -10 °C. The resulting solution was cooled to -78 °C and 2.4-dimethylpenta-3-one (5.00 g, 42.9 mmol) was added to it. After stirring for 2 h at 0 °C, the mixture was cooled to -78 °C and 2-bromo-butyl-1-ol (5.64 g, 45.1 mmol) was added to it. The resulting mixture was allowed to warm to room temperature and left stirring for 24 h. The reaction was quenched at 0 °C by addition of water (15 mL). The aqueous phase was extracted with ether (3 x 20 mL), and the combined organic extracts were washed with brine (20 mL), dried over $MgSO_4$ and concentrated. The crude residue was distilled to afford the keto alcohol 64 (5.06, 73% yield). bP: 96-103 °C (28 mmHg).

A mixture of the above described keto alcohol 64 (5.06 g, 32.0 mmol), imidazole (5.50 g, 80.8 mmol) and *tert*-butyldimethylchloro silicane (7.46 g, 49.5 mmol) in dry DMF was stirred for 48 h. The reaction mixture was quenched as described for the ketone 46. Distillation of the crude residue provided the hexanone 65 (7.22 g, 83% yield). bp: 107-113 °C (0.00 mmHg). ^{1}H NMR δ 0.04 (s, 6H), 0.88 (s, 9H), 1.02 (d, J = 6.6 Hz, 6H), 1.41 (s,

6H), 2.57 (t, J = 7.8 Hz, 2H), 3.04 (m, J = 6.6 Hz, 1H), 3.55 (t, J = 7.8 Hz, 2H).

1,9-Bis-(t-butyldimethylsilyloxy)-6-ethyl-7,7,3-trimethylnon-2-en-4-yn-6-ol (68). A mixture of trans 3-methylpent-3-en-1-yn-5-ol 9 (3.00 g, 31.3 mmol), imidazole (5.33, 78.3 mmol) and *tert*-butyldimethylchloro silicane (7.08 g, 47.0 mmol) in dry DMF (10 mL) was stirred for 24 h. The reaction mixture was treated with water and a solution of ether/hexane = 1:1 as described for the ketone 46. The purification was carried out through a flash chromatography eluted with a solution of hexane/ether = 4:1 to afford trans 5-(t-butyldimethylsilyloxy-3-methylpen-3-en-1-yne (3.50 g, 53% yield). Rf = 0.65. ^{1}H NMR δ 0.05 (s, 6H), 0.88 (s, 9H), 1.77 (s, 3H), 2.77 (s, 1H), 4.22 (d, J = 6.3 Hz, 2H), 5.99 (t, J = 6.3 Hz, 1H).

Method A. To a stirred solution of 3.0 M EtMgBr (0.50 mL, 1.50 mmol, in ether) in anhydrous THF (5 mL) was added a solution of the above described yne (315 mg, 1.5 mmol) in dry THF (2 mL) at room temperature. The resulting mixture was heated to reflex, and after 1 h, a solution of the ketone 46 (258 mg, 1.00 mmol) in dry THF (2 mL) was added to it at room temperature. The reaction mixture was heated to reflex for 5 h, and then cooled to 0 °C and treated with saturated aqueous NH_4Cl solution (5 mL). The aqueous phase was extracted with ether (3 x 20 mL). The combined organic extracts were washed with brine (20 mL), dried over $MgSO_4$ and concentrated. The pure product 68 (178 mg, 38% yield) was

obtained through a flash chromatography (SiO_2, eluent hexane/ether = 6:1). Rf = 0.50.

Method B. To a stirred solution of the ynol 9 (760 mg, 7.74 mmol) in anhydrous THF (2 mL) was added dropwise 1.6 M n-BuLi (9.70 mL, 15.5 mmol) in hexane at -70 °C. After additional 1 h at -70 °C, a solution of the ketone 46 (1.00 g, 3.88 mmol) in dry THF (2 mL) was added to the above mixture. The resulting solution was then allowed to warm to room temperature, stirred for 24 h. The reaction was quenched as described in Method A. The resultant diols (744 mg, 60% yield, recovered the ketone 46 100 mg) was provided by a column chromatography (SiO_2, hexane/ether = 2:1), Rf = 0.25. ^{1}H NMR δ 0.03 (s, 6H), 0.85 (s, 9H), 0.99 (s, 1H), 1.05 (t, J = 7.2 Hz, 3H), 1.10 (s, 6H), 1.59 (t, J = 7.2 Hz, 2H), 1.62 (t, J = 6.3 Hz, 2H), 1.76 (s, 3H), 3.69 (t, J = 6.3 Hz, 2H), 4.14 (d, J = 6.5 Hz, 2H), 5.89 (t, J=6.5 Hz, 1H).

A mixture of the above described diols (744 mg, 2.09 mmol), imidazole (355 mg, 5.23 mmol) and *tert*-butyldimethylchloro silicane (472 mg, 5.23 mmol) in dry DMF was stirred for 24 h at room temperature. The reaction was quenched as described for the ketone 46. The pure product 68 was provided by flash chromatography on silica gel, eluted with hexane/ether = 6:1. Rf = 0.50. ^{1}H NMR δ 0.05 (s, 6H), 0.06 (s, 6H), 0.87 (s, 9H), 0.88 (s, 9H), 1.08 (t, J = 7.2 Hz, 3H), 1.10 (s, 6H), 1.59 (t, J = 7.2 Hz, 2H), 1.64 (t, J = 6.2 Hz, 2H), 1.76 (s, 3H), 3.72 (t, J = 6.2 Hz, 2H), 4.21 (d, J =

6.2 Hz, 2H), 5.85 (t, J = 6.2 Hz, 1H).

1,9-Bis-(t-butyldimethylsilyloxy)-3,7,7-trimethyl-5-vinylnon-2-en-4-yen (69). To a stirred solution of the ynol 68 (785 mg, 1.68 mmol) in anhydrous pyridine (2 mL)was added $POCl_3$ (0.20 mL) at 0 °C. The resulting solution was allowed to warm to room temperature and left stirred for 48 h. A saturated aqueous NH_4Cl solution (2 mL) and ether (5 mL) were added to the above mixture. The organic phase was washed with water (5 mL) and brine (5 mL), dried over $MgSO_4$ and concentrated. After chromatography on silica gel eluted with hexane/ether = 3:1, the recovered starting material 68 (645 mg, Rf = 0.50) and the desired product 69 (86 mg, 64% yield based on recovered the 68, Rf = 0.95) were obtained. ^1H NMR δ 0.01 (s, 6H), 0.05 (s, 6H), 0.85 (s, 9H), 0.88 (s, 9H), 1.08 (s, 6H), 1.70 (t, J = 7.4 Hz, 2H), 1.81 (s, 3H), 1.82 (d, J = 6.6 Hz, 3H), 3.52 (t, J = 7.4 Hz, 2H), 4.24 (d, J = 6.5 Hz, 2H), 5.69 (t, J=6.6 Hz, 1H), 5.88 (t, J=6.5 Hz).

Trans (and Cis triene aldehyde 70. Prepared as the procedure for the triene aldehyde 30, in 87% yield. ^1H NMR for trans isomer δ 0.02 (s, 6H), 0.84 (s, 9H), 1.06 (s, 6H), 1.63 (t, J = 7.6 Hz, 2H), 1.70 (d, J = 6.7 Hz, 3H), 2.30 (s, 3H), 3.47 (t, J = 7.6 Hz, 2H), 5.53 (q, J = 6.7 Hz, 1H), 5.92 (d, J = 8.1 Hz, 1H), 6.20 (d, J = 16.4 Hz, 1H), 6.63 (d, J = 16.4 Hz, 1H), 10.12 (d, J = 8.1 Hz, 1H).

Trans (and C_{13}-cis) pentene ester 71. The Wittig reaction was performed as the procedure for the ester 31. ^1H NMR for the trans

isomer δ 0.01 (s, 6H), 0.85 (s, 9H), 1.10 (s. 6H), 1.25 (t, J = 7.2 Hz, 3H), 1.63 (t, J = 7.6 Hz, 2H), 1.70 (d, J = 6.9 Hz, 3H), 1.98 (s, 3H), 2.33 (s, 3H), 3.48 (t, J = 7.6 Hz, 2H), 4.14 (t, J = 7.2 Hz, 2H), 5.44 (q, J = 6.9 Hz, 1H), 5.76 (s, 1H), 6.17 (d, J = 11.4 Hz, 1H), 6.27 (d, J = 15.1 Hz, 1H), 6.33 (d, J = 16.4 Hz, 1H), 6.51 (d, J = 16.4 Hz, 1H), 6.97 (dd, J = 15.1, 11.4 Hz, 1H). UV (λ_{max} in hexane) 346 nm.

References:

1. A. Knowles & H. J. Dartrell; "*The Eye*" **1977**, *Vol.2B*, H. Darson (Ed.), pp.392, Academic Press, New York.

2. M. D. Bownds; *Photochem. Photobiol.* **1980**, *32*, 487-490.

3. W. A. Hagins; *Annu. Rev. Biophys. Bioeng.* **1972**, *1*, 131-158.

4. T. G. Ebrey & Honig; *Quat. Rev. Biophys. Chem.* **1975**, *8*, 129.

5. M. Chabre; *Annu. Rev. Biophys. Biophys. Chem.* **1985**, *14*, 331-360.

6. H. Schichi; *Biochemistry of Vision* **1983**, Academic Press, New York.

7. D. Oesterhelt & W. Stoeckenius; *Nature, New Biol.* **1971**, *233*, 149.

8. K. Foster, J. Saranak, N. Patel, G. Zarilli, M. Okabe, T. Klone & K. Nakanishi; *Nature* **1984**, *311*, 756-759.

9. K. Foster, J. Saranak, F. Derguini, D. Rao, G. Zarilli, M. Okabe, J. Fang, N. Shimizu & K. Nakanishi; *J. Am. Chem. Soc.* **1988**, *110*, 6588-89.

10. G. Wald & P. K. Bronw; *Proc. Natl. Acad. Sci., USA* **1950**, *36*, 84-92.

11. M. D. Bownds; *Nature (London)* **1967**, *216*, 1178-1181.

12. J. K. Wang, J. H. McDowell & P. A. Hargrave; *Biochemistry* **1980**, *19*, 5111-5117.

13. R. Uhl, T. Borys, N. Semple, J. Pasternak & E. W. Abrahmson; *Biochim. Biophys. Res. Commun.* **1979**, *90*, 58.

14. R. A. Ranbach, P. P. Names & E. A. Dratz; *Exp. Eye Res.* **1974**, *18*, 1-12.

15. C.-W. Wu & L. Stryer; *Proc. Natl. Acad. Sci., USA* **1972**, *69*, 1104-1108.

16. M. M. Dewey, P. K. Davis, J. K. Blasie & L. Barr; *J. Mol. Biol.* **1969**, *39*, 359-405.

17. L. Y. Yan & J.-P. Revel; *J. Cell Biol.* **1974**, *62*, 257-273.

18. J. K. Blasie, M. M. Dewey, A. E. Blarrock & C. R. Wothington; *J. Mol. Biol.* **1965**, *14*, 143-152.

19. J. M. Corless; *Nature (London)* **1972**, *237*, 229-231.

20. M. Chabre; *Biochim. Biophys. Acta* **1975**, *382*, 332-335.

21. M. J. Yeager; *Brookhaven Symp. Biol.* **1975**, *27*, III, 3-35.

22. H. Saibil, M. Chabre & D. Worcester; *Nature (London)* **1976**, *262*, 266-270.

23. A. J. Adams, R. L. Somers & H. Shichi; *Photochem. Photobiol.* **1979**, *29*, 687-692.

24. Y. A. Ovchinnikov; *FEBS Lett.* **1982a**, *148*, 179-191.

25. Y. A. Ovchinnikov, N. G. Abdulaev, M. Y. Feigma, I. D. Artamonov, A. S. Zolotarev, A. I. Miroshnikov, V. I. Martynov, M. B. Kustina, A. B. Kudelin & A. S. Bogachuk; *Bioorg. Khim.* **1982**, *8*, 1011-1014.

26. P. A. Hargrave, J. H. McDowell, D. R. Curitis, J. K. Wang, E. Juszczak, S. L. Fong, J. K. M. Rao & R. Argo; *Biophys. Struct. Mech.* **1983**, *9*, 235-244.

27. J. Nathans & D. S. Hohness; *Cell* **1983**, *34*, 807-814.

28. D. J. Pappin, E. Eliopoulous, M. Brett & J. B. C. Findlay; *Int. J. Biol. Macromol.* **1984**, *6*, 73-76.

29. J. Nathans & D. S. Hohness; *Proc. Natl. Acad. Sci., USA* **1984**, *81*, 4851-4855.

30. E. A. Dratz & P. A. Hargrave; *Trends Biochim. Soc.* **1983**, *8*, 128-131.

31. J. B. C. Findlay, D. J. C. Pappin & E. Eliopoulos; *Prog. Retinal Res.* **1988**, *7*, 63-87.

32. R. H. Callender & B. Honig; *Annu. Rev. Biophys. Bioeng.* **1977**, *6*, 33-55.

33. B. Honig & T. G. Ebrey; *Annu. Rev. Biophys. Bioeng.* **1974**, 3, 151-177.

34. W. Sperling; In "*Biochemistry and Physiology of Visual Pigments.*" **1974**, E. H. Langer (Ed.) pp. 19-28, Springer-Verlag, Berlin and New York.

35. R. R. Birge; *Annu. Rev. Biophys. Bioeng.* **1981**, *10*, 315-354.

36. R. Rowan, A. Warshel, B. O. Sykes & M. Karplus; *Biochemistry* **1974**, *13*, 970-980.

37. G. Wald; *Annu. Rev. Biochem.* **1953**, *22*, 497-526.

38. M. Gogala & Z. Vgl; *Physiol.* **1967**, *57*, 232.

39. K. Hamdorf, J. Schwemer & M. Gogala; *Nature (London)* **1971**, *231*, 458.

40. R. Paulsen & J. Schwemer; *Biochem. Biophys. Acta* **1972**, *238*, 520.

41. F. I. Harosi & Y. Hashimoto; *Science* **1983**, *222*, 1021.

42. F. I. Harosi; *In the Visual System* **1985**, A R. Liss (Ed.) pp. 41, New York.

43. M. E. Heyde, D. Gill, R.G. Kilponen & L. Rimai; *J. Am. Chem. Soc.* **1971**, *93*, 6776-6780.

44. A. Lewis, R. Fafer & E. W. Abranhamson; *J. Raman Spectrosc.* **1973**, *1*, 465.

45. A. R. Oseroff & R. H. Callender; *Biochemistry* **1974**, *13*, 4248.

46. R. A. Mathies, A. R. Oseroff & L. Stryer; *Proc. Natl. Acad. Sci., USA* **1976**, 73, 1-5.

47. K. A. Bagley, V. Balogh-Nair, A. A. Crotean, G. Dollonger, T. G. Ebrey, L. Eisenstein, M. K. Hong, K. Nakanishi & J. Vittitow; *Biochemistry* **1985**, *24*, 6055-6071.

48. S. O. Smith, I. Palings, V. Copie, D. P. Raleigh, J. Courtin, J. A. Pardoen, J. Lugtenburg, R. A. Mathies & R. G. Griffin; *Biochemistry* **1987**, *26*, 1606-1611.

49. J. O. Erickson & P. E. Blatz; Vision Res. **1968**, *8*, 1367.

50. P. E. Blatz, J. H. Mohler & H. V. Navangal; *Biochemistry* **1972**, *11*, 848.

51. See ref.1.

52. B. Honig, U. Dinur, K. Nakanishi, V. Balogh-Nair, M. A. Gawinowiz, M. Arnaboldi & M. G. Motto; *J. Am. Chem. Soc.* **1979**, *101*, 7084-7086.

53. M. Sheves, K. Nakanishi & B. Honig; *J. Am. Chem. Soc.* **1979**, *101*, 7086-7088.

54. K. Nakanishi, V. Balogh-Nair, M. Arnaboldi, K. Tsujimoto & B. Honig; *J. Am. Chem. Soc.* **1980**, *102*, 7945-7947.

55. G. Harbison, S. O. Smith, J. A. Pardoen, J. Courtin, J. Lugtenburg, J. Herzfeld, R. A. Mathies & R. G. Griffin; *Biochemistry* **1985**, *24*, 6955-6962.

56. R. R. Birge, C. M. Einterz, H. P. Knapp & L. P. Murray; *Biophys. J.* **1988**, *53*, 367-385.

57. H. Deng & R. H. Callender; *Biochemistry* **1987**, *26*, 7418-7426.

58. R. H. Gilson & Honig; *J. Am. Chem. Soc.* **1988**, *110*, 1943-1951.

59. P. Hildebrandt & M. Stoekburger; *Biochemistry* **1984**, *23*, 5539-5549.

60. B. Honig; In "*Biophysical Studies of Retinal Protein.*" **1986**, pp. 212-218, University of Illinois Press, Urbana.

61. T. Mogi, L. Stern, T. Marti, B. Chao & H. G. Khorana; *Proc. Natl. Acad. Sci., USA* **1988**, *85*, 4148-4152.

62. T. Baasov, N. Friedman & M. SHeves; *Biochemistry* **1987**, *26*, 3210-3217.

63. E. A. Zhukovsky & D. D. Oprian; *Science* **1989**, *246*, 928.

64. T. P. Sakar, R. R. Franke & H. G. Khorana; *Proc. Natl. Acad. Sci., USA* **1989**, *86*, 8309-8313.

65. J. Nathans; *Biochemistry* **1990**, *29*, 9746-9752.

66. Y. Koutalos, T. G. Ebrey, M. Tsuda, K. Odashima, T. Lien, M. H. Park, N. Shimizu, F. Derguini, K. Nakanishi, H. R. Gilson & B. Honig; *Biochemistry* **1989**, *28*, 2732-2739.

67. L. C. P. Mollevanger, A. P. M. Kentgens, J. A. Pardoen, J. M. L. Courtin, W. S. Veeman, J. Lugtenburg & W. J. deGrip; *Eur. J. Biochem.* **1987**, *163*, 9-14.

68. S. O. Smith, J. Friedlander, I. Palings, J. Courtin, H. deGroot, J. Lugtenburg, R. A. Mathies & R. G. Griffin; *Biophys. J.* **1988**, *13*, 385a.

69. J. G. Chen, T. Nakamura, T. G. Ebrey, H. Ok, K. Konno, F. Derguini, K. Nakanishi & B. Honig; *Biophys. J.* **1989**, *55*, 725-729.

70. H. Shichi, M. S. Lewis, F. Irreverre & A. L. Stone; *J. Biol. Chem.* **1969**, *244*, 529-536.

71. V. Balogh-Nair & K. Nakanishi; In "*New Comprehensive Biochemistry. Vol.3, Stereochemistry.*" Tamn, Ch., Ed.; Elsevier Biochemical Press: Amsterdam, **1982**, Chapter 7, pp.283-334.

72. F. Crescitelli, W. F. H. Momaerts & T. I. Sharv; *Proc. Natl. Acad. Sci., USA* **1966**, *56*, 1792-1743.

73. Y. Shichida, F. Tokunage & T. Yoshizawa; *Biochim. Biophys. Acta* **1978**, *504*, 413-430.

74. H. Shichi & E. Shelton; *J. Struc.* **1974**, *2*, 7.

75. H. Dartnall; In "*Handbook of Sensory Physiology*", M. G. F. Fuortes Ed., **1972**, *Vol. VII/1*, Springer-Verlag, Berlin, p.122.

76. L. Stryer; *Annu. Rev. Neurosi.* **1986**, *9*, 87-119.

77. P. A. Liebman, K. R. Paker & E. A Dratz; *Annu. Rev. Physiol.* **1987**, *49*, 765-791.

78. T. Yoshizawa & G. Wald; *Nature* **1963**, *197*, 1279-1286.

79. T. Yoshizawa & G. Wald; *Nature* **1967**, *214*, 566-571.

80. G. E. Busch, M. L. Applebury, A. A. Lamola & P. M. Rentzesis; *Proc. Natl. Acad. Sci., USA* **1972**, *69*, 2802-2806.

81. T. A. Rosenfeld, A. Alchelel & M. Ottoleghi; In "*Excited States of Biological Molecules.*" J. B. Birks, Ed. **1976**, pp. 540-544, Wiley, New York.

82. T. Kakiton & H. Kakitami; *Photochem. Photobiol.* **1980**, *32*, 707-709.

83. Y. Shichida, Y. S. Matuoko & T. Yoshizawa; *Photochem. Photobiol.* **1984**, *7*, 221-228.

84. M. Matuoaka, Y. Shichida & T. Yoshizawa; *Biochem. Biophys. Acta* **1984**, *165*, 38-42.

85. K. S. Peter, M. L. Alebury & P. M. Rentzepis; *Proc. Natl. Acad. Sci., USA* **1977**, *74*, 3119-3123.

86. K. S. Peter & N. Leontis; In "*Biological Events Probed by Ultra-Fast Laser Spectroscopy.*" A. A. Alfano, Ed., **1982**, pp. 259-269, Academic Press, New York.

87. Y. Shichida; *Photobiochem. Photophys.* **1986**, *13*, 287-307.

88. M. Ottolenghi & M. Sheves; In "*Primary Processes in Photobiology.*" T. Kobayashi, Ed., **1987**, p. 144-153, Springer-Verlag, Berlin.

89. F. Boucher & R. M. Leblanc; *Photochem. Photobiol.* **1985**, *41*, 459-465.

90. A. Cooper; *Nature (London)* **1979**, *282*, 531-533.

91. G. A. Schick, T. M. Cooper, R. A. Holloway, L. P. Murray & R. R. Birge; *Biochemistry* **1987**, *26*, 2556-2562.

92. S. O. Smith, J. Courtin, H. deGroot, R. Gebhard & J. Lugtenburg; *Biochemistry* **1991**, *30*, 7409-7415.

93. K. J. Rothschild & W. J. deGrip; *Photochem. Photobiophys.* **1986**, *13*, 245-258.

94. A. Aleck, N. Friedman, M. Ottolenghi, M. Sheves, C. M. Einterz, S. J. Hug, J. W. Lewis & D. S. Kliger; *Biophys. J.* **1989**, *55*, 233-241.

95. C. M. Einterz, S. J. Hug, J. W. Lewis & D. S. Kliger; *Biochemistry* **1990**, *29*, 1485-1491.

96. U. M. Ganter, T. Kashima, M. Sheves & F. Siebert; *J. Am Chem. Soc.* **1991**, *113*, 4087-4092.

97. T. Okada, H. Kandori, Y. Shichida, T. Yoshizawa, M. Denny, B.-W. Zhang, A. E. Asato & R. S. H. Liu; *Biochemistry* **1991**, *30*, 4796-4802.

98. S. J. Hug, J. W. Lewis, C. W. Einterz, T. E. Thorgeirsson & D. S. Kliger; *Biochemistry* **1990**, *29*, 1475-1485.

99. C. E. Randall, J. W. Lewis, S. J. Hug, S. C. Bjorling, I. Eisner-Shanas, N. Friedman, M. Ottolenghi, M. Sheves & D. S. Kliger; *J. Am. Chem. Soc.* **1991**, *113*, 3473-3485.

100. J. W. Lewis, S. J. Hug, S. E. Wallace-Williams & D. S. Kliger; *J. Am. Chem. Soc.* **1990**, *112*, 6711-6712.

101. T. G. Ebrey & T. Yoshizawa; *Exp. Eye Res.* **1973**, *17*, 545-556.

102. See ref. 71.

103. H. Horiuchi, F. Tokunaga & T. Yoshizawa; *Biochim. Biophys. Acta* **1980**, *591*, 445-457.

104. W. J. deGrip, D. Gray, J. Gillespie, P. H. M. Bovee, E. M. M. van den Berg, J. Lugtenburg & K. J. Rothschild; *Photochem. Photobiol.* **1988**, *48*, 497-504.

105. U. M. Gantyer, N. Gartner & F. Siebert; *Biochemistry* **1988**, *273*, 7480-7488.

106. T. Yoshizawa, Y. Shichida, S. Matuoka, S. Ioshida, H. Kandori & M. Sokabe; In "*Retinal Protein.*" Y. A. Ovchinnikov, Ed., **1987**, pp. 75-84, YNU Science Press, Zeist, The Netherlands.

107. See ref. 94.

108. A. G. Doykas, B. Aton, R. H. Callendar & T. G. Ebrey; *Biochemistry* **1987**, *17*, 2430-2435.

109. D. Emeis & K. P. Hoffmann; *FEBS Lett.* **1981**, *136*, 201-206.

110. C. Longstaff, R. D. Calhoun & R. R. Rando; *Proc. Natl. Acad. Sci., USA* **1986**, *83*, 4209-4213.

111. See ref. 106.

112. D. Emeis, H. Kuhn, J. Riechert & K. P. Hoffmann; *FEBS Lett.* **1982**, *143*, 29-34.

113. See
ref. 5.

114. J. Kibelbek, J. M. Beach & B. J. Litman; *Biophys. J.* **1990**, *57*, 367a.

115. D. C. Mitchell, J. Kibelbek & B. J. Litman; *Biochemistry* **1991**, *30*, 37-42.

116. J. Kibelbek, D. C. Mitchell, J. M. Beach & B. J. Litman; *Biochemistry* **1991**, *30*, 6761-6768.

117. C. Blazynski & S. E. Ostroy; *Vision Res.* **1981**, *21*, 833-841.

118. W. A. Hagins. *Annu. Rev. Biophys. Bioeng.* **1972**, *1*, 131-158.

119. D. A. Bonglor, A. L. Hodgkin & T. Lamb; *J. Physiol. London* **1974**, *242*, 685.

120. M. W. Bitenski, R. E. Groman & W. H. Miller; *Proc. Natl. Acad. Sci., USA* **1971**, *68*, 561.

121. C. Goridis & N. Virmaux; *Nature* **1974**, *248*, 57.

122. K. W. Yan & K. Nakatani; *Nature (London)* **1985**, *313*, 579-582.

123. E. E. Fesenko, S. S. Kolesniko & A. L. Lyubaraky; *Nature (London)* **1985**, *313*, 310-313.

124. K. K. B. Fung & L. Stryer; *Proc. Natl. Acad. Sci., USA* **1980**, *77*, 2500-2504.

125. N. Bennett & Y. DuPont; *J. Biol. Chem.* **1985**, *260*, 4156-4168.

126. See ref. 74.

127. P. Deterre, J. Bigay, F. Forquet, M. Robert & M. Chabre; *Proc. Natl. Acad. Sci., USA* **1988**, *85*, 2424-2428.

128. See ref. 26.

129. See ref. 29.

130. M. Applebury & P. A. Hargrave; *Vision Res.* **1986**, *26*, 1881-1895.

131. G. P. Miljanich, M. F. Brown, S. Mabrey-Gaud & J. M. Sturtevant; *J. Membrane Biol.* **1985**, *85*, 79-86.

132. P. A. Hargrave; *Prog. Retinal. Res.* **1982**, *1*, 1-51.

133. P. A. Hargrave; *Biochim. Biophys. Acta* **1977**, *462*, 83-94.

134. M. D. Davison & J. B. C. Findlay; *Biochem. J.* **1986**, *236*, 1323-1334.

135. P. A. Hargrave, S. L. Fong, J. H. McDowell, M. T. Mas, D. R. Curtis, J. K. Wang & D. P. Smith; *Neurochem. Int.* **1980**, *1*, 231-244.

136. U. Wilden & H. Kuhn; *Biochemistry* **1982**, *21*, 3014-3022.

137. See ref.29.

138. See ref. 30.

139. J. B. C. Findlay, D. J. C. Pappin & E. Eliopoulos; *Prog. Retinal Res.* **1988**, *7*, 63-87.

140. G. Wald; *Science* **1986**, *162*, 230-239.

141. W. Stoeckenius, R. Lozier & R. A. Bogomolni; *Biochim. Biophys. Acta* **1987**, *505*, 215-278.

142. R. Henderson; *Annu. Rev. Biophys. Bioeng.* **1977**, *6*, 87.

143. D. Oesterhelt & W. Stoeckenius; *Proc. Natl. Acad. Sci., USA* **1973**, *70*, 2853.

144. M. Tsuda, N. Hazemoto, M. Kondo, N. Kamo, Y. Kobatake & Y. Terayama; *Biochem. Biophys. Res. Commun.* **1982**, *108*, 970-976.

145. H. Bayley, H.-S. Huang, A. H. Ross, Y. Takagak & H. G. Khorana; *Proc. Natl. Acad. Sci., USA* **1981**, *78*, 2225-2229.

146. D. Oesterhelt & W. Stoeckenius; *Nature New Biol.* **1971**, *233*, 149.

147. R. Henderson & P. N. T. Unwin; *Nature* **1975**, *257*, 28-32.

148. M. J. Pettie, A. Yudd, K. Nakanishi, R. Henselman & W. Stoeckenius; *Biochemistry* **1977**, *16*, 1955.

149. A. Maedea, T. Iwasa & T. Yoshizawa; *J. Biochem.* **1977**, *82*, 1599.

150. M. S. Braiman & R. A. Mathies; *Proc. Natl. Acad. Sci., USA* **1982**, *79*, 403-407.

151. R. A. Mathies, C. H. Brito Cruz, W. T. Pollard & C. V. Shank; *Science* **1988**, *240*, 777-779.

152. R. H. Lozier, R. A. Bogomolni & W. Stoeckenius; *Biophys. J.* **1975**, *15*, 955-962.

153. J. M. Baldwin, R. Henderson, E. Beckman & F. Zemlin; *J. Mol. Biol.* **1988**, *202*, 585-591.

154. R. H. Lozier & W. Niederbeger; *Fed. Proc. Fed. Am. Soc. Exp. Biol.* **1977**, *36*, 1805-1809.

155. J. F. Nagle, L. A. Parodi & R. H. Lozier; *Biophys. J.* **1982**, *38*, 161-174.

156. J. H. Hanamoto, P. Dupuls & M. A. El-Sayed; *Proc. Natl. Acad. Sci., USA* **1988**, *85*, 6385-6361.

157. Zs. Dancshazy, R. Govindjee & T. G. Ebrey; *Proc. Natl. Acad. Sci., USA* **1988**, *81*, 7083-7087.

158. R. Filler & M. Stockburger; *Biochemistry* **1988**, *27*, 7641-7651.

159. H. C. Bitting, D.-J. Jang & M. A. El-Sayed; *Photochem. Photobiol.* **1990**, *51*, 593-598.

160. H. J. Butt, K. Fendler, A. Der & E. Bamberg; *Biophys. J.* **1989**, *56*, 851-859.

161. See ref.141.

162. W. Kouyama, W. Stoeckenius & R. A. Bogomolin; *Biophys. J.* **1985**, *48*, 201-208.

163. L. A. Drachev, A. D. Kaulen & V. P. Skulachev; *FEBS lett.* **1984**, *178*, 331-335.

164. S. Grzessiek & N. A. Dencher; *FEBS Lett.* **1986**, *180*, 337-342.

165. D. Braun, N. A. Dencher, M. Lindau & M. P. Heyn; *Biophys. J.* **1988**, *53*, 617-621.

166. T. Kouyama, A. Nasuda-Kouyama, A. Ikegemi & R. A. Mathies; *Biochemistry* **1988**, *27*, 5855-5863.

167. R. R. Birge & T. M. Cooper; *Biophys. J.* **1983**, *42*, 61-69.

168. R. R. Birge, T. M. Cooper, A. F. Lawrence, M. B. Masthay, C. Vasilakis, C. F. Zhang & R. Zidovetzk; *J. Am. Chem. Soc.* **1989**, *111*, 4063-4074.

169. R. R. Birge; *J. Am. Chem. Soc.* **1991**, *113*, 4327-4328.

170. R. Govindjee, S. P. Balashow & T. G. Ebrey; *Biophys. J.* **1990**, *58*, 597-608.

171. M. S. Braiman & R. A. mathies; *Proc. Natl. Acad. Sci., USA* **1982**, *79*, 403-403.

172. K. Bagley, G. Dollinger, L. Eisenstein, A. K. Singh & L. Zimanyi; *Proc. Natl. Acad. Sci., USA* **1982**, *79*, 4972-4976.

173. S. O. Smith, J. Lugtenburg & R. A. Mathies; *J. Membr. Biol.* **1985**, *85*, 95-109.

174. S. P. A. Fodor, J. B. Ames, R. Gebhard, E. M. M. van den Berd, W. Stoeckenius, J. Lugtenburg & R. A. Mathies; *Biochemistry* **1988**, *27*, 7097-77101.

175. M. S. Braiman, T. Mogi, T. Marti, L. T. Stern, H. G. Khorana & K. J. Rothschild; *Biochemistry* **1988**, *27*, 8516-8520.

176. H. J. Butt, K. Fendler, E. Bamberg, J. Tittor & D. Oesterhelt; *EMBO J.* **1989**, *48*, 1657-1663.

177. R. Diller & M. Stockburger; *Biochemistry* **1988**, *27*, 7641-7651.

178. G. Varo & J. K. Lanyi; *Biochemistry* **1990**, *29*, 2241-2250.

179. G. Varo & J. K. Lanyi; *Biochemistry* **1991**, *30*, 5008-5015.

180. G. Varo & J. K. Lanyi; *Biochemistry* **1991**, *30*, 5016-5022.

181. G. Varo & J. K. Lanyi; *Biochemistry* **1991**, *30*, 7165-7171.

182. P. Ormos; *Proc. Natl. Acad. Sci., USA* **1991**, *88*, 473-477.

183. M. S. Braiman & K. J. Rothschild; *Annu. Rev. Biophys. Biophys. Chem.* **1988**, *17*, 541-570.

184. K. J. Rothschild, M. Zagaeski & W. A. Cantore; *Biochem. Biophys. Res. Commun.* **1981**, *103*, 483-489.

185. F. Siebert, W. Mantele & W. Krentz; *FEBS Lett.* **1987**, *141*, 82-87.

186. M. Engelhard, K. Gerwert, B. Hess, W. Krentz & F. Siebert; *Biochemistry* **1985**, *24*, 400-407.

187. P. Roepe, P. L. Ahl, S. K. DasGupta, J. Herzfeld & K. J. Rothschild; *Biochemistry* **1987** *26*, 6696-6707.

188. L. Eisenstein, S.-L. Lin, G. Dollinger, K. Odashima, J. Termini, K. Konno, W.-O. Ding & K. Nakanishi; *J. Am. Chem. Soc.* **1987**, *109*, 6860-6862.

189. K.-S. Hung, R. Radhakrishman, H. Bayley & H. G. Khorana; *J. Mol. Chem.* **1982**, *257*, 13616-13623.

190. M. Engelhard, K. Gerwert, B. Hess, W. Kreutz & F. Siebert; *Biochemistry* **1985**, *24*, 400-407.

191. T. Mogi, L. J. Stern, T. Marti, B. H. Chao & H. G. Khorana; *Proc. Natl. Acad. Sci., USA* **1988**, *85*, 4148-4152.

192. See ref. 147.

193. See ref. 175.

194. See ref. 191.

195. L. Eisenstein, S.-L. Lin, G. Dollinger, K. Odashima, J. Termini, K. Konno, W.-D. Ding & K. Nakanishi; *J. Am. Chem. Soc.* **1987**, *109*, 6860-6862.

196. H. Otto, T. Marti, M. Holz, T. Mogi, M. Lindau, H. G. Khorana & M. P. Heyn; *Proc. Natl. Acad. Sci., USA* **1989**, *86*, 9228-9232.

197. K. Gerwert, B. Hess, J. Soppa & D. Oesterhelt; *Proc. Natl. Acad. Sci., USA* **1989**, *86*, 4943-4944.

198. R. Henderson, J. M. Baldwin, T. A. Ceska, F. Zemlin, E. Beckman & K. H. Downing; *J. Mol. Biol.* **1990**, *213*, 899-929.

199. K. Gerwert, B. Hess & M. Engelhard; *FEBS Lett.* **1990**, *261*, 449-454.

200. H. Otto, T. Marti, M. Holz, T. Mogi, L. J. Stern, F. Engel, H. G. Khorana & M. P. Heyn; *Proc. Natl. Acad. Sci., USA* **1990**, *87*, 1018-1022.

201. J. M. Fukumoto, J. H. Hanamoto & M. A. El-Sayed; *Photochem. Photobiol.* **1984**, *39*, 75.

202. G. Dollinger, L. Eisenstein, S.-L. Lin, K. Nakanishi & J. Termin; *Biochemistry* **1986**, *25*, 6524.

203. K. J. Rothschild, P. Roepe, P. L. Ahl, T. N. Earnest, R. A. Bogomolni, S. K. DasGupta, C. M. Mulliken & J. Herzfeld; *Proc. Natl. Acad. Sci., USA* **1986**, *83*, 347.

204. T. Mogi, J. L. Stern, N. R. Hackett & H. G. Khorana; *Proc. Natl. Acad. Sci., USA* **1987**, *84*, 5595-5599.

205. See ref. 182.

206. K. Nakanishi; *Pure & Appl. Chem.* **1991**, *63*, 161-170.

207. M. S. Braiman, O. Bousche & K. J. Rotheschild; *Proc. Natl. Acad. Sci., USA* **1991**, *88*, 2388-2392.

208. A. E. Blaurock & W. Stoeckenius; *Nature (London)* **1971**, *233*, 152.

209. See ref. 147.

210. P. N. T. Unwin & R. henderson; *J. Mol. Biol.* **1975**, *94*, 425.

211. Y. A. Ovchinnikov, N. G. Abdulaev, M. Y. Feigina, A. V. Kiselev & N. A. Labanov; *FEBS Lett.* **1979**, *100*, 219-224.

212. H. G. Khorana, G. E. Gerber, W. C. Herlihy, C. P. Gray, R. J. Anderegy, K. Nihei & K. Bieman; *Proc. Natl. Acad. Sci., USA* **1979**, *76*, 5046-5050.

213. R. J. Anderegg, H. Bayley, K. Biemann, S. H. Chang, R. J. Dunn, G. E. Gerber, C. P. Gray, W. C. Herlihy, B. Hojeberg, K.-S. Huang, V. C. Joshi, H. G. Khorana, J. M. McCoy, R. Radhakrishnan, O. L. RajBhandary, A. H. Ross, M. Simsele, Y. Takagaki & D. Wildenauer; In "*Recent Studies on Bacteriorhodopsin.*" **1985**, Proc. 2nd. SUNYA Conversation in the Discipline of Biomolecular Stereodynamics. *Vol 2*, R. H. Sarma; Ed., Academic Press.

214. R. Runn, J. McCoy, M. Simsek, A. Majumdar, S. H. Chang, U. L. RajBhandary & H. G. Khorana; *Proc. Natl. Acad. Sci., USA* **1981**, *78*, 6744-6748.

215. D. M. Engelman, R. Henderson, A. D. McLachlan & B. A. Wallace; *Proc. Natl. Acad. Sci., USA* **1980**, *77*, 2023-2027.

216. H. G. Khorana; *J. Biol. Chem.* **1988**, *263*, 7439-7442.

217. S. B. Harward & R. M. Stroud; *J. Mol. Biol.* **1981**, *151*, 491-517.

218. B. K. Jap, M. F. Maestre, S. B. Hayward & R. M. Glaeser; *Biophys. J.* **1983**, *43*, 81-89.

219. E. Nabedryk, A. M. Badin & J. Breton; *Biophys. J.* **1985**, *48*, 873-876.

220. D. C. Lee, J. A. Hayward, C. J. Restall & D. Chapman; *Biochemistry* **1985**, *24*, 4364-4373.

221. T. N. Earnest & K. Rothschild; *Biophys. J.* **1986**, *49*, 294a.

222. T. N. Earnest; *Ph.D. Dissertation*, Boston University, Boston, MA **1987**, pp.1-193.

223. N. W. Downer, T. J. Bruchman & J. H. Hazzard; *J. Biol. Chem.* **1986**, *261*, 3640-3647.

224. D. C. Lee, E. Herzyk & D. Chapman; *Biochemistry* **1987**, *26*, 5775-5783.

225. B. A. Wallace & C. L. Teeters; *Biochemistry* **1986**, *26*, 65-70.

226. See ref. 198.

227. T. N. Earnest, J. Herzfeld & K. J. Rothschild; *Biophys. J.* **1990**, *58*, 1539-1546.

228. K. Nakanishi, V. Balogh-Nair, M. Arnaboldi, K. Tsujimoto & B. Honig; *J. Am. Chem. Soc.* **1980**, *102*, 7945-7947.

229. M. Arnaboldi, M. G. Motto, K. Tsujimoto, V. Balogh-Nair & K. Nakanishi; *J. Am. Chem. Soc.* **1979**, *101*, 7082-7084.

230. B. Honig, U. Dinur, K. Nakanishi, V. Balogh-Nair, M. Gawinowicz, M. Arnaboldi & M. G. Motto; *J. Am. Chem. Soc.* **1979**, *101*, 7084-7086.

231. B. Pullman, J. Langlet & H. Berthod; *J. Theor. Biol.* **1969**, *23*, 482.

232. B. Honig, B. Hudson, B. D. Sykes & M. Karplus; *Proc. Natl. Acad. Sci., USA* **1980**, 71, *68*, 1289-1293.

233. G. S. Harbison, S. O. Smith, J. A. Pardoen, J. M. L. Courtin, J. Lugtenburg, J. Herzfeld, R. A. Mathies & R. G. Griffin; *Biochemistry* **1985**, *24*, 6955-9662.

234. R. van der Steen, P. L. Biesheuvel, R. A. Mathies & J. Lugtenburg; *J. Am. Chem. Soc.* **1986**, *108*, 6410-6411.

235. R. D. Baselt, S. P. A. Fodor, R. van der Steen, J. Lugtenburg, R. A. Bogomolni & R. A. Mathies; *Biophys. J.* **1989**, *55*, 193-196.

236. F. Derguini, D. Dunn, L. Eisenstein, K. Nakanishi, K. Odashima, V. J. Rao, L. Sastry & J. Termini; *Pure & Appl. Chem.* **1986**, *58*, 719-724.

237. See ref.228.

238. J. Lugtenburg, M. Muradin-Szweykowska, C. Heeremans, J. A. Pardoen, G. S. Harbison, J. Herzfeld, R. G. Griffin, O. S. Smith & R. A. Mathies; *J. Am. Chem. Soc.* **1986**, *108*, 3104.

239. R. van der Steen, P. L. Biesheuvel, C. Erkelens, R. A. Mathies & J. Lugtenburg; *Recl. Trav. Chim. Pay-Bas* **1989**, *108*, 83-93.

240. M. P. Heyn, R. J. Cherry & U. Muller; *J. Mol. Biol.* **1977**, *117*, 607-620.

241. T. N. Earnest, P. Roepe, M. S. Braiman, J. Gillespie & K. J. Rothschild; *Biochemistry* **1986**, *25*, 7793-7798.

242. A. Ikegami, T. Kouyama, K. Kinosta, J. H. Urabe & J. Otomo; In "*Primary Processes in Photobiology.*" T. Kobayashi; Ed., **1987**, *Vol. 20*, pp. 173-182, Springer-Verlay, New York, Inc. NY.

243. M. P. Heyn, J. Westerhausen, I. Wallat & F. Seiff; *Proc. Natl. Acad. Sci., USA* **1988**, *85*, 2146-2150.

244. J. Otomo, A. Tomioka, K. Kinosita, J. H. Miyata, Y. Takenaka, T. Kouyama & A. Ikegami; *Biophys. J.* **1988**, *54*, 57-64.

245. K.-S. Huang, R. Radhakrishman, H. Bayley & H. G. Khorana; *J. Biol. Chem.* **1982**, *257*, 13616-13623.

246. See ref. 198.

247. See ref. 245.

248. J. Y. Huang & A. Lewis; *Biophys. J.* **1989**, *55*, 835-842.

249. S. W. Lin & R. A. Mathies; *Biophys. J.* **1989**, *55*, 653-660.

250. See ref. 175.

251. T. Hauss, S. Grzesiek, H. Otto, J. Westerhausen & M. P. Heyn; *Biochemistry* **1990**, *29*, 4904-4913.

252. S. W. Lin & R. A. Mathies; *Biophys. J.* **1989**, *56*, 653-660.

253. W.-D. Ding, A. Tsipouras, H. OK, T. Yamamoto, M. A. Gawinowioz & K. Nakanishi; *Biochemistry* **1990**, *29*, 4898-4904.

254. M. Seigneuret, J.-M. Neumann, D. Levy & J.-L. Rigaud; *Biochemistry* **1991**, *30*, 3885-3892.

255. V. Balogh-Nair & K. Nakanishi; *Methods Enzymol.* **1982**, *88*, 496-506.

256. V. Balogh-Nair & K. Nakanishi; *New Copr. Biochem.* **1982**. *3*, 283-334.

257. R. S. H. Liu & A. E. Asato; *Tetrahedron* **1984**, *40*, 1931-1969.

258. F. Frickel; In " *The Retinoids.*" M. Sporn, A. B. Roberts & P. E. Goodman; Ed. **1984**, *Vol. 1*, pp.7-145, Academic, New York.

259. W. K. Chan, K. Nakanishi, T. G. Ebrey & B. Honig; *J. Am. Chem. Soc.* **1974**, *96*, 3642-3644.

260. T. G. Ebrey, R. Govindjee, B. Honig, E. Pollock, W. K. Chan, R. Crouch, A. Yudd & K. Nakanishi; *Biochemistry* **1975**, *14*, 3933-3941.

261. K. Nakanishi; *Pure & Appl. Chem.* **1985**, *57*, 769-776.

262. R. S. H. Liu, A. E. Asato, M. Denny & D. Mead; *J. Am. Chem. Soc.* **1984**, *106*, 8289-8300.

263. A. E. Asato, M. Denny, H. Matsumoto, T. Mirzadegan, W. C. Ripka, F. Crescitelli & R. S. H. Liu; *Biochemistry* **1986**, *25*, 7021-7026.

264. M. Ito, A. Kodama, K. Tsukida, Y. Fukada, Y. Shichida & T. Yoshizawa; *Chem. Pharm. Bull.* **1982**, *30*, 1913-1916.

265. Y. Fukada, Y. Shichida, T. Yoshizawa, M. Ito, A. Kodama & K. Tsukida; *Chem. Pharm. Bull.* **1982**, *30*, 1913-1916.

266. M. Ito. T. Hiroshima, K. Tsukida, Y. Shichida & T. Yoshizawa; *J. Chem. Soc. Chem. Commu.* **1985**, 1443-1444.

267. R. Crouch, B. R. Nodes, J. I. Perlman, D. R. Pepperberg, H. Akita & K. Nakanishi; *Invest. Ophthalm. and Vis. Sci.* **1984**, *25*, 419-428.

268. R. Hubbard & G. Wald; *J. Gen. Physiol.* **1952**, *36*, 269-315.

269. G. Wald, P. K. Brown, R. Hubbard & W. Orosnik; *Proc. Natl. Acad. Sci., USA* **1955**, *41*, 438-451.

270. W. Orosnik, P. K. Brown, R. Hubbard & G. Wald; *Proc. Natl. Acad. Sci., USA* **1956**, *42*, 578-580.

271. Y. Shichida, K. Nakamura, T. Yoshizawa, A. Trehan, M. Denny & R. S. H. Liu; *Biochemistry* **1988**, *27*, 6495-6499.

272. A. Kropt; *Nature (London)* **1976**, *264*, 92-94.

273. W. H. Waddel, M. Uemura & J. L. West; *Tetrahedron Lett.* **1978**, 3223-3226.

274. W. Gartner, H. Hopt, W. E. Hull, D. Oesterhelt, D. Scheutzov & P. Towner; *Tetrahedron Lett.* **1980**, 347-350.

275. A. Kropf, P. Whittenberger, S. Goff & A. S. Waggoner; *Exp. Eye Res.* **1973**, *17*, 591-606.

276. R. Crouch & Y. S. Or; *FEBS Lett.* **1983**, *158*, 139-142.

277. V. Jayahirtha, J. P. Zingoni, R. Crouch, M. Denny & R. S. H. Liu; *Biochemistry* **1985**, *25*, 171-174.

278. F. Derguini, C. F. Bigge, A. A. Croteau, V. Balogh-Nair & K. Nakanishi; *Photochem. Photobiol.* **1984**, *39*, 661-665.

279. K. Nakanishi; *Pure & Appl. Chem.* **1991**, *63*, 161-170.

280. Y. Koutalos, T. G. Ebrey, M. Tsuda, K. Odashima, T. Lien, M. H. Park, N. Shimizu, F. Derguini, K. Nakanishi, H. R. Gilson & B. Honig; *Biochemistry* **1989**, *28*, 2732-2739.

281. V. Chowdhry & F. H. Westheimer; *Annu. Rev. Biochem.* **1979**, *48*, 239.

282. J. Knowles; *Accts. Chem. Res.* **1972**, *5*, 155.

283. H. Bayley & J. R. Knomles; *Meth. Enzymol.* **1977**, *46*, 69.

284. E. A. Dratz, G. P. Milianich, P. Names, J. E. Gaw & Schwartz; *Photochem. Photobiol.* **1979**, *29*, 661.

285. H. Saibil, M. Chabre & D. Worcester; *Nature (London)* **1976**, *262*, 266.

286. R. Sen, A. Singh, V. Balogh-Nair & K. Nakanishi; *Tetrahedron* **1984**, *40*, 483.

287. J.-M. Fang, J. D. Carriker, V. Balogh-Nair & K. Nakanishi; *J. Am. Chem. Soc.* **1983**, *105*, 5162.

288. R. van der Steen, P. L. Biesheuvel, R. Mathies & Lugtenburg; *J. Am. Chem. Soc.* **1988**, *108*, 6410.

289. K. Nakanishi; *Pure & Appl. Chem.* **1985**, *57*, 769.

290. M. G. Motto, M. Sheves, K. Tsujimoto, V. Balogh-Nair & K. Nakanishi; *J. Am. Chem. Soc.* **1980**, *102*, 7947.

291. F. Derguini, C. F. Bigge, A. A. Crotoan, V. Balogh-Nair & K. Nakanishi; *Photochem. Photobiol.* **1984**, *39*, 661.

292. V. Balogh-Nair, J. D. Carriker, B. Honig, V. Kamat, M. G. Motto, K. Nakanishi, R. Sen, M. Sheves, M. Araboldi Tania & K. Tsujimoto; *Photochem. Photobiol.* **1981**, *33*, 483.

293. H. Bayley, R. Radhakrishknan, K. S. Huang & H. G. Khorana; *J. Biol. Chem.* **1981**, *256*, 3797.

294. P. Umadevi, M. Sheves, V. Rosenbach & M. Ottolenghi; *Photochem. Photobiol.* **1983**, *38*, 197.

295. A. Maeda, A. E. Asato & R. S. H. Liu; *Biochemistry* **1984**, *23*, 2507.

296. T. Baasov & M. Sheves; *J. Am. Chem. Soc* . **1987**, *109*, 1594.

297. Y. Kimura, A. Ikegami & W. Stoeckenius; *Photochem. Photobiol.* **1984**, *40*, 641-646.

298. G. H. Chang, J. G. Chen, R. Govindjee & Y. Ebrey; *Proc. Natl. Acad. Sci., USA* **1985**, *82*, 396-400.

299. D. Oesterhelt & Stoeckenius; *Nat. New Biol.* **1971**, *233*, 149-152.

300. U. Fischer & D. Oesterhelt; *Biophys. J.* **1979**, *28*, 211-230.

301. A. Albeck, N. Friedman, M. Sheves & Ottolenghi; *Biophys. J.* **1989**, *56*, 1259-1265.

302. R. Sen, J. D. Carriker, V. Balogh-Nair & K. Nakanishi; *J. Am. Chem. Soc.* **1982**, *104*, 3214.

303. M. Ito; *Pure & Appl. Chem.* **1991**, *63*, 13-22.

304. S. D. Young, C. T. Buse & C. H. Heathcock; *Org. Synth.* **1984**, *Vol.63*, 79-88.

305. F. Derguini, V. Balogh-Nair & K. Nakanishi; *Tetrahedron Lett.* **1979**, *20*, 4899-4902.

306. G. Pattenden & B. C. L. Weedon; *J. Chem. Soc.(C)* **1968**, 1984.

307. W. S. Wadsworth; *Org. React.* (N. Y.) **1977**, 73-253.

308. J. Boutagy & R. Thomas; *Chem. Rev.* **1974**, *74*, 87-99.

309. H. Pommer; *Angew. Chem.* **1977**, *89*, 437-443.

310. B. Maryanoff & A. B. Reitz; *Chem. Rev.* **1989**, *89*, 863.

311. See ref. 305.

312. G. L. Olson, H.-G. Cheung, K. D. Morgan, R. Borer & G. Saucy; *Helv. Chim. Acta* **1976**, *59*, 567-585.

313. Y. Hanzawa, A. Yamada & Y. Kobayash; *Tetrahedron Lett.* **1985**, *26*, 2881-2884.

314. H. Lindlar & R. Ruegg; **1952**, *U. S. patent* 2,610, 207; *Chem. Abstr.* **1953**, *4*, 12418e.

315. Y. Hanzawa, A. Yamada & Y. Kobayashi; *Tetrahedron Lett.* **1985**, *26*, 2881-2884.

316. *J. Org. Chem.* **1978**, *43*, 1020.

317. *Org. Syn.* Vol.65, p.12.12. P. J. Stang, Z. Rappoport, M. C. Hanack & L. R. Subramanian; *Vinyl Cations*; Academic, New York, **1979.**

318. P. J. Stang, Z. Rappoport, M. C. Hanack & L. R. Subramanian; *Vinyl Cation*, Academic, New York, **1979.**

319. J. E. McMurry & W. J. Scott; *Tetrahedron Lett.* **1983**, *24*, 979-982.

320. W. J. Scott & J. E. McMurry; *Acc. Chem. Res.* **1988**, *21*, 47-54.

321. W. J. Scott, M. R. Pena, K. Sward, S. J. Stoessel & J. K. Stille; *J. Org. Chem.* **1985**, *50*, 2302-2308.

322. E. J. Corey, D. Enders & M. G. Bock; *Tetrahedron Lett.* **1976**, *17*, 7-10.

323. M. E. Krafft & R. E. Holton; *Tetrahedron Lett.* **1983**, *24*, 1345-1348.

324. W. J. Scott & J. K. Stille; *J. Am. Chem. Soc.* **1986**, *108*, 3033-3040.

325. W. J. Scott, M. R. Pena, K. Sward, S. J. Stoessel & J. K. Stille; *J. Org. Chem.* **1985**, *50*, 2302-2308.

326. W. C. Stille, M. Kahn & A. Mitra; *J. Org. Chem.* **1978**, *43*, 2923.

327. V. Balogh-Nair & K. Nakanishi; in "*New Comprehensive Biochemistry. Vol.3. Stereochemistry*". Tamm.Ch., Ed., Elsevier, biomedical Press: Amsterdam, **1982**, Chapter 7, 283-334.

328. a. H. Matsumoto, K, Horiuchi & T. Yoshizawa; *Biochim. Biophys. Acta* **1978**, *501*, 257-268; b. A. Albeck, N. Friedman, M. Ottolenghi, M. Sheves, C. M. Einterz, S. J. Hug, J. W. Lewis & D. S. Kliger; *Biophys. J.* **1989**, *55*, 233-241.

329. M. Arnaboldi, M. G. Motto, K. Tsujimoto, V. Balogh-Nair & K. Nakanishi; *J. Am. Chem. Soc.* **1979**, *101*, 7082-7084.

330. F. G. Pilkiewicz, M. J. Pettei, A. P. Yudd & K. Nakanishi; *Exp. Eye Res.* **1977**, *24*, 421-423.

331. S. P. A. Fodor, W. T. Pollard, R. Gebhard, E. M. M. van den Berg, J. Lugtenburg & R. A. Mathies; *Proc. Natl. Acad. Sci., USA* **1988**, *85*, 2156-2160.

332. R. L. Christensen & B. E. Kohler; *Photochem. Photobiol.* **1973**, *18*, 293-301.

333. R. R. Birge, D. F. Bocian & L. M. Hubbard; *J. Am. Chem. Soc.* **1982**, *104*, 1196-1207.

334. R. Henderson; *Annu. Rev. Biophys. Bioeng.* **1977**, *6*, 87.

335. J. Y. Huang & A. Lewis; *Biophys. J.* **1989**, *55*, 835-842.

336. S. W. Lin & R. A. Mathies; *Biophys. J.* **1989**, *55*, 653-660.

337. R. Henderson & et al; *J. Mol. Biol.* **1990**, *213*, 899-929.

338. F. M. Menger & L. L. D'Angelo; *J. Am. Chem. Soc.* **1988**, *110*, 8241-8242.

339. N. M. Green, L. Konieczny, E. J. Toms & R. C. Valentine; *Biochemistry* **1972**, *125*, 781-791.

340. F. Derguini & K. Nakanishi; *Photobiochem. Photobiophys.* **1986**, *13*, 259-283.

341. D. S. Papermaster & W. J. Dreyer; *Biochemistry* **1974**, *13*, 2438.

342. Y. Shichida, T. Ono, T. Yoshizawa, H. Matsumoto, A. E. Asato, J. P. Zingoni & R. S. H. Liu; *Biochemistry* **1987**, *26*, 4422-4428.

343. A. Kropf; *Vision Res.* **1982**, *22*, 495-497.

344. R. Navarrette & R. Serrano; *Biochim. Biophys. Acta* **1983**, *728*, 403.

345. R. Hubbard & G. Wald; *J. Gen. Phsiol.* **1952**, *36*, 269-315.

346. G. Wald, P. K. Brown, R. Hubbard & W. Orosnik; *Proc. Natl. Acad. Sci., USA* **1955**, *41*, 438-451.

347. W. Orosnik, P. K. Brown, R. Hubbard & G. Wald; *Proc. Natl. Acad. Sci., USA* **1956**, *42*, 578-580.

348. R. S. H. Liu, H. Matsumoto, A. Kini, A. E. Asato, M. Denny, A. Kropf & W. J. Degrip; *Tetrahedron* **1984**, *40*, 437-482.

349. R. S. H. Liu & A. E. Asato; *Tetrahedron* **1984**, *40*, 1931-1969.

350. A. E. Asato, M. Denny, H. Matsumoto, T. Mirzadegam, W. C. Ripka, F. Crescitelli & R. S. H. Liu; *Biochemistry* **1986**, *25*, 7021-7026.

351. See ref. 345.

352. W. H. Waddell & D. L. Hopkins; *J. Am. Chem. Soc.* **1977**, *99*, 6457.

353. M. Denny & R. S. H. Liu; *J. Am. Chem. Soc.* **1977**, *99*, 4865-4867.

354. R. Hubbard, R. I. Gregerman & G. Wald; *J. Gen. Physiol.* **1952**, *36*, 415.

355. P. K. Brown & G. Wald; *J. Biol. Chem.* **1956**, *222*, 865.

356. R. S. H. Liu & A. E. Asato; *Methods Enzymol.* **1982**, *88*, 506-516.

357. V. Chowdyry & F. H. Westheimer; *Ann. Rev. Biochem.* **1979**, *48*, 239.

358. J. Knowles; *Accts. Chem. Res.* **1972**, *5*, 155.

359. W. Lwowski; *Ann. N.Y. Acad. Sci.* **1980**, *346*, 491-500.

360. T. A. Nakayama & H. G. Khorana; *J. Org. Chem.* **1990**, *55*, 4953-4956.

361. T. A. Nakayama & H. G. Khorana; *J. Biol. Chem.* **1990**, *256*, 15762-15769.

362. R. Sen, J. D. Carriker, V. Balogh-Nair & K. Nakanishi; *J. Am. Chem. Soc.* **1982**, *104*, 3214-3216.

363. R. Sen, A. K. Singh, V. Balogh-Nair & K. Nakanishi; *Tetrahedron* **1984**, *40*, 493-500.

364. E. F. V. Scriven; *Chem. Soc. Rev.* **1983**, 129-161.

365. B. Neises & W. Steglich; *Angew. Chem. Int. Ed. Engl.* **1978**, *17*, 522-523.

366. E. J. Corey & A. G. Myers; *Tetrahedron Lett.* **1984**, *25*, 3559-3562.

367. F. Kazmierczak & P. Helquist; *J. Org. Chem.* **1989**, *54*, 3988-3992.

368. I. Mori, K. Ishihara & C. H. Heathcock; *J. Org. Chem.* **1990**, *55*, 1114-1117.

369. E. Piers & A. V. Gavai; *J. Org. Chem.* **1990**, *55*, 2380-2390.

370. W. J. Scott & J. E. McMurry; *Acc. Chem. Res.* **1988**, *21*, 47-54.

371. H. Kotsuki, I. Kadota & M. Ochiai; *Tetrahedron Lett.* **1990**, *32*, 4609-4612.